



# CONTENTS

Relevance of the work.....	6
Input.....	7
Fuselage structure.....	7
Cabin volume and pressure .....	10
Cabin cross-section .....	12
1 Floor beam arrangement.....	15
2 Airplane load analysis .....	17
3 Freebody diagram and determination of analyzed cross section. ....	25
4 Normal and shear stress finding .....	28
5 Buckling analysis .....	42
5.1 Local Buckling .....	43
5.2 Column buckling (Euler).....	48
5.3 Chord crippling and Jonson-Euler column buckling. ....	52
5.4 Web buckling. ....	57
6. Floor beam with Frame Joint. Static and fatigue analysis .....	65
6.1 Static strengths analysis .....	65
6.2 Fatigue joint analysis.....	70
.....	76
Startup .....	77
Conclusion.....	78
Bibliography.....	79

## **Relevance of the work**

Today, the plane is the fastest and safest type of transport. Because of this, dozens of aircraft per day are produced in the world. Against this background, there is growing competition between aircraft manufacturers. Since the aircraft must be fast with a minimum weight, maximum load capacity, minimum fuel consumption and maximum life.

In view of this, airplanes are constantly improving improving their weight and economic efficiency, but they still should be the most safety transport due to many safety requirements in FAR and other standards.

In current work is designed floor beam waffle construction with using semi-empirical methods with optimal cross section sizes which satisfied static and fatigue strength and requirements from FAR 25.

## **Input**

### **Fuselage structure**

Aircraft fuselages consist of thin sheets of material stiffened by large numbers of longitudinal stringers together with transverse frames. Generally, they carry bending moments, shear forces, and torsional loads, which induce axial stresses in the stringers and skin, together with shear stresses in the skin; the resistance of the stringers to shear forces is generally ignored. Also, the distance among the adjacent stringers is usually small, so that the variation in shear flow in the connecting panel is small. It is, therefore, reasonable to assume that the shear flow is constant among the adjacent stringers, so that the analysis simplifies to the analysis of an idealized section in which the stringers/booms carry all the direct stresses while the skin is effective only in shear. The direct stress carrying capacity of the skin may be allowed for by increasing the stringer/boom areas. The analysis of fuselages, therefore, involves the calculation of direct stresses in the stringers and the shear stress distributions in the skin; the latter are also required in the analysis of transverse frames.

The fuselage is a critical component in aircraft. Typically found in the middle section, it's responsible for securing crew, passengers and cargo. Depending on the number of engines the aircraft has, it may contain the engine as well. Furthermore, the fuselage works to position and stabilize the aircraft for improved performance and maneuverability. But there are many different types of aircraft fuselage, some of which we're going to explore in this blog post.

#### **Truss Structure**

Often used in lightweight aircraft, a truss structure fuselage is typically made of welded steel tube trusses (though it can also be made of wood). They are often rounded and feature lightweight stringers to achieve a greater aerodynamic shape.

#### **Geodesic Structure**

Used for the British Vickers during World War II, geodesic fuselage structures seek to enhance the aircraft's shape to reduce drag and improve speed. Multiple strip stringers are intertwined around the formers in varying spiral directions, similar to a wicker basket. Geodesic fuselage structures are lightweight, strong, and ultra-durable. They were typically

made of either wood and/or aluminum, featuring a fabric covering the shell for greater comfortable and aesthetic value.

### Monocoque

In the monocoque shell structure, the fuselage is designed within the aircraft's primary structure. The Lockheed Vega is an example of an early model aircraft with a monocoque shell structure. It was build with molded plywood, featuring multiple layers that cover a plug in the mold. Other versions of the monocoque shell include a fiberglass-type cloth with polyester resin, as well as a variant of this design with epoxy resin. With that said, no fuselage featuring plywood is truly monocoque.

### Semi-Monocoque

There's also a semi-monocoque fuselage design, which lives up to its namesake by featuring characteristics of its counterpart. According to Wikipedia, the semi-monocoque fuselage structure is preferred when constructing an all-aluminum fuselage. It features frames designed to create the shell of the fuselage, which are secured via cross sections on a rigid fixture. Stringers are attached to join with the fixture.

These are just a few of the most common fuselage structures used in aircraft design. From small single-engine aircraft to larger commercial aircraft, all planes need a fuselage. It's a critical component that allows plans to transport people and cargo. However, aircraft manufacturers must choose the right fuselage for the job when designing planes.

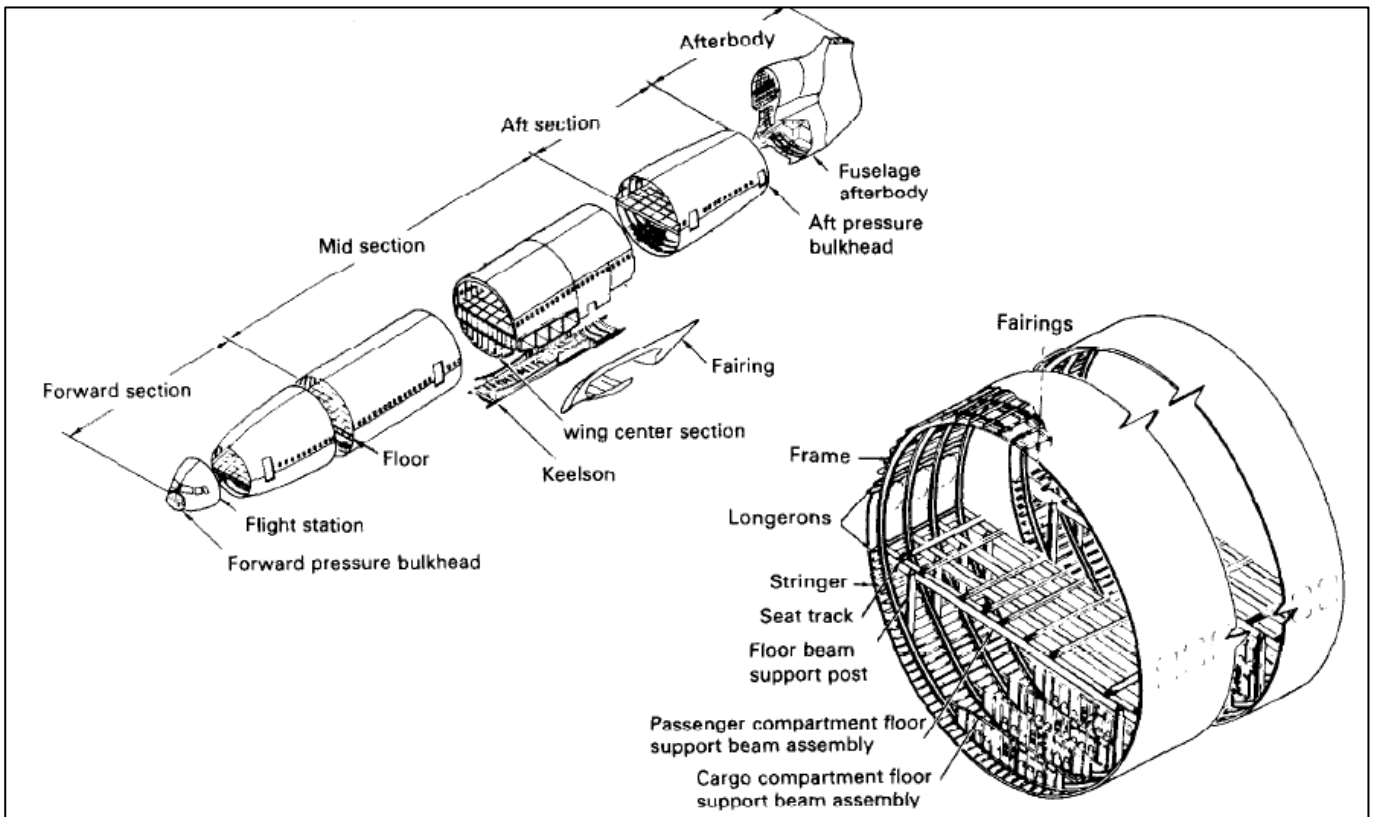


Figure 1 – Typical fuselage configuration [1]

The fuselage is that portion of the aircraft wherein the payload is carried. In jet transports the payload consists of the passengers and their baggage and/or cargo. Primary considerations when designing the airplane's fuselage are as follows:

- Low aerodynamic drag.
- Minimum aerodynamic instability.
- Comfort and attractiveness in terms of seat design, placement, and storage space.
- Safety during emergencies such as fires, cabin depressurization, ditching, and proper placement of emergency exits, oxygen systems, etc.
- Ease of cargo handling in loading and unloading, safe and robust cargo hatches and doors.
- Structural support for wing and tail forces acting in flight, as well as for landing and ground operation forces.
- Structural optimization to save weight while incorporating protection against corrosion and fatigue.

- Flight deck optimization to reduce pilot workload and protect against crew fatigue and intrusion by passengers.
- Convenience, size, and placement of galleys, lavatories, and coat racks.
- Minimization of noise and control of all sounds so as to provide a comfortable, secure environment.
- Climate control within the fuselage including air conditioning, heating, and ventilation.
- Provision for housing a number of different subsystems required by the aircraft, including auxiliary power units, hydraulic system, air conditioning system, etc.

Though these factors must be taken into account in fuselage design, they are constrained by the need to minimize overall structural weight and aerodynamic drag because they affect performance and initial cost, as well as impacting operating costs. The overall shape and dimensions very much dictate the effectiveness of the design and these are in turn influenced by the mission.

[5]

### **Cabin volume and pressure**

The pressurized cabin of a commercial airliner, as shown schematically in Figure 2, includes the flight deck in the nose cone, the passenger cabin and cargo areas, and terminates at the aft pressure bulkhead. The cross-sectional shape of the cabin is generally circular, or close to circular, because of the structural and manufacturing benefits of such a shape. To simplify the analysis attention is focused on the passenger cabin, which comprises the major portion of the fuselage volume. The fuselage width is proportional to the number of seats abreast, their width, and the width of any aisles between the seats.

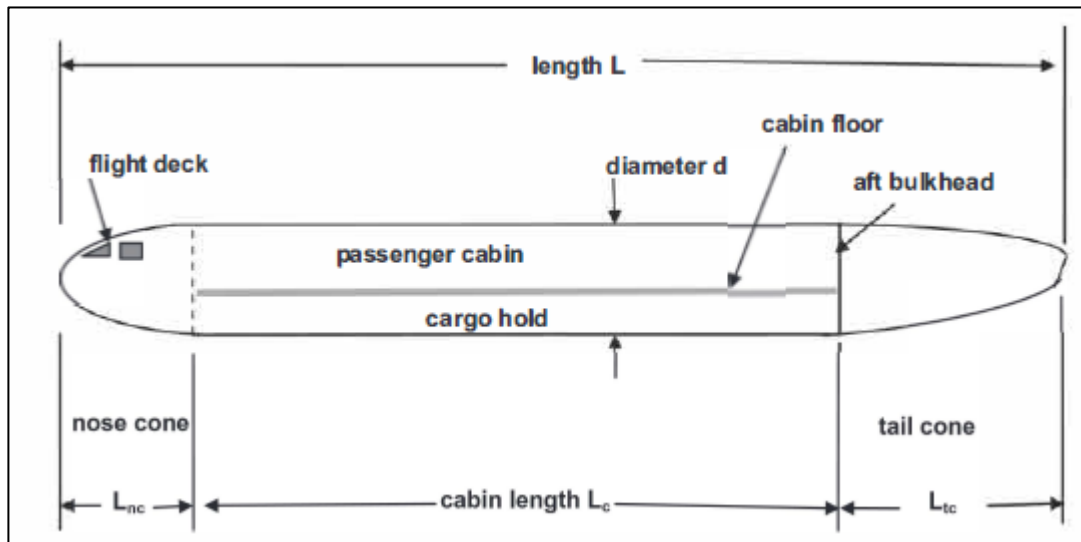


Figure 2 - Schematic diagram of fuselage showing passenger cabin.

The approximation sign is used to note that we tacitly assume the number of seats abreast to be a constant. On some aircraft there may be a few rows that have a different number of seats abreast for various operational or design reasons.

We may consider two volume measures, the pressurized volume and the free volume. The free volume is defined as that volume readily accessible to the passengers in the cabin neglecting the volume occupied by seats and partitions.

At the normal stratospheric cruising altitudes of 30,000-38,000ft, the outside pressure is 0.3-0.2 atm, respectively, while the cabin pressure is maintained at a level equal to that found at altitudes between about 5500ft and 8000ft, or between about 0.8 and 0.7 atm. This is normally tolerable for healthy adults without serious difficulties, but on long-duration flights noticeable effects may arise which are similar to what is commonly called mountain sickness. As the pressure in the cabin was decreased to levels corresponding to altitudes between 7000ft and 8000ft, blood oxygen levels were found to decrease as much as 4.4%. At these lower cabin pressures the volunteers were more likely to complain of headaches, fatigue, muscle cramps, and stomach aches. The general conclusion reached in these studies is that for long-duration flights the cabin pressure should be maintained at a level of about 6000ft or less to reduce the probability of passenger discomfort. New long-

range aircraft, like the Boeing 787, have incorporated increased cabin pressures, at about the 6000ft altitude level, to address this aspect of passenger comfort.

### **Cabin cross-section**

The typical passenger cabin is designed to be cylindrical in cross-section as closely as possible. There are a number of reasons for this:

- A circle has the greatest cross-sectional area per unit perimeter. The drag of a typical fuselage, which has a rather large fineness ratio, that is, the ratio of length to diameter, is dominated by the skin friction component, as will be seen later on in the design analysis.
- A circular cross-section is strongest under internal pressure. At the normal stratospheric cruising altitudes of 30,000-38,000ft, the outside pressure is 0.3-0.2 atm, respectively, while the internal pressure is maintained at a level equal to that found at 8000ft, or about 0.7 atm. Therefore the pressure difference across the thin skin of the cabin ranges from 0.4 to as much as 0.5 atm, or  
6- 7psi (40-50kPa).
- A circular cylinder can more easily accommodate growth in  $N_p$  in terms of manufacturing since cylindrical sections, called plugs, can be readily added to an existing fuselage to create a so-called stretched version of a given aircraft. There are disadvantages to circular cross-section cabins as well, and these are related to limited space outside the passenger compartment for auxiliary systems and cargo. It is evident that the passenger compartment must be located in the vicinity of a diameter of the circle since this gives the greatest width for seats and aisles.

The diameter of the fuselage is the most important parameter of the fuselage design since it sets the maximum frontal area of the airplane, and it is essential to make it as small as possible while remaining consistent with passenger comfort and safety. Most commercial airlines require aircraft to be easily configured so as to provide at least two cabin seating arrangements, first class and economy class, with the great majority of seats (80% or more) in the latter category and this arrangement will set the diameter of the cabin. Seats, carry-on luggage (and therefore overhead bins), cargo containers, and galley carts (and therefore

aisles) are standardized so that there is a good deal of constraint on the layout. Any increase in cabin interior diameter without a corresponding change in external diameter is a major achievement.

[5]

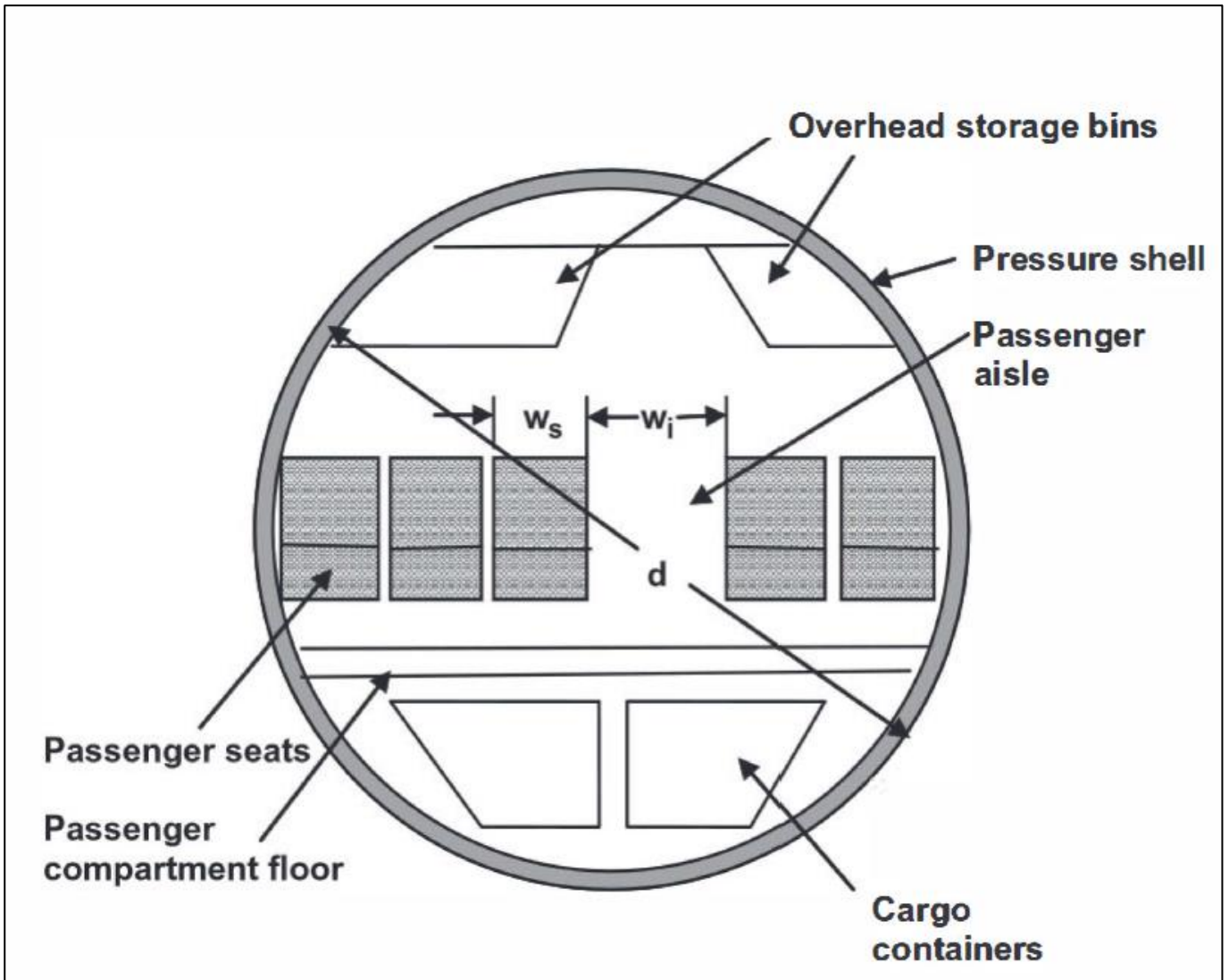


Figure 3 - Schematic diagram of typical passenger cabin cross-section.

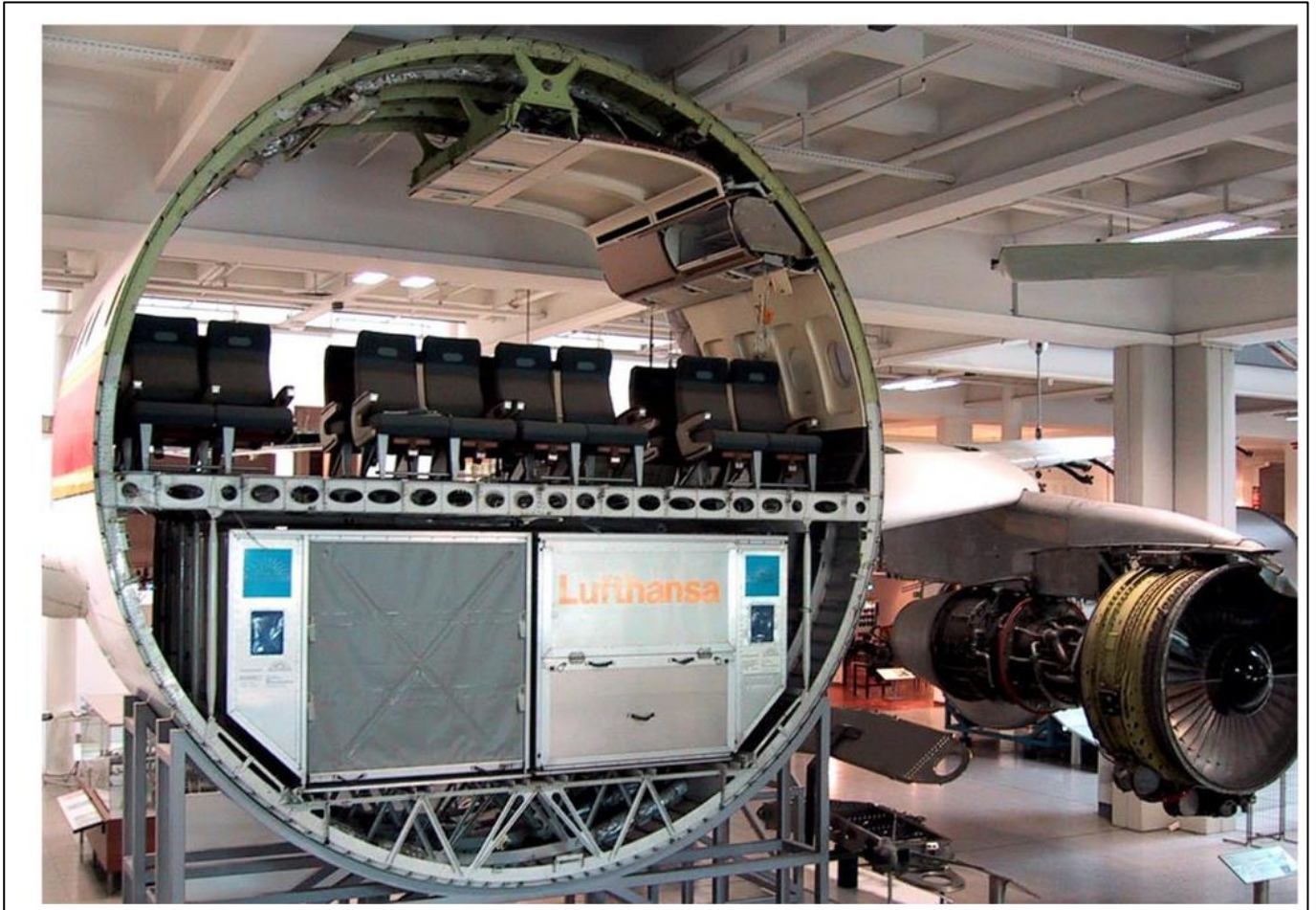


Figure 4 - Cabin cross-section.

## **1 Floor beam arrangement**

Structures, systems and methods provide a load-bearing aircraft flooring within an aircraft's fuselage. Load-supporting aircraft flooring systems preferably are provided with a longitudinally separated series of transverse bridges having an upper doubler flange which defines latitudinally separated upper openings, and a latitudinally separated series of beams which include an upper flange and a pair of separated depending web flanges received within respective upper openings of transverse bridges. The upper flanges and web flanges of the beams may thus be connected to the transverse bridges. The transverse bridges may include latitudinally separated Y-shaped supports which define the upper openings thereof. According to certain embodiments, the Y-shaped supports include an upper fork region and a lower support post region. The beams may include opposed bridge fixation fingers protruding outwardly from the upper flange of the beam for joining the beams to a respective underlying one of the transverse bridges. Aircraft flooring panels may thus be connected to the beams, preferably by means of flooring fixation fingers protruding outwardly from the upper flange of the beams. Seat tracks for attaching aircraft seats and/or other interior aircraft structures/monuments are preferably fixed to the upper flanges of the beams coincident with its longitudinal axis.

In current work is designed floor beam waffle construction. See typical cross-section view and sizes on figure 1.1.

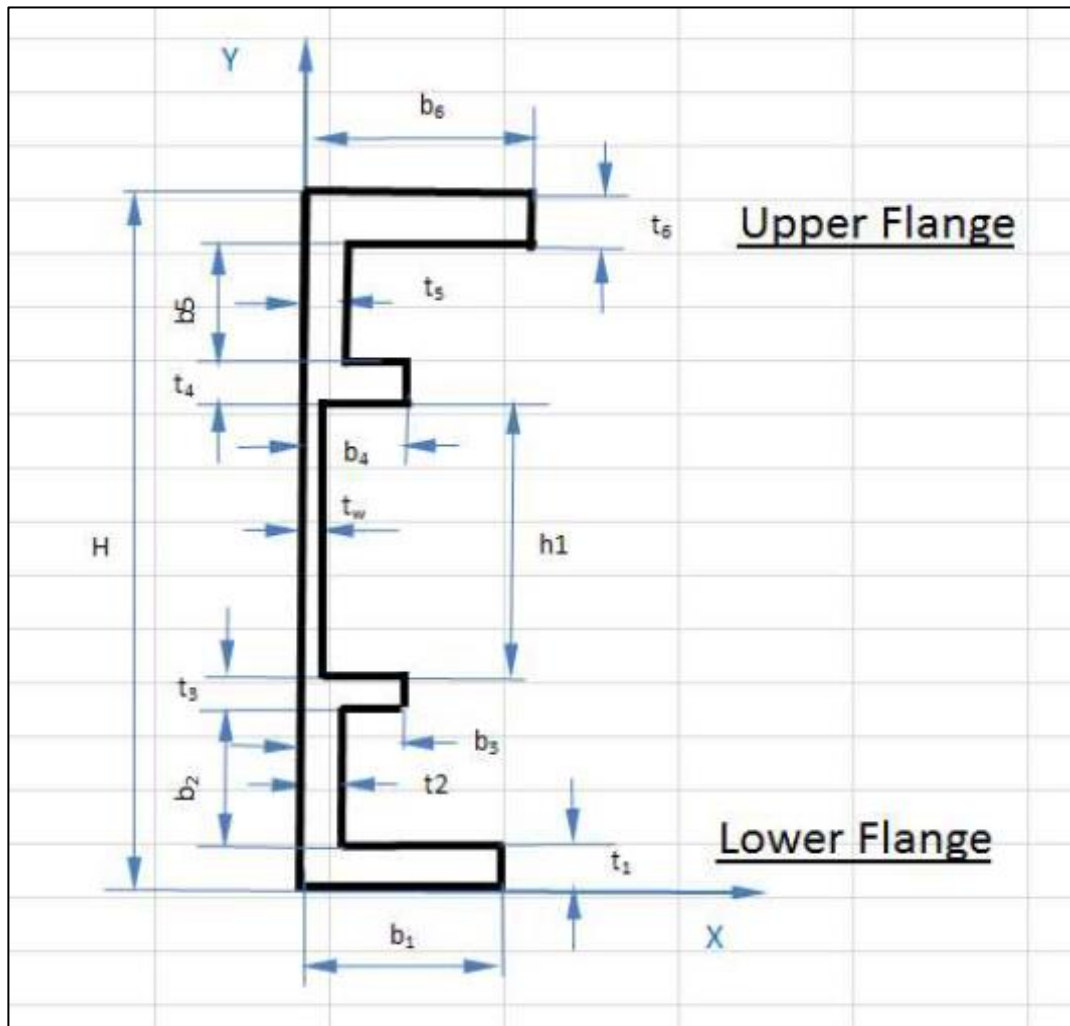


Figure 1.1 - Typical cross-section view and sizes

## 2 Airplane load analysis

[2]

Strength requirements are specified in terms of limit loads (the maximum loads to be expected in service) and ultimate loads (limit load multiplied by prescribed factors of safety). Unless otherwise provided, prescribed loads are limit loads. Unless otherwise provided, the specified air, ground, and water loads must be placed in equilibrium with inertia forces, considering each item of mass in the airplane. These loads must be distributed to conservatively approximate or closely represent actual conditions. Methods used to determine load intensities and distribution must be validated by flight load measurement unless the methods used for determining those loading conditions are shown to be reliable. If deflections under load would significantly change the distribution of external or internal loads, this redistribution must be taken into account. Unless otherwise specified, a factor of safety of 1.5 must be applied to the prescribed limit load which are considered external loads on the structure. When a loading condition is prescribed in terms of ultimate loads, a factor of safety need not be applied unless otherwise specified.

Flight load factors represent the ratio of the aerodynamic force component (acting normal to the assumed longitudinal axis of the airplane) to the weight of the airplane. A positive load factor is one in which the aerodynamic force acts upward with respect to the airplane. Considering compressibility effects at each speed, compliance with the flight load requirements of this subpart must be shown.

At each critical altitude within the range of altitudes selected by the applicant; At each weight from the design minimum weight to the design maximum weight appropriate to each particular flight load condition;

And For each required altitude and weight, for any practicable distribution of disposable load within the operating limitations recorded in the Airplane Flight Manual. Enough points on and within the boundaries of the design envelope must be investigated to ensure that the maximum load for each part of the airplane structure is obtained. The significant forces acting on the airplane must be placed in equilibrium in a rational or conservative manner. The linear inertia forces must be considered in equilibrium with the

thrust and all aerodynamic loads, while the angular (pitching) inertia forces must be considered in equilibrium with thrust and all aerodynamic moments, including moments due to loads on components such as tail surfaces and nacelles. Critical thrust values in the range from zero to maximum continuous thrust must be considered.

Current floor beam was analyzed for 8 load cases:

Load Case #1 and #7 (Far 25.365. Pressurized compartment loads).

The airplane structure must be strong enough to withstand the flight loads combined with pressure differential loads from zero up to the maximum relief valve setting.

The external pressure distribution in flight, and stress concentrations and fatigue effects must be accounted for.

If landings may be made with the compartment pressurized, landing loads must be combined with pressure differential loads from zero up to the maximum allowed during landing.

The airplane structure must be designed to be able to withstand the pressure differential loads corresponding to the maximum relief valve setting multiplied by a factor of 1.33 for airplanes to be approved for operation to 45,000 feet or by a factor of 1.67 for airplanes to be approved for operation above 45,000 feet, omitting other loads.

Any structure, component or part, inside or outside a pressurized compartment, the failure of which could interfere with continued safe flight and landing, must be designed to withstand the effects of a sudden release of pressure through an opening in any compartment at any operating altitude resulting from each of the following conditions:

The penetration of the compartment by a portion of an engine following an engine disintegration;

Any opening in any pressurized compartment up to the size  $H_0$  in square feet; however, small compartments may be combined with an adjacent pressurized compartment and both considered as a single compartment for openings that cannot reasonably be expected to be confined to the small compartment.

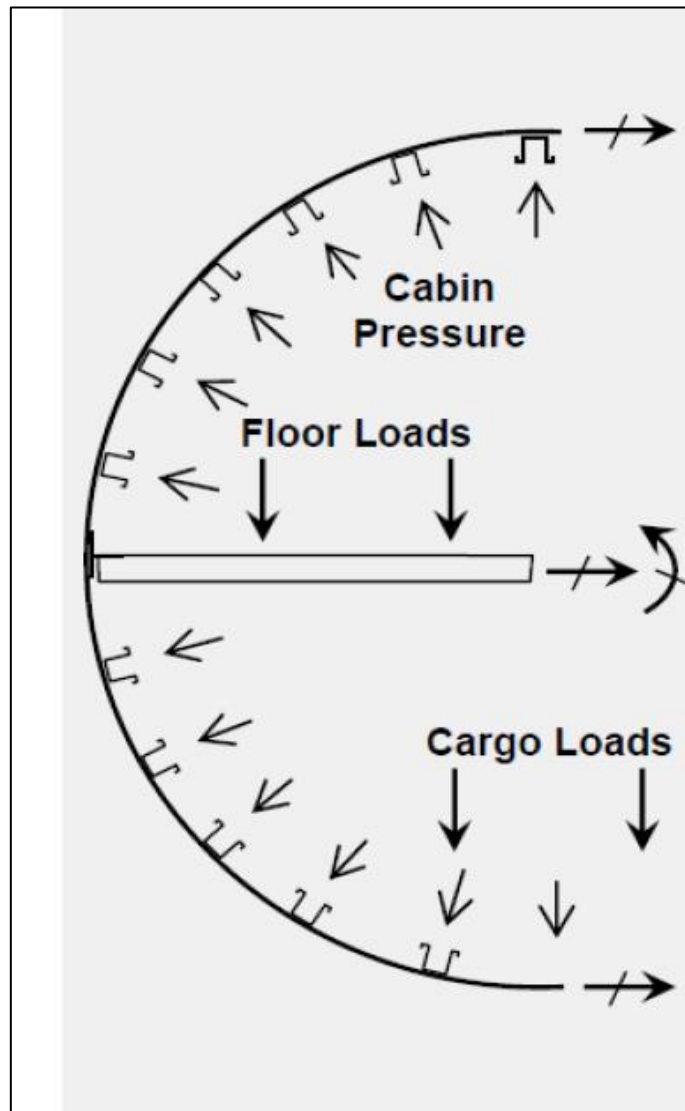


Figure 1.2 - Load case #1

The maximum opening caused by airplane or equipment failures not shown to be extremely improbable.

In complying with paragraph (e) of this section, the fail-safe features of the design may be considered in determining the probability of failure or penetration and probable size of openings, provided that possible improper operation of closure devices and inadvertent door openings are also considered. Furthermore, the resulting differential pressure loads must be combined in a rational and conservative manner with 1-g level flight loads and any loads arising from emergency depressurization conditions. These loads may be considered as ultimate conditions; however, any deformations associated with these conditions must

not interfere with continued safe flight and landing. The pressure relief provided by intercompartment venting may also be considered.

Bulkheads, floors, and partitions in pressurized compartments for occupants must be designed to withstand the conditions specified in paragraph (e) of this section. In addition, reasonable design precautions must be taken to minimize the probability of parts becoming detached and injuring occupants while in their seats.

LC 1: 18.8psi axial P=6807 lbs								
BL in	0	11.33	33.99	64.75	75.92	97	98.58	115.96
V lbs	17	26	23	8	-8	-8	-987	-987
M lbs*in	-3319	-3219	-2544	-3576	-3492	-3334	-1854	15296

Figure 1.3 - Load for load case #1

LC 7: 2.78psi UP P=5004 lbs								
BL in	0	11.33	33.99	64.75	75.92	97	98.58	115.96
V lbs	-252	1147	1799	-2799	-4296	-4296	2996	2444
M lbs*in	-112100	-109598	-83604	-2432	28823	119372	111807	59760

Figure 1.4 - Load for load case #7

Load Case #2 , #3 and #8 (Far 25.561. General).

The airplane, although it may be damaged in emergency landing conditions on land or water, must be designed as prescribed in this section to protect each occupant under those conditions. The structure must be designed to give each occupant every reasonable chance of escaping serious injury in a minor crash landing when:

- Proper use is made of seats, belts, and all other safety design provisions;
- The wheels are retracted (where applicable).

LC 2: 6.0 g DOWN P=-1640 lbs								
BL in	0	11.33	33.99	64.75	75.92	97	98.58	115.96
V lbs	197	-1112	-1734	2531	3599	3599	-3661	-3661
M lbs*in	99498	97673	72546	-1505	-29655	-105529	-97602	-33992

Figure 1.5 - Load for load case #2

LC 3: 4.5 g DOWN axial P=3465 lbs								
BL in	0	11.33	33.99	64.75	75.92	97	98.58	115.96
V lbs	257	-925	-1474	2433	3653	3653	-2934	-2383
M lbs*in	125100	121845	93982	93	-36047	-138497	-129381	-61555

Figure 1.6 - Load for load case #3

LC 8: 3.0 g Up P=2865 lbs								
BL in	0	11.33	33.99	64.75	75.92	97	98.58	115.96
V lbs	277	-1697	-2626	3788	5408	5408	-4381	-4381
M lbs*in	152980	150131	111682	1765	-40554	-154543	-144317	-68197

Figure 1.7 - Load for load case #8

Load Case #4,#5,#6 (Far 25.341. Gust and turbulence loads).

The airplane is assumed to be subjected to symmetrical vertical and lateral gusts in level flight. Limit gust loads must be determined in accordance with the provisions:

- Loads on each part of the structure must be determined by dynamic analysis. The analysis must take into account unsteady aerodynamic characteristics and all significant structural degrees of freedom including rigid body motions.
- A sufficient number of gust gradient distances in the range 30 feet to 350 feet must be investigated to find the critical response for each load quantity.
- The following reference gust velocities apply:
  - At airplane speeds between VB and VC: Positive and negative gusts with reference gust velocities of 56.0 ft/sec EAS must be

considered at sea level. The reference gust velocity may be reduced linearly from 56.0 ft/sec EAS at sea level to 44.0 ft/sec EAS at 15,000 feet. The reference gust velocity may be further reduced linearly from 44.0 ft/sec EAS at 15,000 feet to 20.86 ft/sec EAS at 60,000 feet.

- At the airplane design speed  $V_D$ : The reference gust velocity must be 0.5 times the value obtained under § 25.341(a)(5)(i).

When a stability augmentation system is included in the analysis, the effect of any significant system nonlinearities should be accounted for when deriving limit loads from limit gust conditions.

Continuous turbulence design criteria. The dynamic response of the airplane to vertical and lateral continuous turbulence must be taken into account. The dynamic analysis must take into account unsteady aerodynamic characteristics and all significant structural degrees of freedom including rigid body motions. The limit loads must be determined for all critical altitudes, weights, and weight distributions as specified in § 25.321(b), and all critical speeds within the ranges indicated in § 25.341(b)(3).

Supplementary gust conditions for wing-mounted engines. For airplanes equipped with wing-mounted engines, the engine mounts, pylons, and wing supporting structure must be designed for the maximum response at the nacelle center of gravity derived from the following dynamic gust conditions applied to the airplane:

- A discrete gust determined in accordance with § 25.341(a) at each angle normal to the flight path, and separately;
- A pair of discrete gusts, one vertical and one lateral. The length of each of these gusts must be independently tuned to the maximum response in accordance with § 25.341(a). The penetration of the airplane in the combined gust field and the phasing of the vertical and lateral component gusts must be established to develop the maximum response to the gust pair.

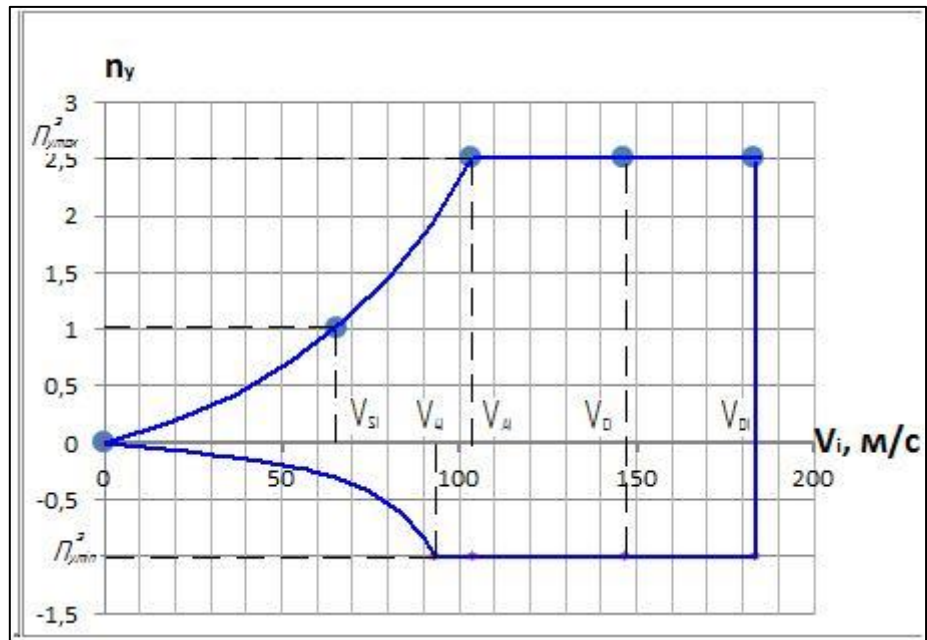


Figure 1.8 - Typical view of Envelopes of flight modes during maneuvering overloads.

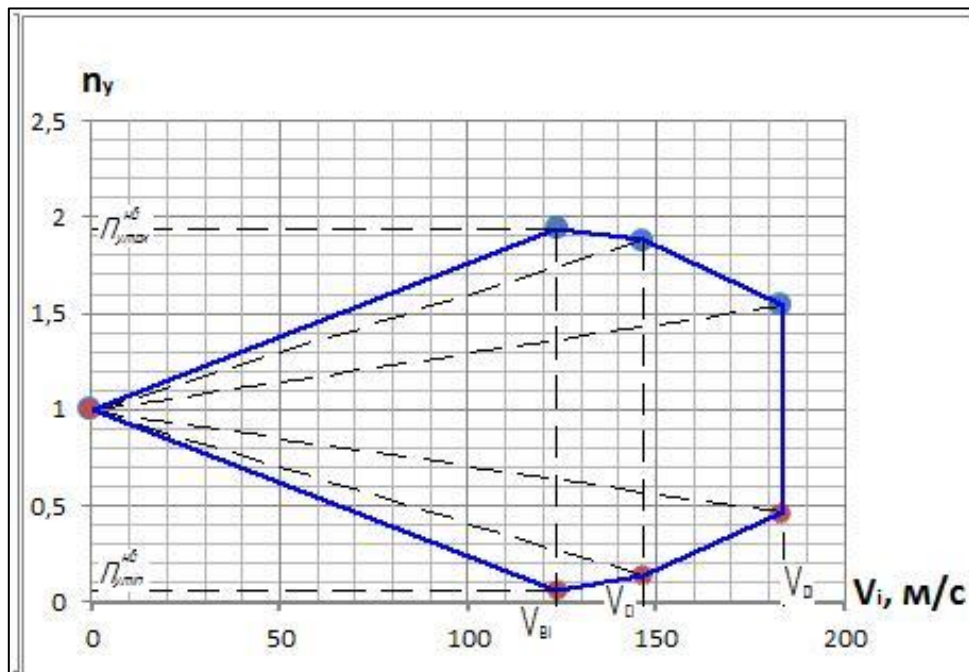


Figure 1.9 - Typical view of Envelopes flying in turbulent air.

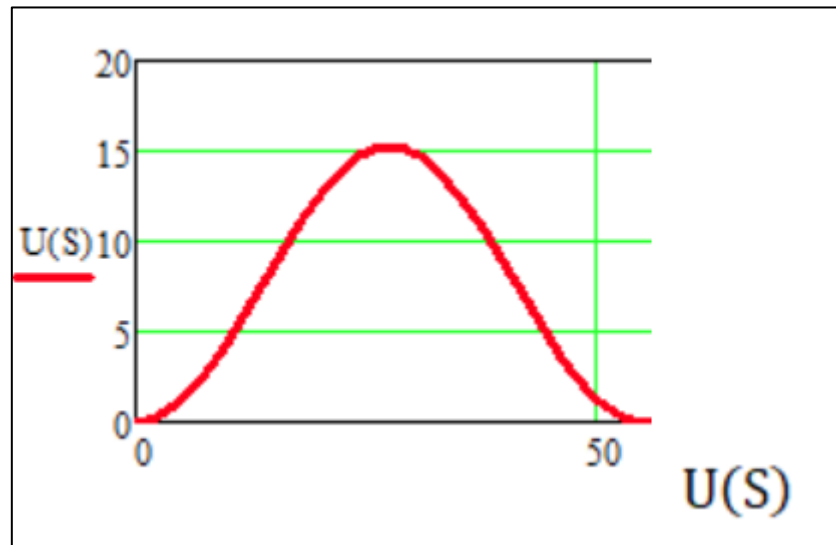


Figure 1.10 - Typical view of rush shape.

LC 4: 1.0g DOWN+2.09psi P=1134 lbs								
BL in	0	11.33	33.99	64.75	75.92	97	98.58	115.96
V lbs	-7	1278	1895	-2180	-3835	-3835	2668	2668
M lbs*in	-100551	-100668	-71755	-5828	18487	99283	91555	45191

Figure 1.11 - Load for load case #4

LC 5: 1.0g DOWN+2.09psi P=-1476 lbs								
BL in	0	11.33	33.99	64.75	75.92	97	98.58	115.96
V lbs	-7	1278	1895	-2180	-3835	-3835	2668	2668
M lbs*in	-100551	-100668	-71755	-5828	18487	99283	91555	45191

Figure 1.12 - Load for load case #5

LC 6: 2,0 g UP+14.1psi P=7008 lbs								
BL in	0	11.33	33.99	64.75	75.92	97	98.58	115.96
V lbs	-246	1157	1807	-2801	-4299	-4299	2616	2065
M lbs*in	-113373	-110798	-84580	-3776	27483	118093	111098	65526

Figure 1.13 - Load for load case #6

### 3 Freebody diagram and determination of analyzed cross section.

A free body diagram for a beam is a beam with elastic restrains.

It is assumed that the beam is loaded with concentrated forces coming from the so-called. seat tracks - longitudinal power elements of the airplane floor to which passenger seats are attached.

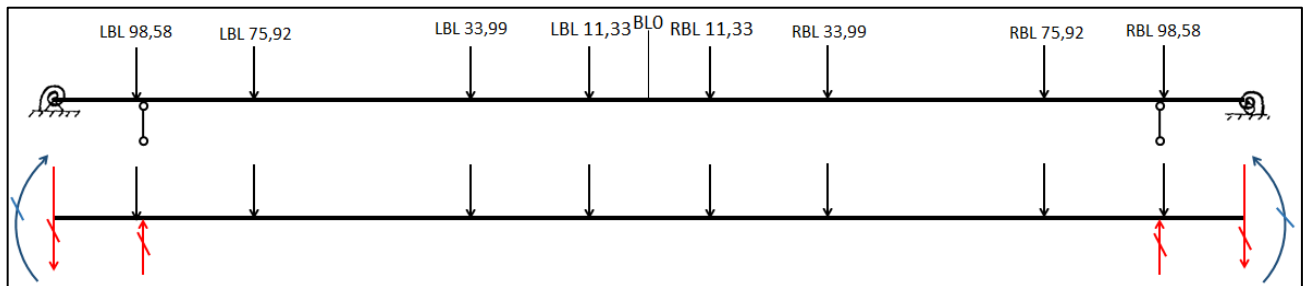


Figure 3.1 Freebody diagram for floor beam

Bending moment diagrams Fig 3.2 and shear force diagrams Fig 3.3 for each LC.

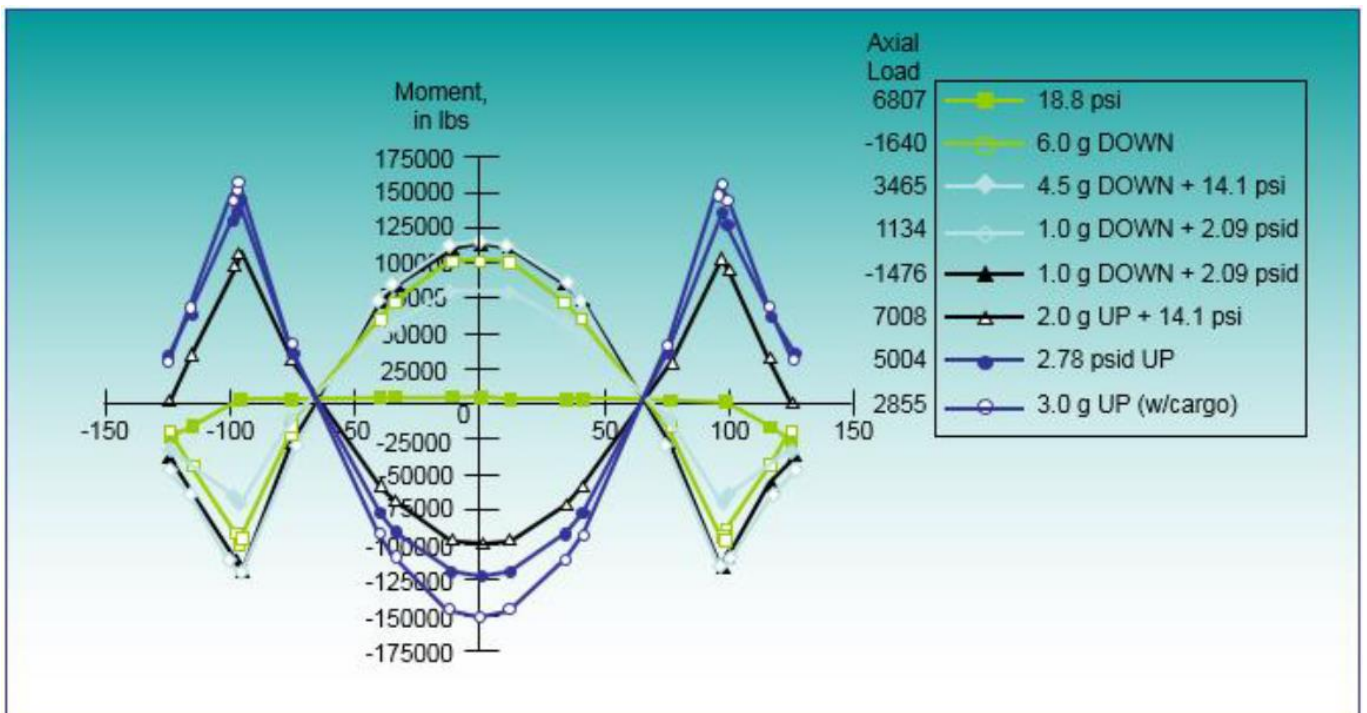


Figure.3.2 – Bending moment diagram

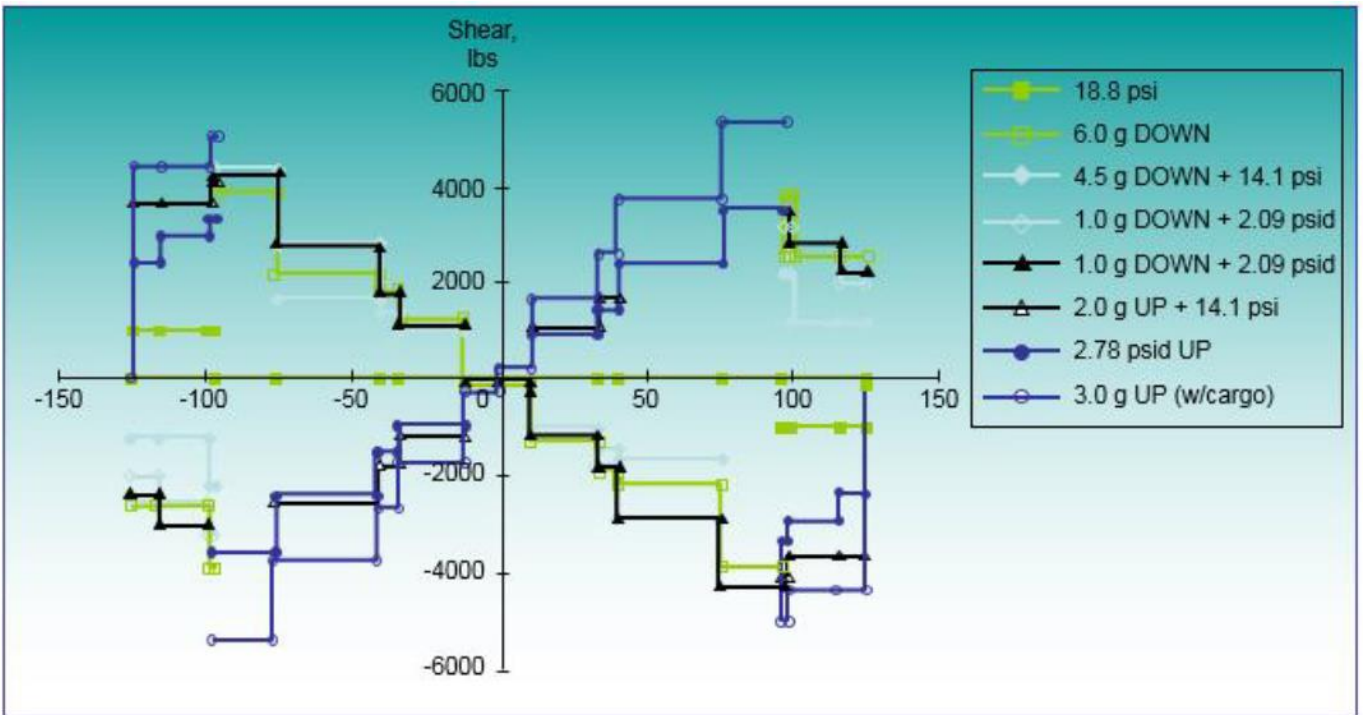


Figure.3.3 – Shear force diagram

On figure 3.4 is showing six zone which will be analyzed in current analysis. For this zone will be taken loads that are more critical for this zones from figures 3.2 and 3.3.

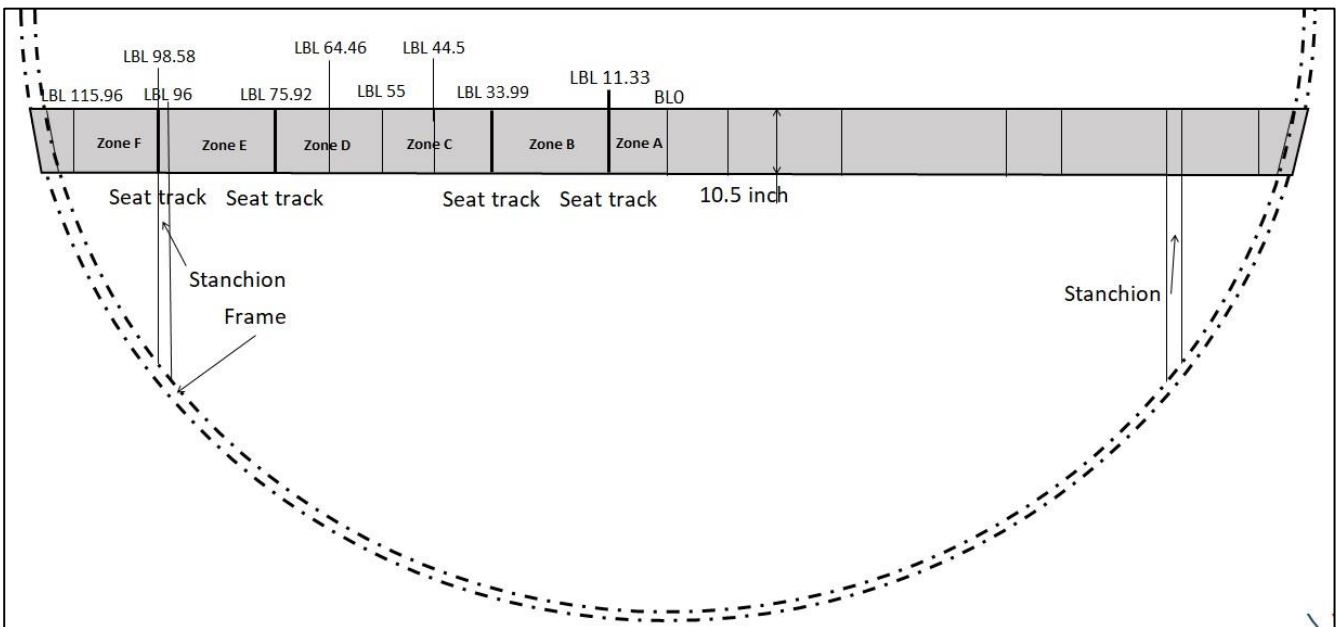


Figure.3.4 – Analyzed zones

The beam made of aluminum alloy 7075-T651.

Table 3.1 – Mechanical properties 7075-T651

Form	Plate
Temper	T651
Ultimate Tensile Stress (Psi)	$F_{tu(L)}=78000$ (Psi) $F_{tu(LT)}=79000$ (Psi)
Yield Compressive Stress (Psi)	$F_{tu(L)}=68000$ (Psi) $F_{tu(LT)}=73000$ (Psi)
Ultimate Shear Stress (Psi)	$F_{su}=45000$ (Psi)
Yield Tensile Stress (Psi)	$F_{ty(L)}=71000$ (Psi)
Yield Shear Stress (Psi)	$F_{su}=40962$ (Psi)
Ultimate Bearing Stress (Psi)	$F_{bru}=147000$ (Psi)
Yield Bearing Stress (Psi)	$F_{brv}=120000$ (Psi)
Elastic modulus for Tension (Psi)	$E=10300000$ (Psi)
Elastic modulus for Compression (Psi)	$E_c=10600000$ (Psi)
Poisson Ratio	$\mu=0.33$
Material shape parameter	$n=19$

Material properties for Table 3.1 taken form figure 3.4

Specification	AMS 4045 and AMS-QQ-A-250/12 <sup>a</sup>																				
	Sheet									Plate											
	T6 and T62 <sup>b</sup>									T651											
Form																					
Temper																					
Thickness, in.																					
	0.008-0.011	0.012-0.039	0.040-0.125	0.126-0.249	0.250-0.499	0.500-1.000	1.001-2.000	2.001-2.500	2.501-3.000	3.001-3.500	3.501-4.000										
Basis																					
	S	A	B	A	B	A	B	A	B	A	B	A	B	A	B	A	B	A	B		
Mechanical Properties:																					
$F_{up}$ , ksi:																					
L	...	76	78	78	80	78	80	77	79	77	79	76	78	75	77	71	73	70	72	66	68
LT	74	76	78	78	80	78	80	78	80	78	80	77	79	76	78	72	74	71	73	67	69
ST	...	...	...	...	...	...	...	...	...	...	...	...	...	70 <sup>c</sup>	71 <sup>c</sup>	66 <sup>c</sup>	68 <sup>c</sup>	65 <sup>c</sup>	67 <sup>c</sup>	61 <sup>c</sup>	63 <sup>c</sup>
$F_{yp}$ , ksi:																					
L	...	69	72	70	72	71	73	69	71	70	72	69	71	66	68	63	65	60	62	56	58
LT	63	67	70	68	70	69	71	67	69	68	70	67	69	64	66	61	63	58	60	54	56
ST	...	...	...	...	...	...	...	...	...	...	...	...	...	59 <sup>c</sup>	61 <sup>c</sup>	56 <sup>c</sup>	58 <sup>c</sup>	54 <sup>c</sup>	55 <sup>c</sup>	50 <sup>c</sup>	52 <sup>c</sup>
$F_{cp}$ , ksi:																					
L	...	68	71	69	71	70	72	67	69	68	70	66	68	62	64	58	60	55	57	51	52
LT	...	71	74	72	74	73	75	71	73	72	74	71	73	68	70	65	67	61	64	57	59
ST	...	...	...	...	...	...	...	...	...	...	...	...	...	67	70	64	66	61	63	57	59
$F_{br}$ , ksi:																					
(e/D = 1.5)	...	118	121	121	124	121	124	117	120	117	120	116	119	114	117	108	111	107	110	101	104
(e/D = 2.0)	...	152	156	156	160	156	160	145	148	145	148	143	147	141	145	134	137	132	135	124	128
$F_{br}$ , ksi:																					
(e/D = 1.5)	...	100	105	102	105	103	106	97	100	100	103	100	103	98	101	94	97	89	93	84	87
(e/D = 2.0)	...	117	122	119	122	121	124	114	118	117	120	117	120	113	117	109	112	104	108	98	103
e, percent (S-Basis):																					
LT	5	7	...	8	...	8	...	9	...	7	...	6	...	5	...	5	...	5	...	3	...
$E$ , 10 <sup>3</sup> ksi	10.3																				
$E_c$ , 10 <sup>3</sup> ksi	10.5																				
$G$ , 10 <sup>3</sup> ksi	3.9																				
$\mu$	0.33																				
Physical Properties:																					
$\omega$ , lb/in. <sup>3</sup>	0.101																				
C, K, and $\alpha$	See Figure 3.7.7.0																				

a Mechanical properties were established under MIL-QQ-A-250/12.  
 b Design allowables were based upon data obtained from testing T6 temper sheet and from testing samples of sheet, supplied in the O or F temper, which were heat treated to demonstrate response to heat treatment by suppliers. Properties obtained by the user may be lower than those listed if the material has been formed or otherwise cold-worked, particularly in the annealed temper, prior to solution heat treatment.  
 c Caution: This specific alloy, temper, and product form exhibits poor stress-corrosion cracking resistance in this grain direction. It corresponds to an SCC resistance rating of D, as indicated in Table 3.1.2.3.1(a).  
 d Bearing values are "dry pin" values per Section 1.4.7.1. See Table 3.1.2.1.1.

Figure.3.4 - The main mechanical characteristics of the material 7075-T651 [4]

## 4 Normal and shear stress finding

In general, a structural member that supports loads perpendicular to its longitudinal axis is referred to as a beam. The structure of aircraft provides excellent examples of beam units, such as the wing and fuselage. Very seldom do bending forces act alone on a <sup>major</sup> aircraft structural unit, but are accompanied by axial and torsional forces. However, the bending forces and the resulting beam stresses due to bending of the beam are usually of primary importance in the design of the beam structure.

Typical cross-section view and sizes are shown on figure 4.1.

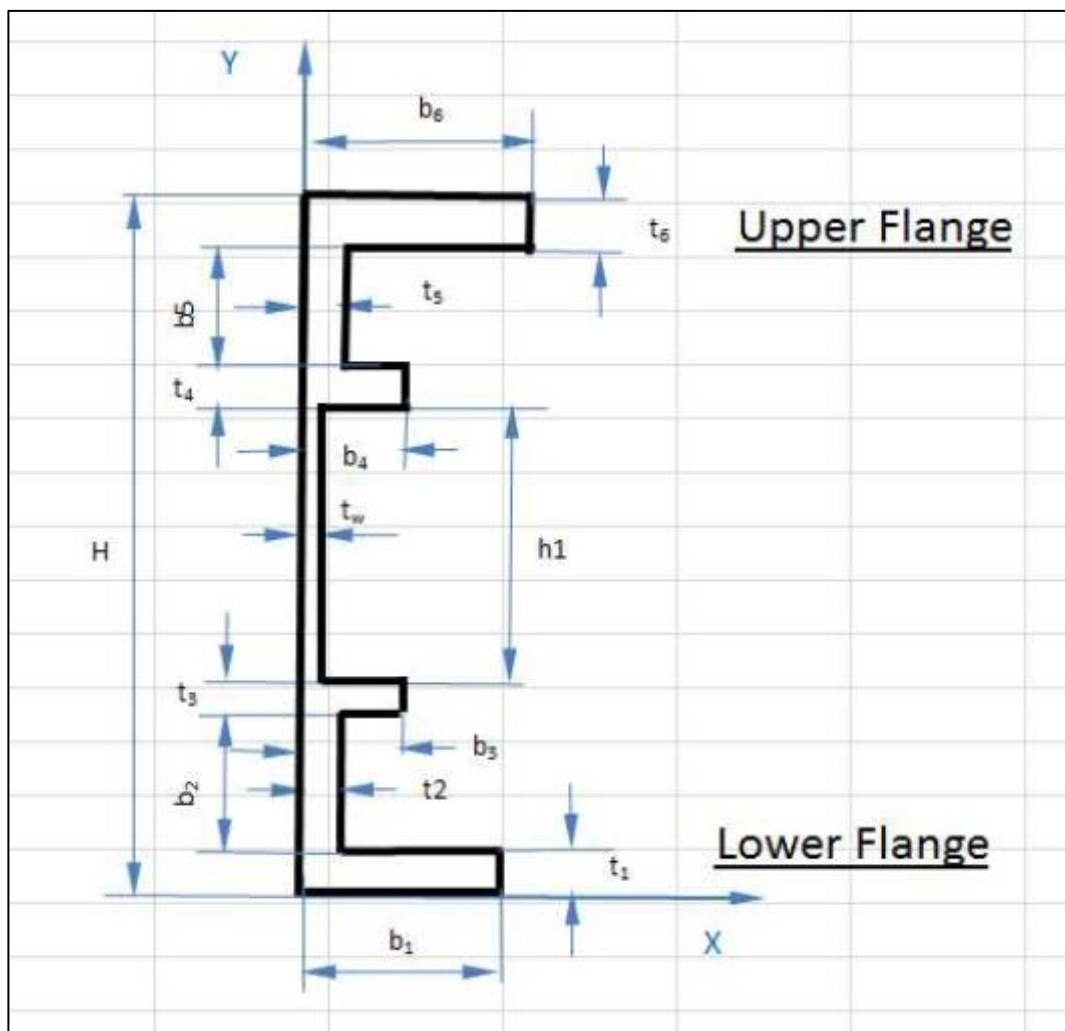


Figure.4.1 - Typical cross-section view and sizes.

The following formulas are used to determine the stresses acting on any structure.

Normal stresses from the action of axial force [1]:

$$f = \frac{P}{A} \quad (4.1)$$

Where:

F - normal stresses in section;

P- axial force that acts on the section;

A - cross-sectional area.

Typical equation for finding normal stress:

$$f_b = -\frac{M_x}{I_x}y + \frac{M_y}{I_y}x + \frac{M_z}{F} \quad (4.2)$$

where  $f_b$  - normal stresses in section;

$M_y$  - bending moment relative to the y-axis;

$M_x$  - bending moment relative to the x-axis;

$I_x$  - axial moment of inertia of the section relative to the x-axis;

$I_y$  - axial moment of inertia of the section relative to the y-axis;

$I_{xy}$  - centrifugal moment of inertia of the section;

x - coordinate x of the point at which the stresses are calculated;

y - coordinate y of the point at which the stresses are calculated.

Beam cross-sections are not symmetrical, so below shown equation for finding normal stress for this case:

$$f_b = -\frac{M_x \cdot I_{xy} + M_y \cdot I_x}{I_x \cdot I_y - I_{xy}^2} \cdot X + \frac{M_y \cdot I_{xy} + M_x \cdot I_y}{I_x \cdot I_y - I_{xy}^2} \cdot Y \quad (4.3)$$

Typical equation for calculation shear stress:

$$f_s = \frac{VQ}{Ib} \quad (4.4)$$

where

$f_s$ -tangent stresses in section;

V-value of the transverse force that the action in section;

Q-first moment (resistance moment) of the cut-off section;

I-axial moment of inertia of the entire section;

b-width of the cross-section element to the exact points where the stresses are calculated.

Beam cross-sections are not symmetrical, so below shown equation for finding normal stress for this case is given by [3]:

$$f_{sh} = \frac{Vy \cdot I_{xy} - Vx \cdot I_x}{(Ix \cdot Iy - I_{xy}^2) \cdot t} \cdot \sum Ai \cdot Xi - \frac{Vy \cdot Iy - Vx \cdot I_{xy}}{(Ix \cdot Iy - I_{xy}^2) \cdot t} \cdot \sum Ai \cdot Yi \quad (4.5)$$

The strength of the projected structure is determined according to the characteristics of the material, the shape and dimensions of the cross-section, loading conditions.

The strength of the structure is characterized by a factor of margin of safety (Margin of safety), which is determined by the formula:

$$MS = \frac{F}{f} - 1 \quad (4.6)$$

where

F - the permissible stresses, which are displayed in accordance with the material used;

f - acting in section of voltage.

All eight load cases were analyzed and found that LC 7 and LC 8 are determinative for beam size, therefore, shown only these two load cases calculations.

Bending moments for both load cases are shown on figures 4.2 and 4.3.

Bending moments for both load cases are shown on figures 4.4 and 4.5.

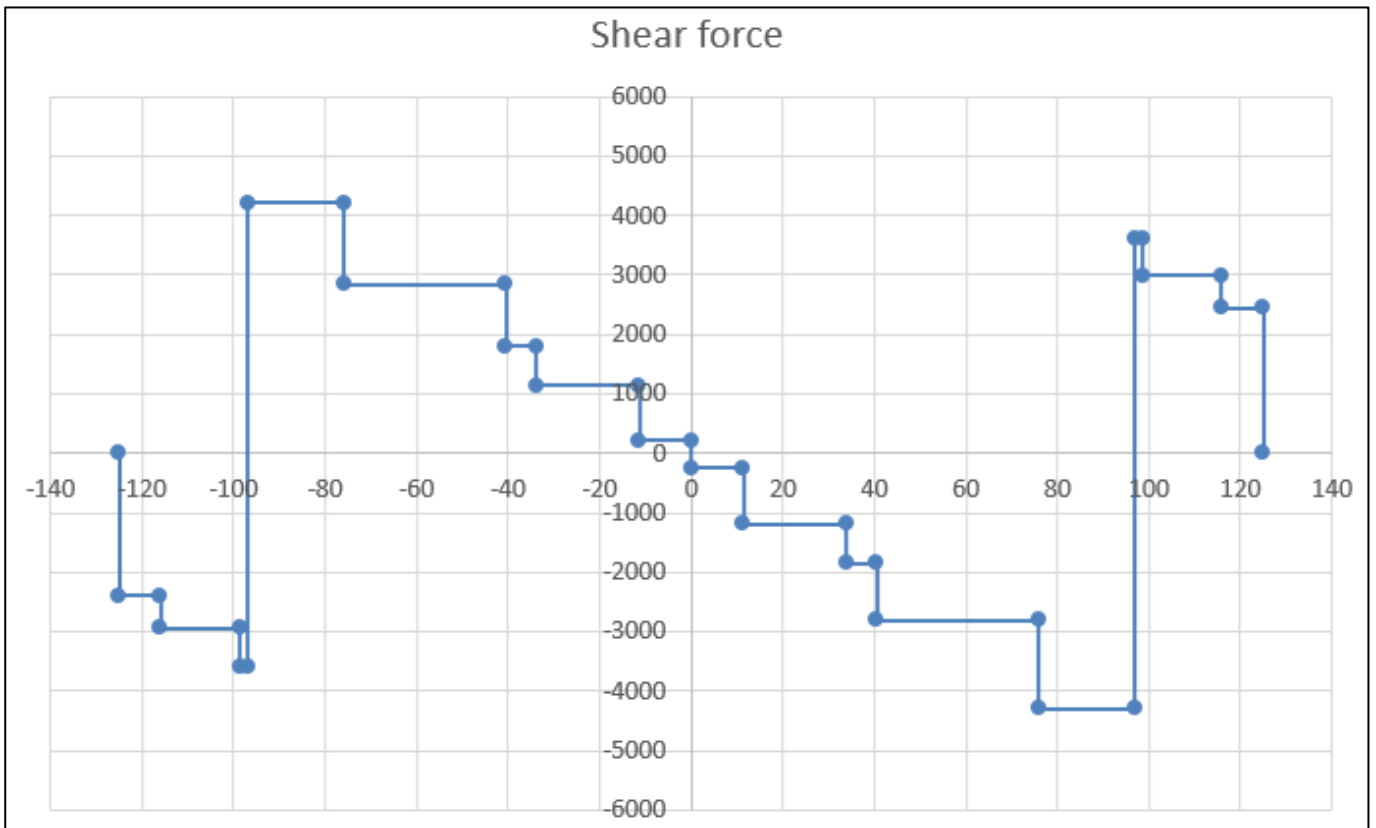


Figure.4.2 – Shear force for LC 7

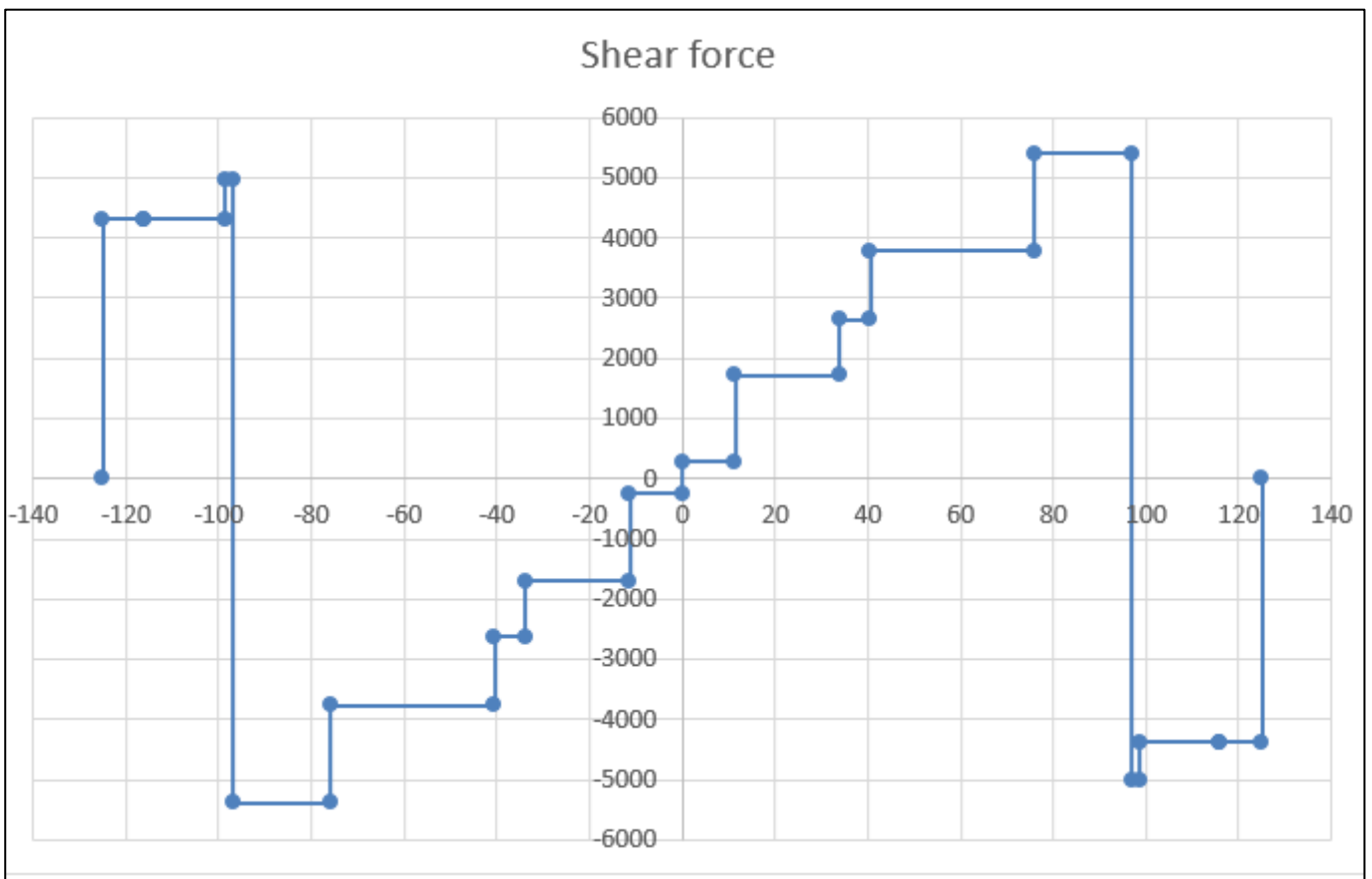


Figure.4.3 – Shear force for LC 8

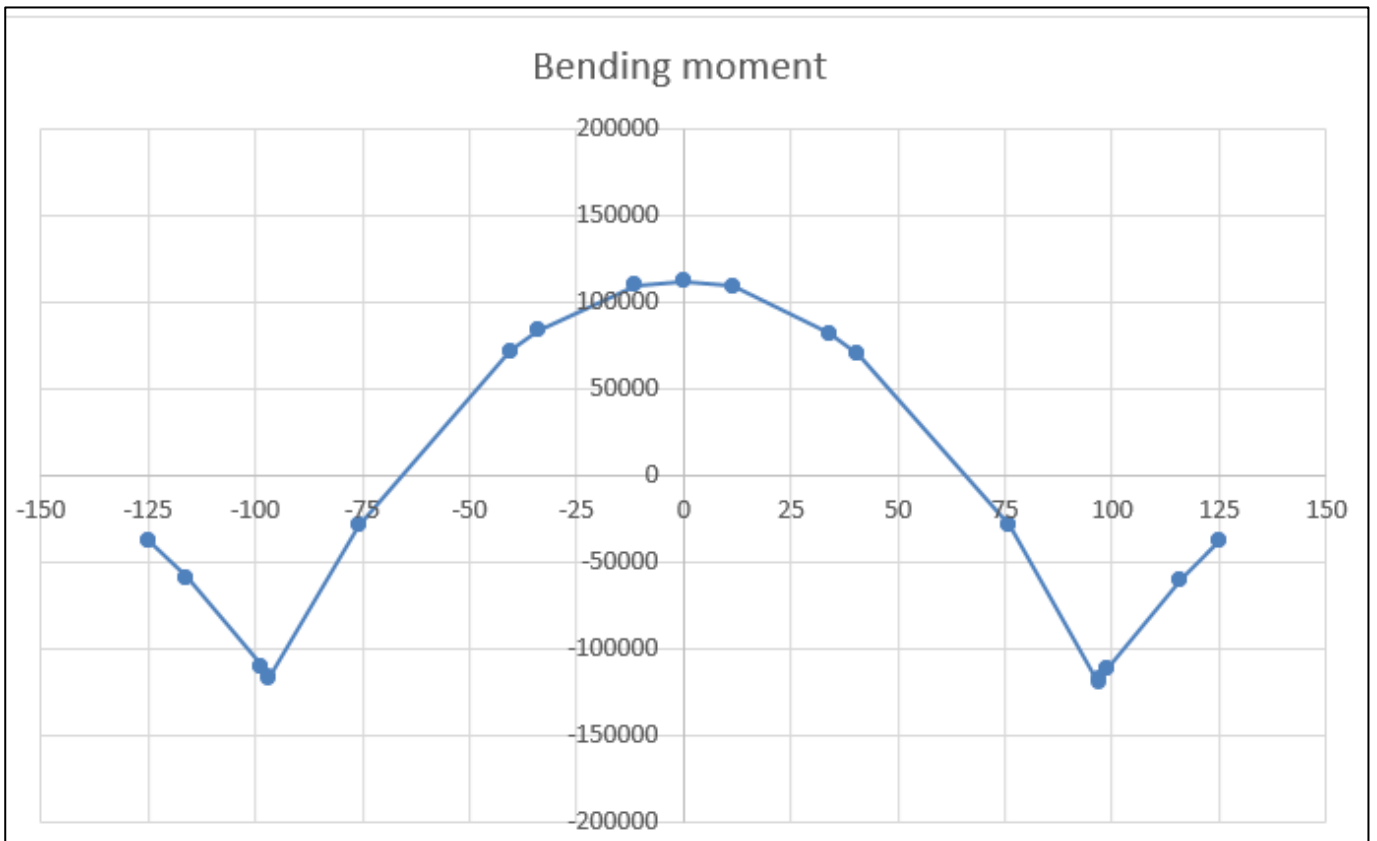


Figure.4.4 – Bending moment for LC 7

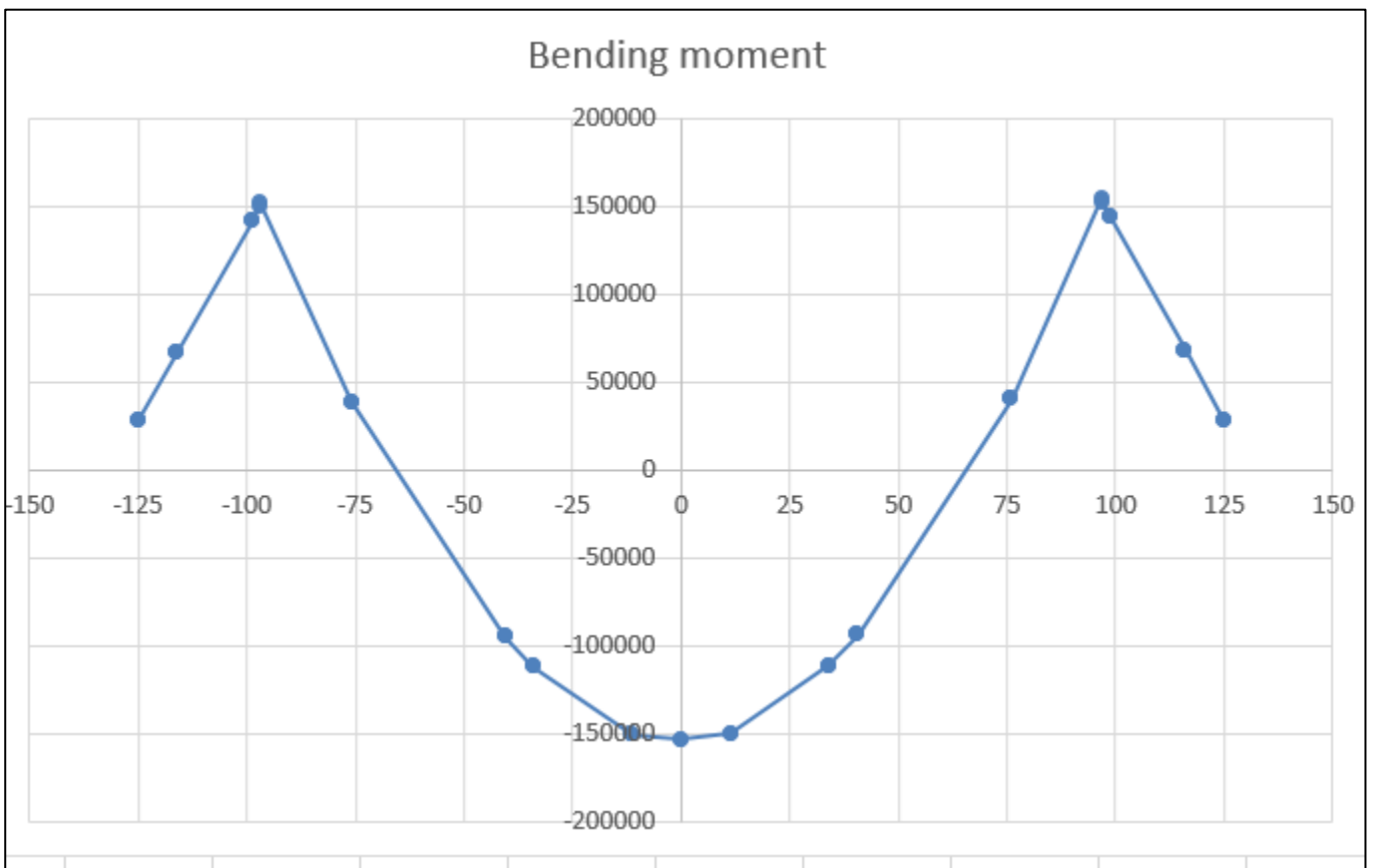


Figure.4.5 – Bending moment for LC 8

Critical load and calculated cross-section, which were determinate on figure 3.4, are shown on figure 4.6.

Cross-section	LC	7			8		
	Coordanates	V	Axial	M	V	Axial	M
A-A	0-11.33	-1191	5004	112100	1721	2855	-152980
B-B	33.99	-1844	5004	82243	2652	2855	-110854
C-C	40.55	-2799	5004	70149	3788	2855	-93455
D-D	75.92	-4296	5004	-28823	5408	2855	40554
E-E	98.58	-4296	5004	-119372	5408	2855	154543
F-F	115.96	2996	5004	-59760	-4381	2855	68197

Figure.4.6 – Loads for calculated cross-sections.

Normal and shear stress were found for several points which are shown on figure 4.7.

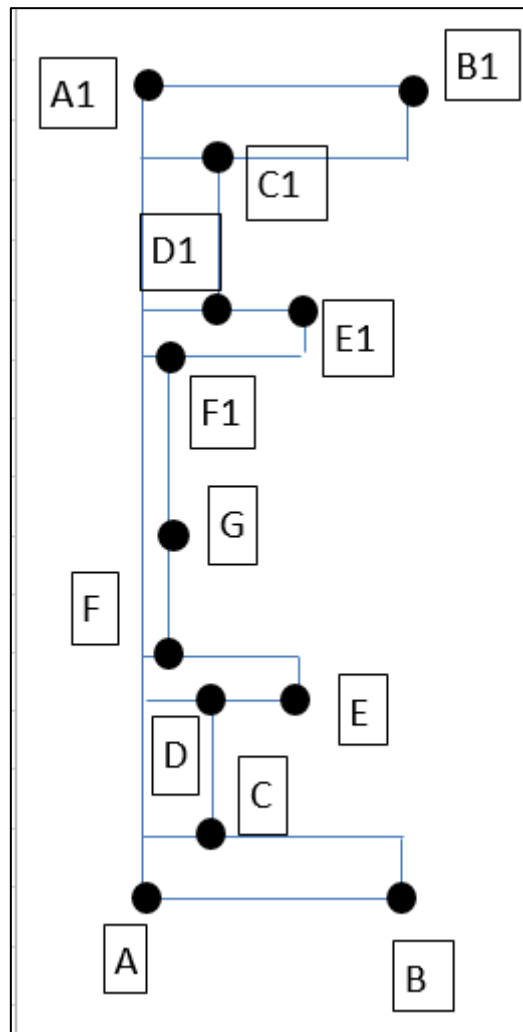


Figure.4.7 – Calculated points

Cross-sections sizes and properties for each cross-sections are shown on figures 4.8 – 4.13

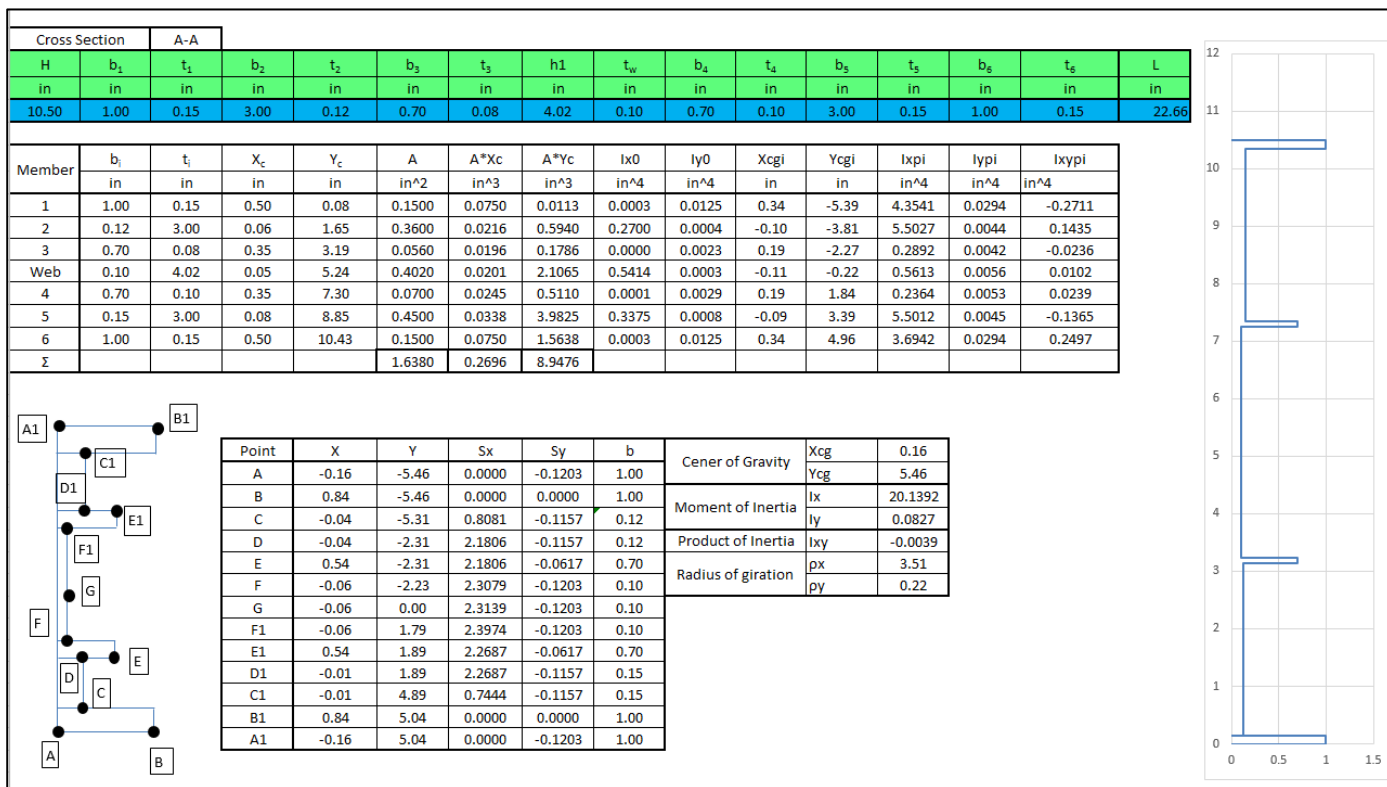


Figure.4.8 – Sizes and properties for cross-section A-A.

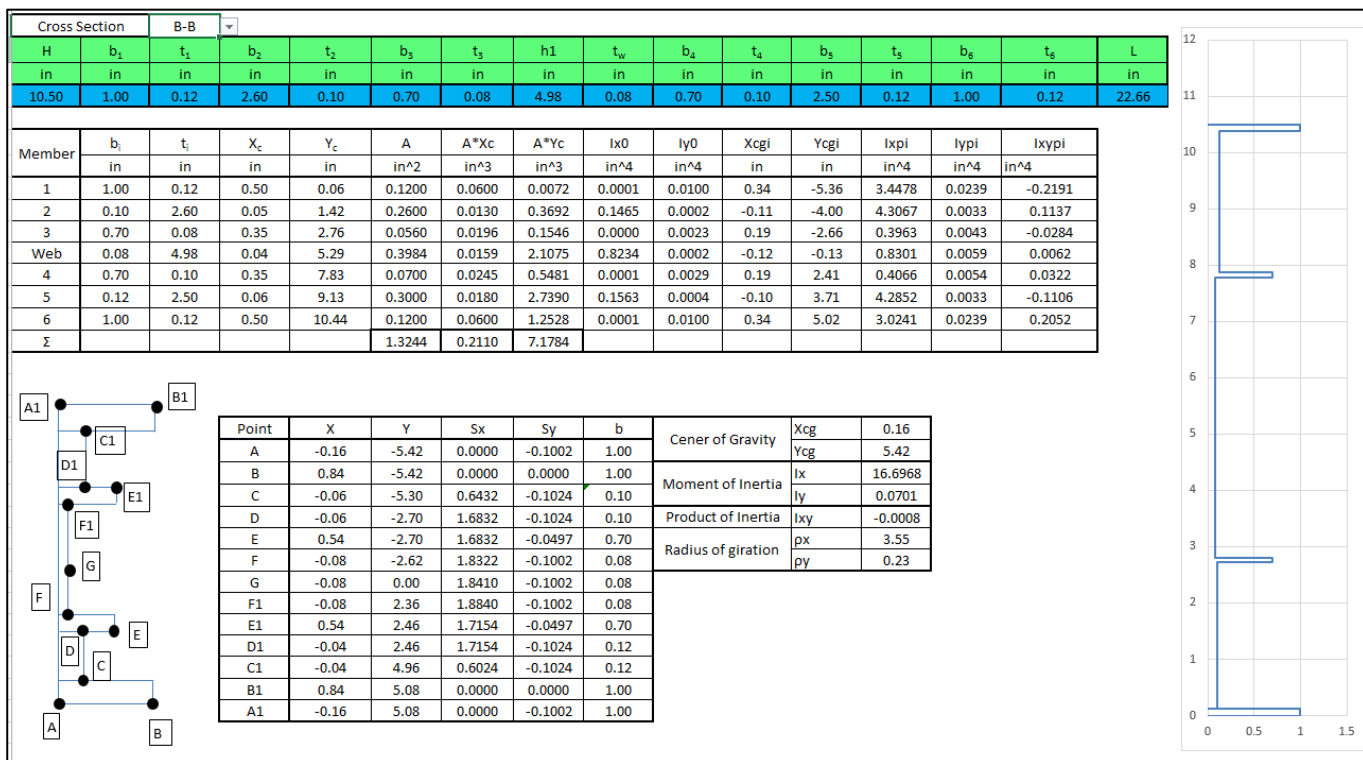


Figure.4.9 – Sizes and properties for cross-section B-B.

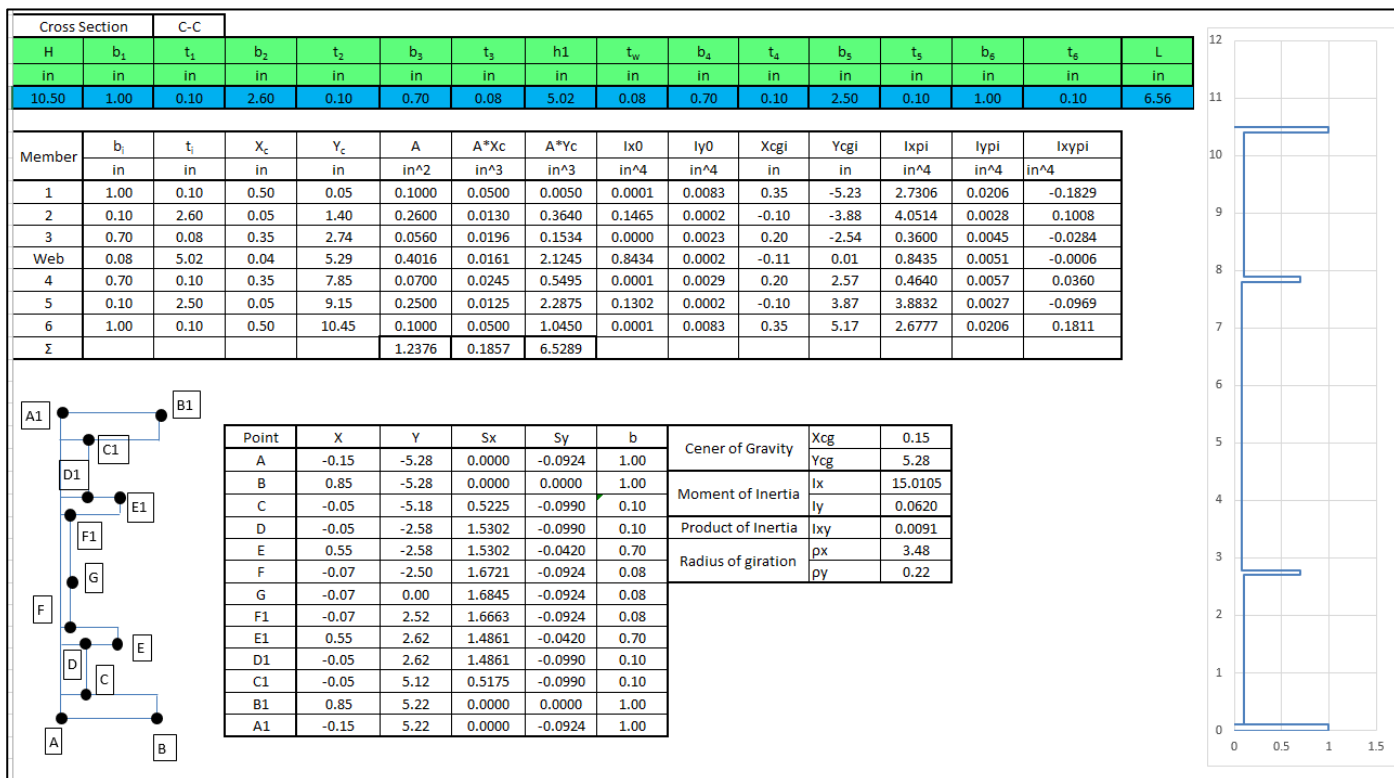


Figure.4.10 – Sizes and properties for cross-section C-C.

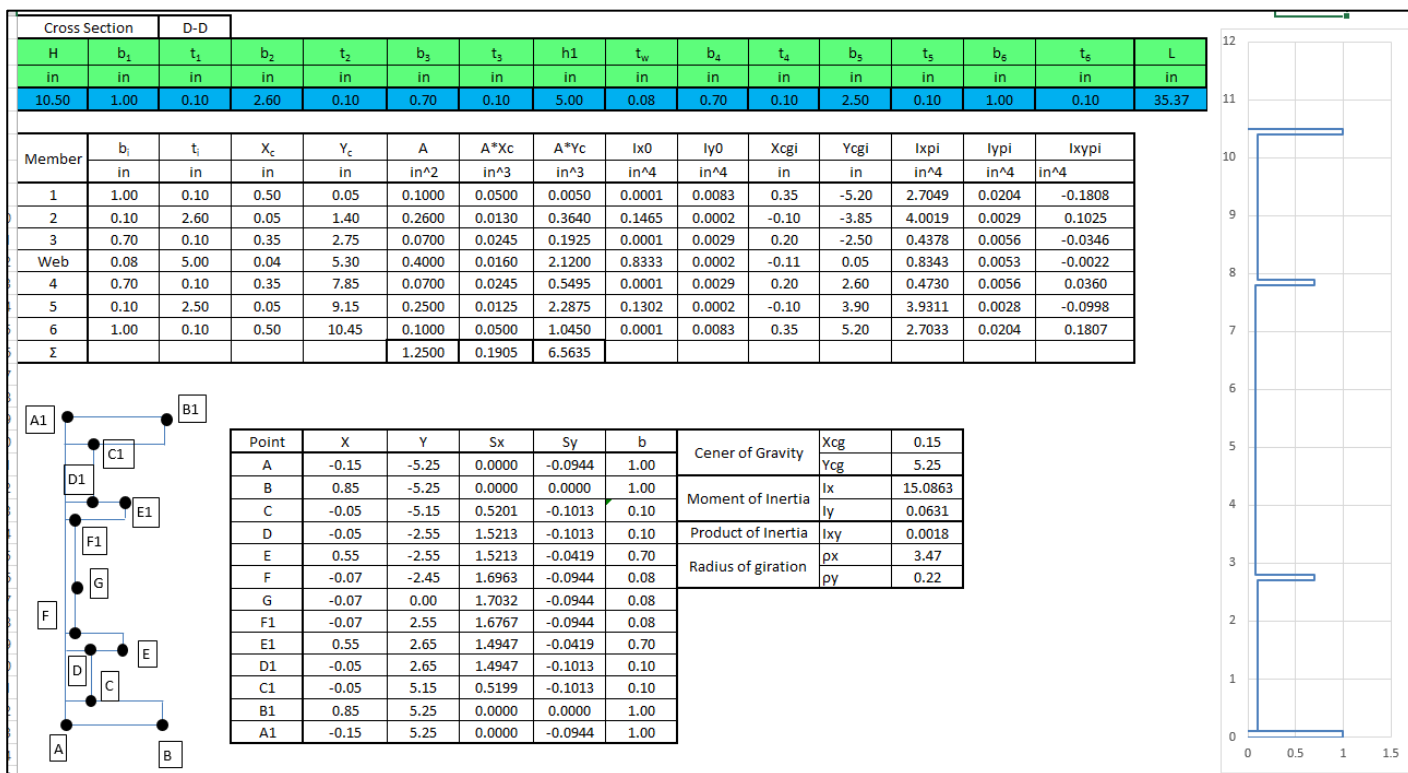


Figure.4.11 – Sizes and properties for cross-section D-D.

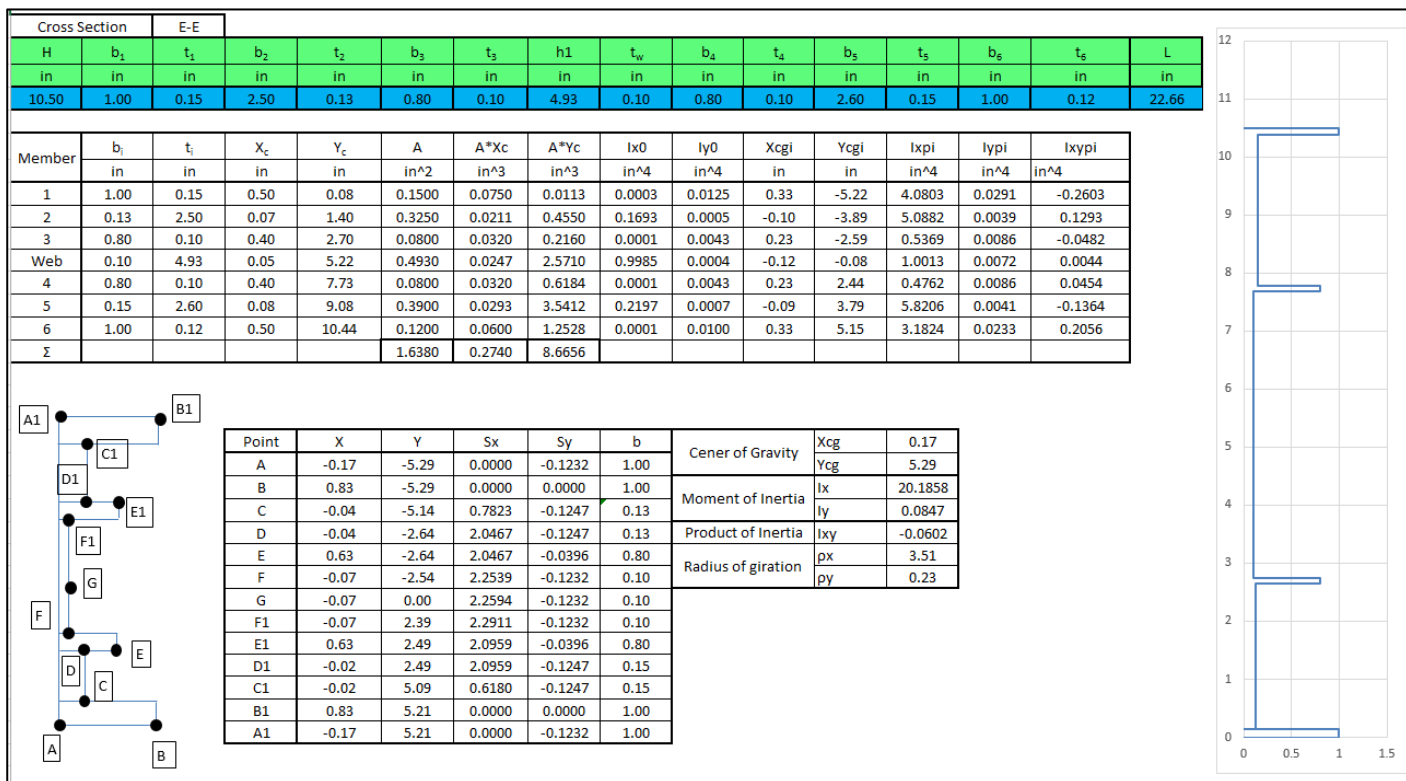


Figure.4.12 – Sizes and properties for cross-section E-E.

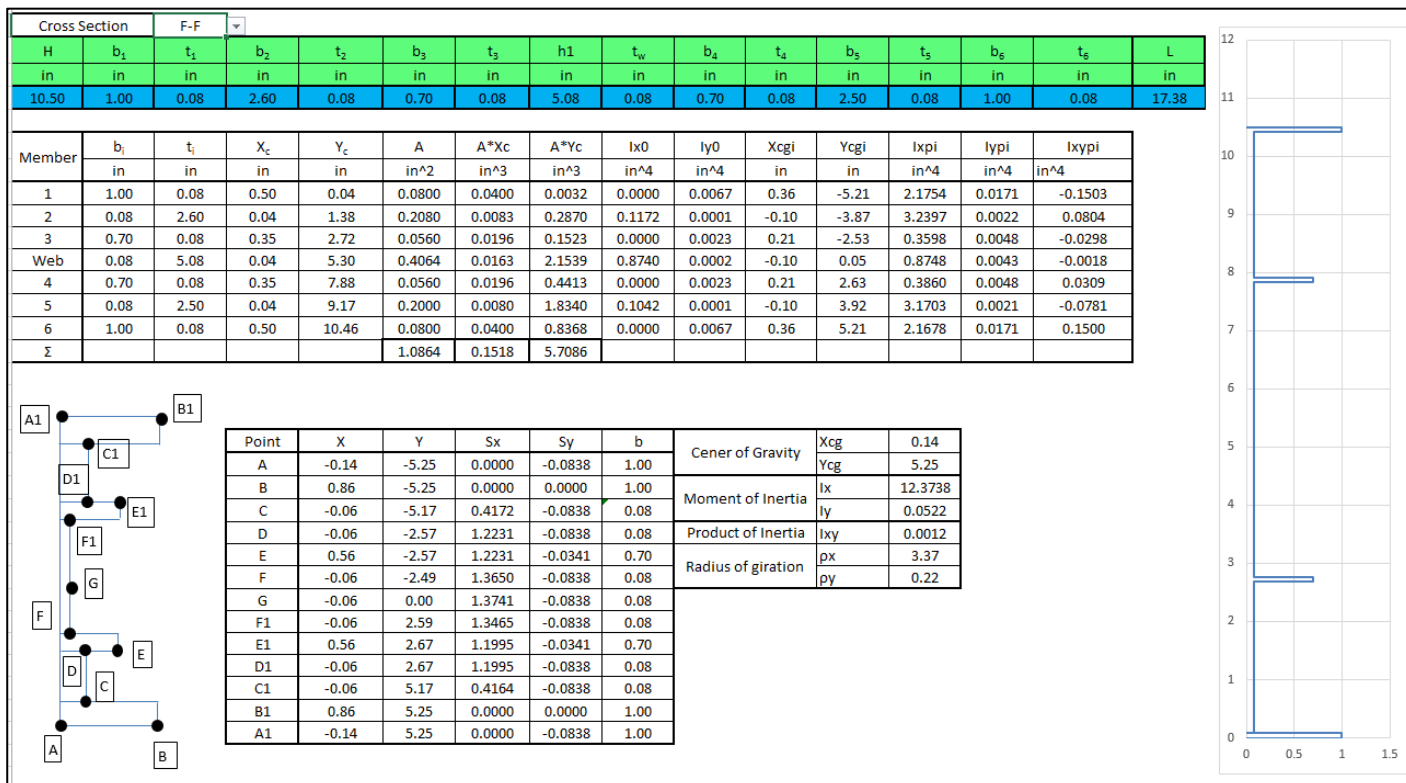


Figure.4.13 – Sizes and properties for cross-section F-F.

Normal and shear stress a for each cross-sections are shown on figures 4.14 – 4.19

LC 8				LC 7			
Loads	Vy	Px	Mx	Loads	Vy	Px	Mx
	lbs	lbs	lbs-in		lbs	lbs	lbs-in
	1721	2855	-152980		-1191	5004	112100

Point	Normal			Shear	Lower flange	Point	Normal			Shear
	Axial	Bending	Total				Axial	Bending	Total	
A	1743	41553	43296	0		A	3055	-30449	-27394	0
B	1743	41195	42938	0		B	3055	-30187	-27132	0
C	1743	40371	42114	579		C	3055	-29583	-26528	-401
D	1743	17582	19325	1557		D	3055	-12884	-9829	-1077
E	1743	17375	19118	267		E	3055	-12732	-9677	-184
F	1743	16982	18725	1977		F	3055	-12444	-9389	-1368
G	1743	23	1766	1982		G	3055	-17	3038	-1372
F1	1743	-13555	-11812	2054		F1	3055	9933	12988	-1421
E1	1743	-14529	-12786	277	E1	3055	10647	13702	-192	
D1	1743	-14332	-12589	1296	D1	3055	10502	13557	-897	
C1	1743	-37121	-35378	427	C1	3055	27201	30256	-296	
B1	1743	-38565	-36822	0	B1	3055	28259	31314	0	
A1	1743	-38207	-36464	0	A1	3055	27997	31052	0	
					Upper flange					

Figure.4.14 – Normal and shear stress for cross-section A-A

LC 8				LC 7			
Loads	Vy	Px	Mx	Loads	Vy	Px	Mx
	lbs	lbs	lbs-in		lbs	lbs	lbs-in
	2652	2855	-110854		-1844	5004	82243

Point	Normal			Shear	Lower flange	Point	Normal			Shear
	Axial	Bending	Total				Axial	Bending	Total	
A	2156	35998	38153	0		A	3778	-26707	-22928	0
B	2156	35921	38077	0		B	3778	-26650	-22872	0
C	2156	35193	37349	1024		C	3778	-26110	-22332	-712
D	2156	17931	20087	2675		D	3778	-13303	-9525	-1860
E	2156	17885	20041	382		E	3778	-13269	-9491	-266
F	2156	17402	19557	3640		F	3778	-12910	-9132	-2531
G	2156	6	2162	3657		G	3778	-4	3774	-2543
F1	2156	-15662	-13506	3743		F1	3778	11620	15398	-2603
E1	2156	-16373	-14217	389	E1	3778	12147	15926	-271	
D1	2156	-16329	-14173	2272	D1	3778	12114	15893	-1580	
C1	2156	-32927	-30771	799	C1	3778	24429	28207	-555	
B1	2156	-33791	-31635	0	B1	3778	25069	28848	0	
A1	2156	-33714	-31559	0	A1	3778	25013	28791	0	
					Upper flange					

Figure.4.15 – Normal and shear stress for cross-section B-B

LC 8				LC 7			
Loads	Vy	Px	Mx	Loads	Vy	Px	Mx
	lbs	lbs	lbs-in		lbs	lbs	lbs-in
	3788	2855	-93455		-2799	5004	70149

Point	Normal			Shear	Lower flange	Upper flange	Point	Normal			Shear
	Axial	Bending	Total					Axial	Bending	Total	
A	2307	32710	35017	-3	Lower flange		A	4043	-24553	-20510	3
B	2307	33627	35934	0			B	4043	-25241	-21198	0
C	2307	32179	34486	1282			C	4043	-24154	-20111	-947
D	2307	15990	18297	3825			D	4043	-12003	-7959	-2826
E	2307	16540	18847	549			E	4043	-12415	-8372	-406
F	2307	15474	17781	5232			F	4043	-11615	-7572	-3866
G	2307	-64	2243	5271			G	4043	48	4091	-3895
F1	2307	-15783	-13476	5214	Upper flange		F1	4043	11847	15891	-3853
E1	2307	-15838	-13531	534			E1	4043	11888	15931	-394
D1	2307	-16388	-14081	3714			D1	4043	12301	16344	-2744
C1	2307	-31954	-29647	1269			C1	4043	23985	28029	-938
B1	2307	-31752	-29445	0			B1	4043	23833	27877	0
A1	2307	-32668	-30361	-3			A1	4043	24521	28565	3

Figure.4.16 – Normal and shear stress for cross-section C-C

LC 8				LC 7			
Loads	Vy	Px	Mx	Loads	Vy	Px	Mx
	lbs	lbs	lbs-in		lbs	lbs	lbs-in
	5408	2855	40554		-4296	5004	-28823

Point	Normal			Shear	Lower flange	Upper flange	Point	Normal			Shear
	Axial	Bending	Total					Axial	Bending	Total	
A	2284	-14103	-11819	-1	Lower flange		A	4003	10024	14027	1
B	2284	-14180	-11896	0			B	4003	10078	14081	0
C	2284	-13842	-11558	1854			C	4003	9838	13841	-1473
D	2284	-6853	-4569	5443			D	4003	4871	8874	-4324
E	2284	-6899	-4615	778			E	4003	4903	8906	-618
F	2284	-6583	-4299	7589			F	4003	4678	8682	-6029
G	2284	6	2290	7620			G	4003	-4	3999	-6053
F1	2284	6858	9142	7501	Upper flange		F1	4003	-4874	-871	-5959
E1	2284	7079	9363	765			E1	4003	-5032	-1028	-608
D1	2284	7125	9409	5348			D1	4003	-5064	-1061	-4248
C1	2284	13846	16130	1853			C1	4003	-9841	-5837	-1472
B1	2284	14046	16330	0			B1	4003	-9983	-5979	0
A1	2284	14122	16406	-1			A1	4003	-10037	-6034	1

Figure.4.17 – Normal and shear stress for cross-section D-D

LC 8				LC 7			
Loads	Vy	Px	Mx	Loads	Vy	Px	Mx
	lbs	lbs	lbs-in		lbs	lbs	lbs-in
	5408	2855	154543		-4296	5004	-119372

Point	Normal			Shear	Lower flange	Point	Normal			Shear
	Axial	Bending	Total				Axial	Bending	Total	
A	1743	-41502	-39759	24		A	3055	32057	35112	-19
B	1743	-36048	-34305	0		B	3055	27844	30899	0
C	1743	-39642	-37899	1799		C	3055	30620	33675	-1429
D	1743	-20461	-18718	4410		D	3055	15805	18860	-3503
E	1743	-16807	-15064	696		E	3055	12982	16037	-553
F	1743	-19857	-18115	6286		F	3055	15338	18393	-4994
G	1743	-367	1376	6301		G	3055	283	3338	-5005
F1	1743	17967	19710	6386		F1	3055	-13878	-10823	-5073
E1	1743	22551	24294	713	E1	3055	-17419	-14364	-566	
D1	1743	19007	20750	3910	D1	3055	-14681	-11626	-3106	
C1	1743	38955	40698	1265	C1	3055	-30089	-27034	-1005	
B1	1743	44511	46254	0	B1	3055	-34381	-31326	0	
A1	1743	39057	40800	24	A1	3055	-30169	-27114	-19	
Point	Normal			Shear	Upper flange	Point	Normal			Shear
	Axial	Bending	Total				Axial	Bending	Total	
A	2628	-28942	-26314	1		A	4606	25361	29967	0
B	2628	-29073	-26445	0		B	4606	25476	30082	0
C	2628	-28511	-25883	-1837		C	4606	24984	29590	1257
D	2628	-14182	-11554	-5404		D	4606	12427	17033	3696
E	2628	-14263	-11635	-618		E	4606	12498	17105	423
F	2628	-13741	-11113	-6032		F	4606	12041	16647	4125
G	2628	8	2636	-6072		G	4606	-7	4599	4153
F1	2628	14257	16885	-5951		F1	4606	-12493	-7887	4069
E1	2628	14617	17245	-606	E1	4606	-12809	-8202	415	
D1	2628	14698	17326	-5300	D1	4606	-12880	-8274	3624	
C1	2628	28477	31105	-1834	C1	4606	-24954	-20348	1254	
B1	2628	28797	31425	0	B1	4606	-25234	-20628	0	
A1	2628	28928	31556	1	A1	4606	-25349	-20743	0	

Figure.4.18 – Normal and shear stress for cross-section E-E

LC 8				LC 7			
Loads	Vy	Px	Mx	Loads	Vy	Px	Mx
	lbs	lbs	lbs-in		lbs	lbs	lbs-in
	-4381	2855	68197		2996	5004	-59760

Point	Normal			Shear	Lower flange	Point	Normal			Shear
	Axial	Bending	Total				Axial	Bending	Total	
A	2628	-28942	-26314	1		A	4606	25361	29967	0
B	2628	-29073	-26445	0		B	4606	25476	30082	0
C	2628	-28511	-25883	-1837		C	4606	24984	29590	1257
D	2628	-14182	-11554	-5404		D	4606	12427	17033	3696
E	2628	-14263	-11635	-618		E	4606	12498	17105	423
F	2628	-13741	-11113	-6032		F	4606	12041	16647	4125
G	2628	8	2636	-6072		G	4606	-7	4599	4153
F1	2628	14257	16885	-5951		F1	4606	-12493	-7887	4069
E1	2628	14617	17245	-606	E1	4606	-12809	-8202	415	
D1	2628	14698	17326	-5300	D1	4606	-12880	-8274	3624	
C1	2628	28477	31105	-1834	C1	4606	-24954	-20348	1254	
B1	2628	28797	31425	0	B1	4606	-25234	-20628	0	
A1	2628	28928	31556	1	A1	4606	-25349	-20743	0	
Point	Normal			Shear	Upper flange	Point	Normal			Shear
	Axial	Bending	Total				Axial	Bending	Total	
A	2628	-28942	-26314	1		A	4606	25361	29967	0
B	2628	-29073	-26445	0		B	4606	25476	30082	0
C	2628	-28511	-25883	-1837		C	4606	24984	29590	1257
D	2628	-14182	-11554	-5404		D	4606	12427	17033	3696
E	2628	-14263	-11635	-618		E	4606	12498	17105	423
F	2628	-13741	-11113	-6032		F	4606	12041	16647	4125
G	2628	8	2636	-6072		G	4606	-7	4599	4153
F1	2628	14257	16885	-5951		F1	4606	-12493	-7887	4069
E1	2628	14617	17245	-606	E1	4606	-12809	-8202	415	
D1	2628	14698	17326	-5300	D1	4606	-12880	-8274	3624	
C1	2628	28477	31105	-1834	C1	4606	-24954	-20348	1254	
B1	2628	28797	31425	0	B1	4606	-25234	-20628	0	
A1	2628	28928	31556	1	A1	4606	-25349	-20743	0	

Figure.4.19 – Normal and shear stress for cross-section F-F

Bigger stress and MS for comparing with material allowable are shown on figures 4.20 – 4.25

LC 8			LC 7		
Max tension stress	ft_max	43296	Max tension stress	ft_max	31314
MS for tension		0.62	MS for tension		1.24
Max shear stress	fs_max	2054	Max shear stress	fs_max	1421
		20.91	MS for shear		30.66
Max compression stress	fc_max	36822	Max compression stress	fc_max	27394
MS for compression		0.5415	MS for compression		0.4029

Figure.4.20 – Stress and MS for cross-section A-A

LC 8			LC 7		
Max tension stress	ft_max	38153	Max tension stress	ft_max	28848
MS for tension		0.84	MS for tension		1.43
Max shear stress	fs_max	3743	Max shear stress	fs_max	2603
		11.02	MS for shear		16.29
Max compression stress	fc_max	31635	Max compression stress	fc_max	22928
MS for compression		0.4652	MS for compression		0.3372

Figure.4.21 – Stress and MS for cross-section B-B

LC 8			LC 7		
Max tension stress	ft_max	35934	Max tension stress	ft_max	28565
MS for tension		0.95	MS for tension		1.46
Max shear stress	fs_max	5271	Max shear stress	fs_max	3895
		7.54	MS for shear		10.55
Max compression stress	fc_max	30361	Max compression stress	fc_max	21198
MS for compression		0.4465	MS for compression		0.3117

Figure.4.22 – Stress and MS for cross-section C-C

LC 8			LC 7		
Max tension stress	ft_max	16406	Max tension stress	ft_max	14081
MS for tension		3.28	MS for tension		3.99
Max shear stress	fs_max	7620	Max shear stress	fs_max	6053
		4.91	MS for shear		6.43
Max compression stress	fc_max	11896	Max compression stress	fc_max	6034
MS for compression		0.1749	MS for compression		0.0887

Figure.4.23 – Stress and MS for cross-section D-D

LC 8			LC 7		
Max tension stress	ft_max	46254	Max tension stress	ft_max	35112
MS for tension		0.52	MS for tension		1.00
Max shear stress	fs_max	6386	Max shear stress	fs_max	5073
		6.05	MS for shear		7.87
Max compression stress	fc_max	39759	Max compression stress	fc_max	31326
MS for compression		0.5847	MS for compression		0.4607

Figure.4.24 – Stress and MS for cross-section E-E

LC 8			LC 7		
Max tension stress	ft_max	31556	Max tension stress	ft_max	30082
MS for tension		1.22	MS for tension		1.33
Max shear stress	fs_max	1	Max shear stress	fs_max	0
		63758.96	MS for shear		93234.11
Max compression stress	fc_max	26445	Max compression stress	fc_max	20743
MS for compression		0.3889	MS for compression		0.3050

Figure.4.25 – Stress and MS for cross-section F-F

## 5 Buckling analysis

[1]

In science, **buckling** is an instability that leads to structural failure. The failure modes can in simple cases be found by simple mathematical solutions. For complex structures the failure modes are found by numerical tools.

When a structure is subjected to compressive axial stress, buckling may occur. Buckling is characterized by a sudden sideways deflection of a structural member. This may occur even though the stresses that develop in the structure are well below those needed to cause failure of the material of which the structure is composed. As an applied axial load is increased on a member, such as a column, it will ultimately become large enough to cause the member to become unstable and it is said to have buckled. Further loading will cause significant and somewhat unpredictable deformations, possibly leading to complete loss of the member's load-carrying capacity. If the deformations that occur after buckling do not cause the complete collapse of that member, the member will continue to support the load that caused it to buckle. If the buckled member is part of a larger assemblage of components such as a building, any load applied to the buckled part of the structure beyond that which caused the member to buckle will be redistributed within the structure.

In a mathematical sense, buckling is a bifurcation in the solution to the equations of static equilibrium. At a certain point, under an increasing load, any further load is able to be sustained in one of two states of equilibrium: a purely compressed state (with no lateral deviation) or a laterally-deformed state.

In this work are analyzed next type of buckling:

- 1) Local buckling.
- 2) Column buckling
- 3) Chord crippling
- 4) Web buckling.

## 5.1 Local Buckling

[1]

Local buckling is an extremely important facet of cold formed steel sections on account of the fact that the very thin elements used will invariably buckle before yielding. Thinner the plate, the lower will be the load at which the buckles will form.

It has been shown in the chapter on “Introduction to Plate Buckling” that a flat plate simply supported on all edges and loaded in compression (as shown in Fig. 5.1) will buckle at an elastic critical stress given by

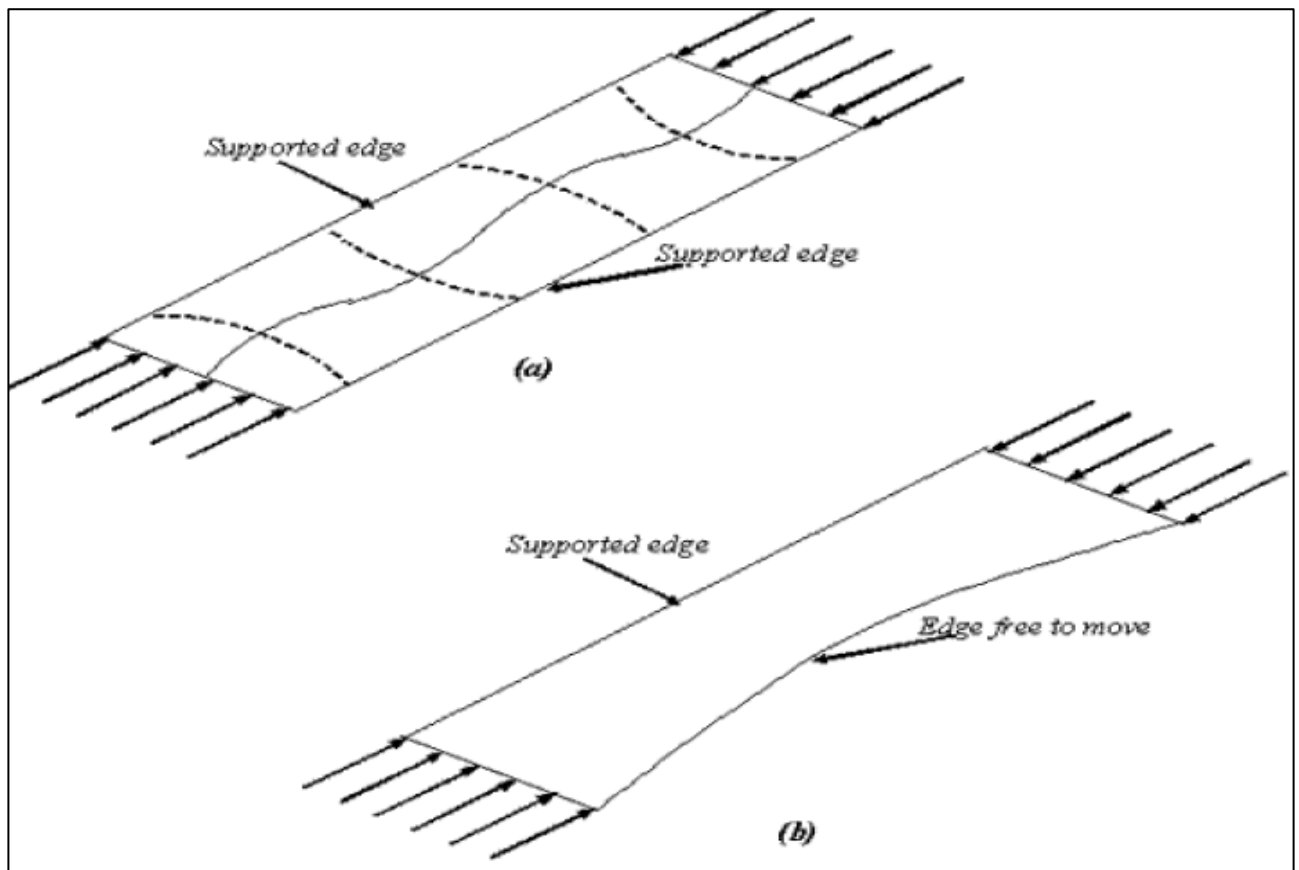


Figure.5.1- Axially compressed plate simply supported on all edges.

The buckling compressive stress for a long flange is [1]:

$$F_{cr} = K_c E_c n_c \left( \frac{t}{b} \right)^2 \quad (5.1)$$

Where  $k_c$  – compressive-buckling coefficients for flat rectangular plates, Fig 5.2,  $E_c$  – Elastic modulus for Compression,  $\nu$  – Poisson ratio,  $t$  – flange thickness,  $b$  – flange width;  $n_c$  – plasticity reduction factor in compression load.

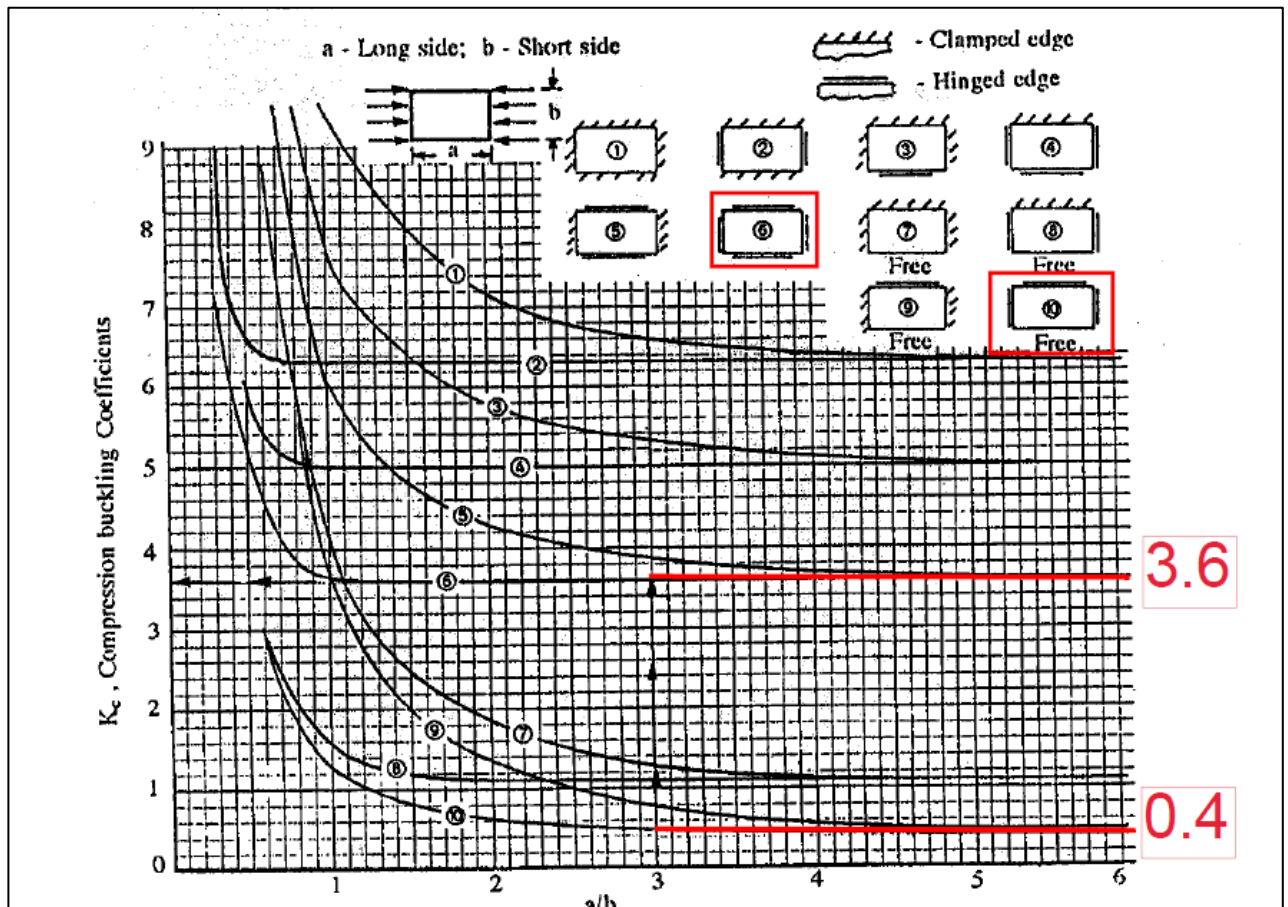


Figure.5.2- Compressive-buckling coefficients. [1]

Find allowable stress without reduction factor and find stress with reduction factor per graphic from [1]. (See Figure 5.3).

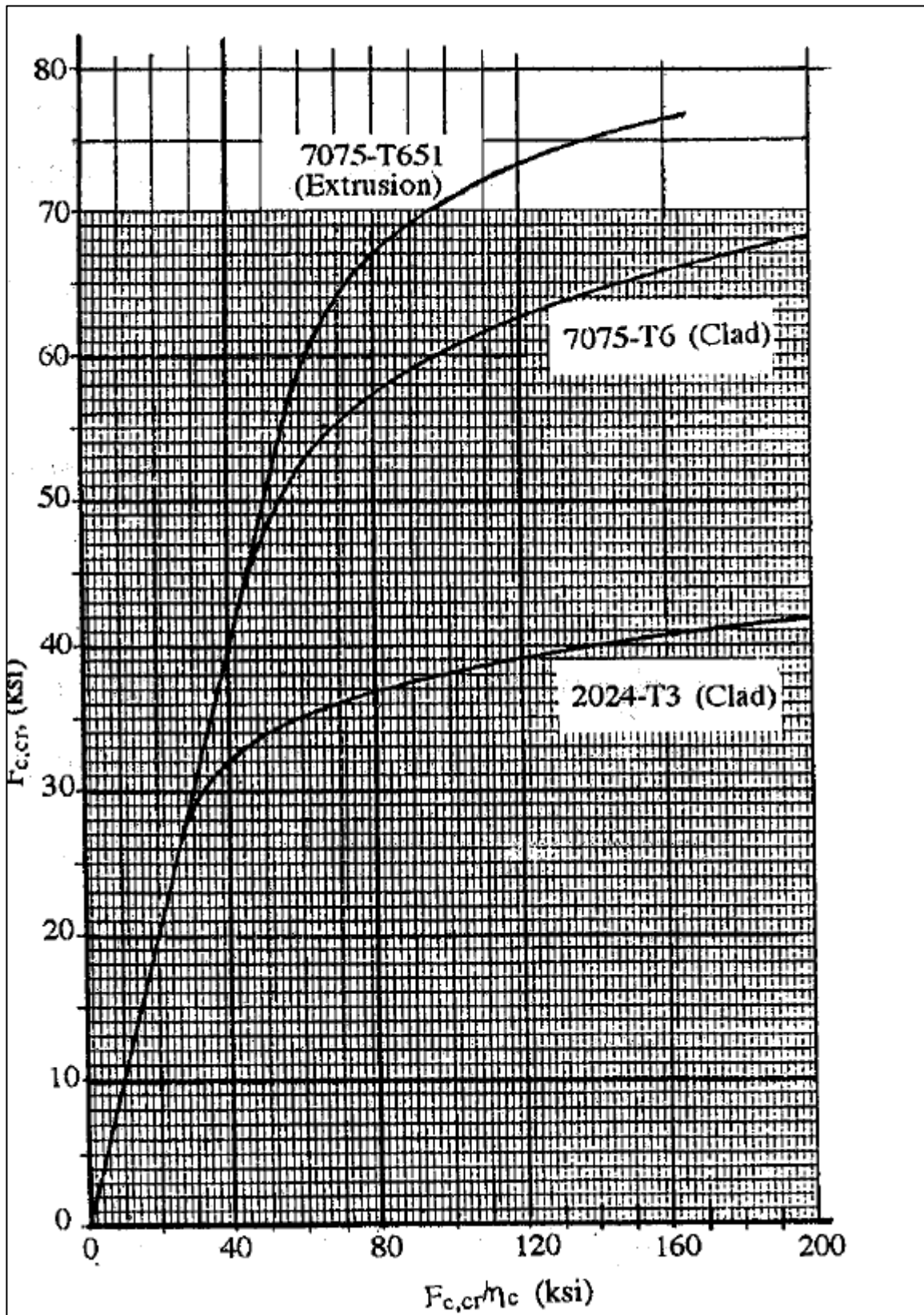


Figure.5.3- Compressive Buckling stress. [1]

Critical local buckling stress and MS for each elements from each cross-sections are shown on figures 5.4 – 5.9

Local buckling				fc_max		Upper	36822			
						lower	27394			
Flange	Element	b, in	t, in	L, in	L/b	Kc	(t/b)^2	Fcr/n	Fcr, ksi	MS
Lower	1	1.00	0.15	22.66	22.66	0.4	0.0225	95.4	59675	1.17836
	2	3.00	0.12	22.66	7.55333	3.6	0.0016	61.056	53018.67	0.93538
	3	0.70	0.08	22.66	32.3714	0.4	0.01306	55.3796	51126.53	0.86631
Upper	4	0.70	0.10	22.66	32.3714	0.4	0.02041	86.5306	58421.77	0.5866
	5	3.00	0.15	22.66	7.55333	3.6	0.0025	95.4	59675	0.62063
	6	1.00	0.15	22.66	22.66	0.4	0.0225	95.4	59675	0.62063

Figure.5.4 - Local buckling stress and MS for elements from A-A cross-section.

Local buckling				fc_max		Upper	31635			
						lower	22928			
Flange	Element	b, in	t, in	L, in	L/b	Kc	(t/b)^2	Fcr/n	Fcr, ksi	MS
Lower	1	1.00	0.12	22.66	22.66	0.4	0.0144	61.056	53018.67	1.31236
	2	2.60	0.10	22.66	8.71538	3.6	0.00148	56.4497	51483.23	1.24539
	3	0.70	0.08	22.66	32.3714	0.4	0.01306	55.3796	51126.53	1.22984
Upper	4	0.70	0.10	22.66	32.3714	0.4	0.02041	86.5306	58421.77	0.84674
	5	2.50	0.12	22.66	9.064	3.6	0.0023	87.9206	58653.44	0.85407
	6	1.00	0.12	22.66	22.66	0.4	0.0144	61.056	53018.67	0.67595

Figure.5.5 - Local buckling stress and MS for elements from B-B cross-section.

Local buckling				fc_max		Upper	30361			
						lower	21198			
Flange	Element	b, in	t, in	L, in	L/b	Kc	(t/b)^2	Fcr/n	Fcr, ksi	MS
Lower	1	1.00	0.10	6.56	6.56	0.4	0.01	42.4	42400	1.00022
	2	2.60	0.10	6.56	2.52308	3.6	0.00148	56.4497	51483.23	1.42872
	3	0.70	0.08	6.56	9.37143	0.4	0.01306	55.3796	51126.53	1.41189
Upper	4	0.70	0.10	6.56	9.37143	0.4	0.02041	86.5306	58421.77	0.92421
	5	2.50	0.10	6.56	2.624	3.6	0.0016	61.056	53018.67	0.74625
	6	1.00	0.10	6.56	6.56	0.4	0.01	42.4	42400	0.39651

Figure.5.6 - Local buckling stress and MS for elements from C-C cross-section.

Local buckling				fc_max		Upper	11896			
						lower	6034			
Flange	Element	b, in	t, in	L, in	L/b	Kc	(t/b)^2	Fcr/n	Fcr, ksi	MS
Lower	1	1.00	0.10	35.37	35.37	0.4	0.01	42.4	42400	6.02694
	2	2.60	0.10	35.37	13.6038	3.6	0.00148	56.4497	51483.23	7.5323
	3	0.70	0.10	35.37	50.5286	0.4	0.02041	86.5306	58421.77	8.68222
Upper	4	0.70	0.10	35.37	50.5286	0.4	0.02041	86.5306	58421.77	3.91112
	5	2.50	0.10	35.37	14.148	3.6	0.0016	61.056	53018.67	3.45692
	6	1.00	0.10	35.37	35.37	0.4	0.01	42.4	42400	2.56428

Figure.5.7 - Local buckling stress and MS for elements from D-D cross-section.

Local buckling				fc_max		Upper	39759				
						lower	31326				
Flange	Element	b, in	t, in	L, in	L/b	Kc	(t/b)^2	Fcr/n	Fcr, ksi	MS	
Lower	1	1.00	0.15	22.66	22.66	0.4	0.0225	95.4	59675	0.90497	
	2	2.50	0.13	22.66	9.064	3.6	0.0027	103.185	60648.08	0.93603	
	3	0.80	0.10	22.66	28.325	0.4	0.01563	66.25	54562.5	0.74176	
Upper	4	0.80	0.10	22.66	28.325	0.4	0.01563	66.25	54562.5	0.37234	
	5	2.60	0.15	22.66	8.71538	3.6	0.00333	127.012	63033.4	0.5854	
	6	1.00	0.12	22.66	22.66	0.4	0.0144	61.056	53018.67	0.33351	

Figure.5.8 - Local buckling stress and MS for elements from E-E cross-section.

Local buckling				fc_max		Upper	26445				
						lower	20743				
Flange	Element	b, in	t, in	L, in	L/b	Kc	(t/b)^2	Fcr/n	Fcr, ksi	MS	
Lower	1	1.00	0.08	17.38	17.38	0.4	0.0064	27.136	27136	0.30818	
	2	2.60	0.08	17.38	6.68462	3.6	0.00095	36.1278	36127.81	0.74167	
	3	0.70	0.08	17.38	24.8286	0.4	0.01306	55.3796	51126.53	1.46473	
Upper	4	0.70	0.08	17.38	24.8286	0.4	0.01306	55.3796	51126.53	0.93331	
	5	2.50	0.08	17.38	6.952	3.6	0.00102	39.0758	39075.84	0.47762	
	6	1.00	0.08	17.38	17.38	0.4	0.0064	27.136	27136	0.02613	

Figure.5.9 - Local buckling stress and MS for elements from F-F cross-section.

## 5.2 Column buckling (Euler)

[1]

Column buckling is a curious and unique subject. It is perhaps the only area of structural mechanics in which failure is not related to the strength of the material. A column buckling analysis consists of determining the maximum load a column can support before it collapses. But for long columns, the collapse has nothing to do with material yield. It is instead governed by the column's stiffness, both material and geometric.

This page will derive the standard equations of column buckling using two approaches. It will first cover the usual development of the equations, i.e., Euler Buckling Theory. This is the derivation found in text books and presented in engineering courses. But I have never liked it. Not because it is incorrect (it is correct), but because I don't think it satisfactorily presents the physical mechanisms governing the buckling process. That is why a second derivation of the buckling equations will also be presented.

Curiously, objects are referred to as columns when they are loaded axially in compression, as is the case here, but they are referred to as beams when they are loaded transversely.

The design is designed for the mind by the minds, but the bullets are shaped and described by the formulas:

### 1. Euler's formula

$$P_E = \frac{\pi^2 EI}{L^2} \quad (5.2)$$

Where

$P_E$ - Euler's power of three times the speed;

$E$ -module of the spring material on the clamp;

$I$ -minimnalny axial momentinertsii pererizu;

$L'$ -effective dovina of the rod,  $L' = L / c$ .

$c$  – fixity coefficient which shown on figure Figure.5.10

At the transition of voltages, we get

$$F_{cr} = \frac{\pi^2 E}{\left(\frac{L'}{\rho}\right)^2} \quad (5.3)$$

With the decrease of majesty  $\left(\frac{L'}{\rho}\right)^2$  there is a change in the nature of the design failure.

It begins to lose stability not much earlier than the compression force of critical value, but much earlier.

Column shape and end fixity		End fixity coefficient	Column shape and end fixity		End fixity coefficient
	Uniform column, axially loaded, pinned ends	$c = 1$ $\frac{1}{\sqrt{c}} = 1$		Uniform column, distributed axis load, one end fixed, one end free	$c = 0.794$ $\frac{1}{\sqrt{c}} = 1.12$
	Uniform column, axially loaded, fixed ends	$c = 4$ $\frac{1}{\sqrt{c}} = 0.5$		Uniform column, distributed axis load, pinned ends	$c = 1.87$ $\frac{1}{\sqrt{c}} = 0.732$
	Uniform column, axially loaded, one end fixed, one pinned end	$c = 2.05$ $\frac{1}{\sqrt{c}} = 0.7$		Uniform column, distributed axis load, fixed ends	$c = 7.5$ (Approx.) $\frac{1}{\sqrt{c}} = 0.365$
	Uniform column, axially loaded, one end fixed, one end free	$c = 0.25$ $\frac{1}{\sqrt{c}} = 2$		Uniform column, distributed axis load, one end fixed, one end pinned	$c = 6.08$ $\frac{1}{\sqrt{c}} = 0.406$

Figure.5.10 - fixity coefficient

Take coefficient 1 for each sections. It is conservative.

Assume elements 1, 2 and 3 as one beam.

And elements 4, 5 and 6 as one beam.

Calculate their section properties and find allowable compression stress.

Due to cross section nearly to symmetrical shown only more critical upper chord.

Critical Euler buckling stress and MS for each upper chord from each cross-sections are shown on figures 5.11 – 5.16

Element	b, in	t, in	A, in <sup>2</sup>	Xc, in	Yc, in	Qy, in <sup>3</sup>	Qx, in <sup>3</sup>	Ixx, in <sup>4</sup>	Iyy, in <sup>4</sup>
4	0.70	0.10	0.07	0.35	0.05	0.0245	0.0035	0.21215	0.004457
5	3.00	0.15	0.45	0.075	1.6	0.03375	0.72	0.0172	0.344406
6	1.00	0.15	0.15	0.5	3.175	0.075	0.47625	0.28774	0.026101
Σ			0.67			0.13325	1.19975	0.51709	0.374964
	Xcg, in	0.19888		Fcr, psi	114025		MS		
	Yxg, in	1.79067					2.09665		
	L', in	22.66		c	1				
	ρ <sub>min</sub>	0.7481		L'/ρ <sub>min</sub>	30.2902				

Figure.5.11 - Euler buckling stress and MS for upper chord from A-A cross-section

Element	b, in	t, in	A, in <sup>2</sup>	Xc, in	Yc, in	Qy, in <sup>3</sup>	Qx, in <sup>3</sup>	Ixx, in <sup>4</sup>	Iyy, in <sup>4</sup>
4	0.70	0.10	0.07	0.35	0.05	0.0245	0.0035	0.14422	0.004246
5	2.50	0.12	0.3	0.06	1.35	0.018	0.405	0.00584	0.162927
6	1.00	0.12	0.12	0.5	2.66	0.06	0.3192	0.16579	0.020149
Σ			0.49			0.1025	0.7277	0.31585	0.187322
	Xcg, in	0.20918		Fcr, psi	77889.4		MS		
	Yxg, in	1.4851					1.46213		
	L', in	22.66		c	1				
	ρ <sub>min</sub>	0.6183		L'/ρ <sub>min</sub>	36.6491				

Figure.5.12 - Euler buckling stress and MS for upper chord from B-B cross-section

Element	b, in	t, in	A, in <sup>2</sup>	Xc, in	Yc, in	Qy, in <sup>3</sup>	Qx, in <sup>3</sup>	Ixx, in <sup>4</sup>	Iyy, in <sup>4</sup>
4	0.70	0.10	0.07	0.35	0.05	0.0245	0.0035	0.13586	0.004287
5	2.50	0.10	0.25	0.05	1.35	0.0125	0.3375	0.00236	0.136382
6	1.00	0.10	0.1	0.5	2.65	0.05	0.265	0.1458	0.01691
Σ			0.42			0.087	0.606	0.28403	0.157579
	Xcg, in	0.20714		Fcr, psi	912107		MS		
	Yxg, in	1.44286					29.0416		
	L', in	6.56		c	1				
	ρ <sub>min</sub>	0.61253		L'/ρ <sub>min</sub>	10.7098				

Figure.5.13 - Euler buckling stress and MS for upper chord from C-C cross-section

Element	b, in	t, in	A, in <sup>2</sup>	Xc, in	Yc, in	Qy, in <sup>3</sup>	Qx, in <sup>3</sup>	Ixx, in <sup>4</sup>	Iyy, in <sup>4</sup>
4	0.70	0.10	0.07	0.35	0.05	0.0245	0.0035	0.13586	0.004287
5	2.50	0.10	0.25	0.05	1.35	0.0125	0.3375	0.00236	0.136382
6	1.00	0.10	0.1	0.5	2.65	0.05	0.265	0.1458	0.01691
Σ			0.42			0.087	0.606	0.28403	0.157579
	Xcg, in	0.20714		Fcr, psi	31375		MS		
	Yxg, in	1.44286					1.63748		
	L', in	35.37		c	1				
	ρ <sub>min</sub>	0.61253		L'/ρ <sub>min</sub>	57.7446				

Figure.5.14 - Euler buckling stress and MS for upper chord from D-D cross-section

Element	b, in	t, in	A, in <sup>2</sup>	Xc, in	Yc, in	Qy, in <sup>3</sup>	Qx, in <sup>3</sup>	Ixx, in <sup>4</sup>	Iyy, in <sup>4</sup>
4	0.80	0.10	0.08	0.4	0.05	0.032	0.004	0.16678	0.007293
5	2.60	0.15	0.39	0.075	1.4	0.02925	0.546	0.00415	0.226343
6	1.00	0.12	0.12	0.5	2.76	0.06	0.3312	0.19261	0.020407
Σ			0.59			0.12125	0.8812	0.36353	0.254043
	Xcg, in	0.20551		Fcr, psi	87728.4		MS		
	Yxg, in	1.49356					1.20653		
	L', in	22.66		c	1				
	ρ <sub>min</sub>	0.65619		L'/ρ <sub>min</sub>	34.5329				

Figure.5.15 - Euler buckling stress and MS for upper chord from E-E cross-section

Element	b, in	t, in	A, in <sup>2</sup>	Xc, in	Yc, in	Qy, in <sup>3</sup>	Qx, in <sup>3</sup>	Ixx, in <sup>4</sup>	Iyy, in <sup>4</sup>
4	0.70	0.08	0.056	0.35	0.04	0.0196	0.00224	0.10701	0.003527
5	2.50	0.08	0.2	0.04	1.33	0.008	0.266	0.0018	0.109363
6	1.00	0.08	0.08	0.5	2.62	0.04	0.2096	0.11483	0.01381
Σ			0.336			0.0676	0.47784	0.22364	0.1267
	Xcg, in	0.20119		Fcr, psi	130600		MS		
	Yxg, in	1.42214					3.93853		
	L', in	17.38		c	1				
	ρ <sub>min</sub>	0.61407		L'/ρ <sub>min</sub>	28.303				

Figure.5.16 - Euler buckling stress and MS for upper chord from F-F cross-section

### 5.3 Chord crippling and Jonson-Euler column buckling.

[1]

Empirical techniques have been developed using coefficients derived from tests since there is no analytical basis for the prediction of crippling strength. The crippling stress for a particular cross-section area is calculated as if the stress were uniform over the entire section. Furthermore, the maximum crippling strength of a member is calculated as a function of its cross-section rather than its length. In reality, parts of the section buckle well below the crippling stress. This results in the more stable areas, such as corners and intersections, reaching a higher stress than buckled elements. At failure, the stress in the corners and intersections is always above the material yield stress although the “crippling” stress, which is an average value, may be considerably less than the yield stress. The compression yield strength is used as the crippling strength cut-off since there is not sufficient data to permit an exact solution at higher stress values for most materials.

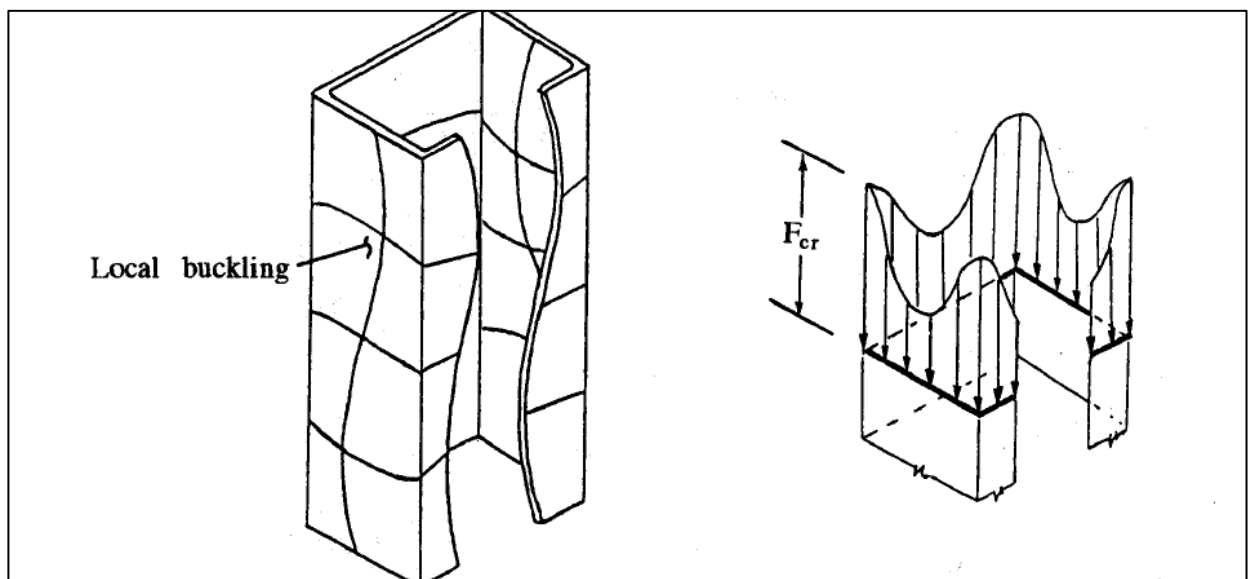


Figure.5.17 – Cross section subjected to Crippling stress

Cripling allowable stress depend on quantity free edge (one or two) and  $b/t$  ratio as shown on figure 5.18

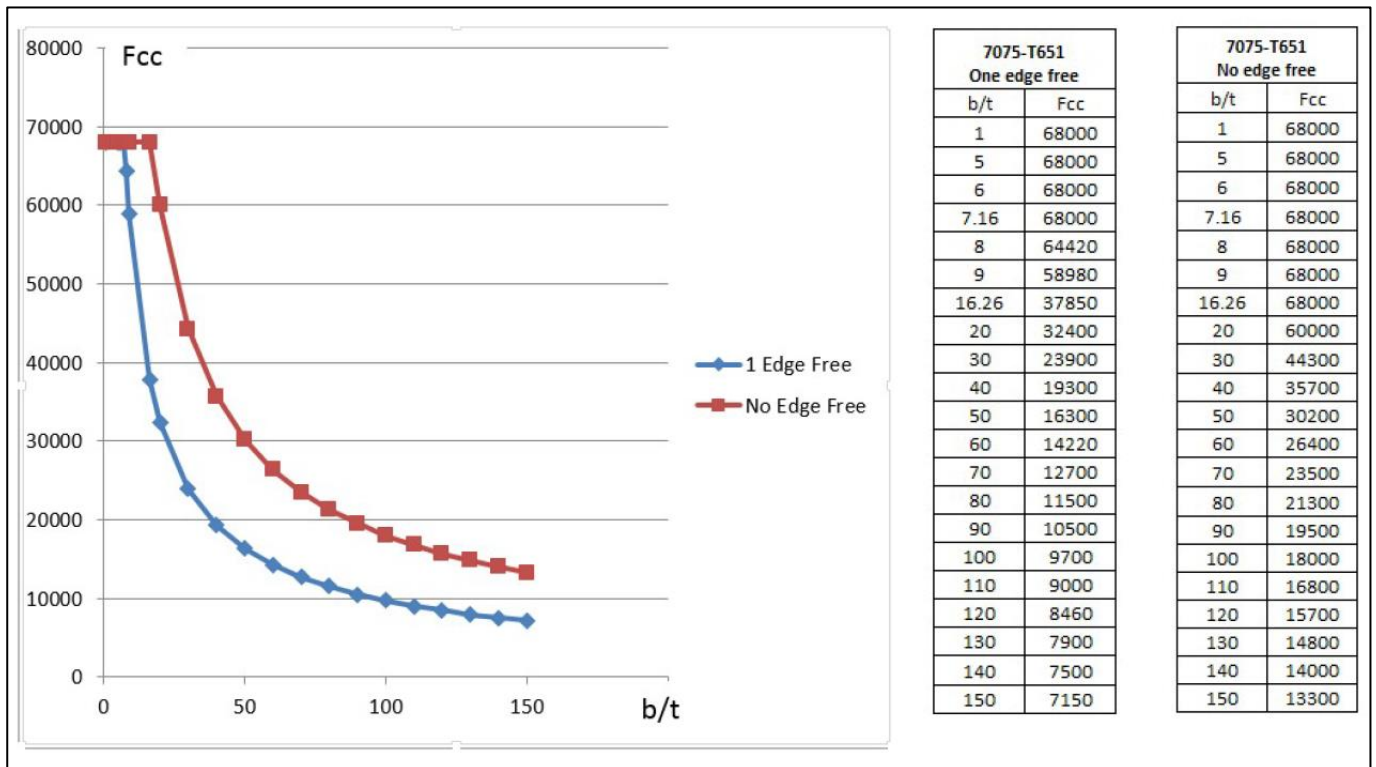


Figure.5.18 – Crippling Stress of Extruded Sections (7075-T651)

Crippling stress calculated for each flange and after than calculate allowable stress for own cross-section :

$$F_{cc} = \frac{\sum b_n \cdot t_n \cdot F_{ccn}}{\sum b_n \cdot t_n} \quad (5.4)$$

Where  $b_n$  – length of each segment,  $t_n$  – thickness of each segment,  $F_{ccn}$  – allowable crippling stress for each segment.

Experiments show that the character of stability loss can be depicted in the following graph [1] and divided into 3 sections.

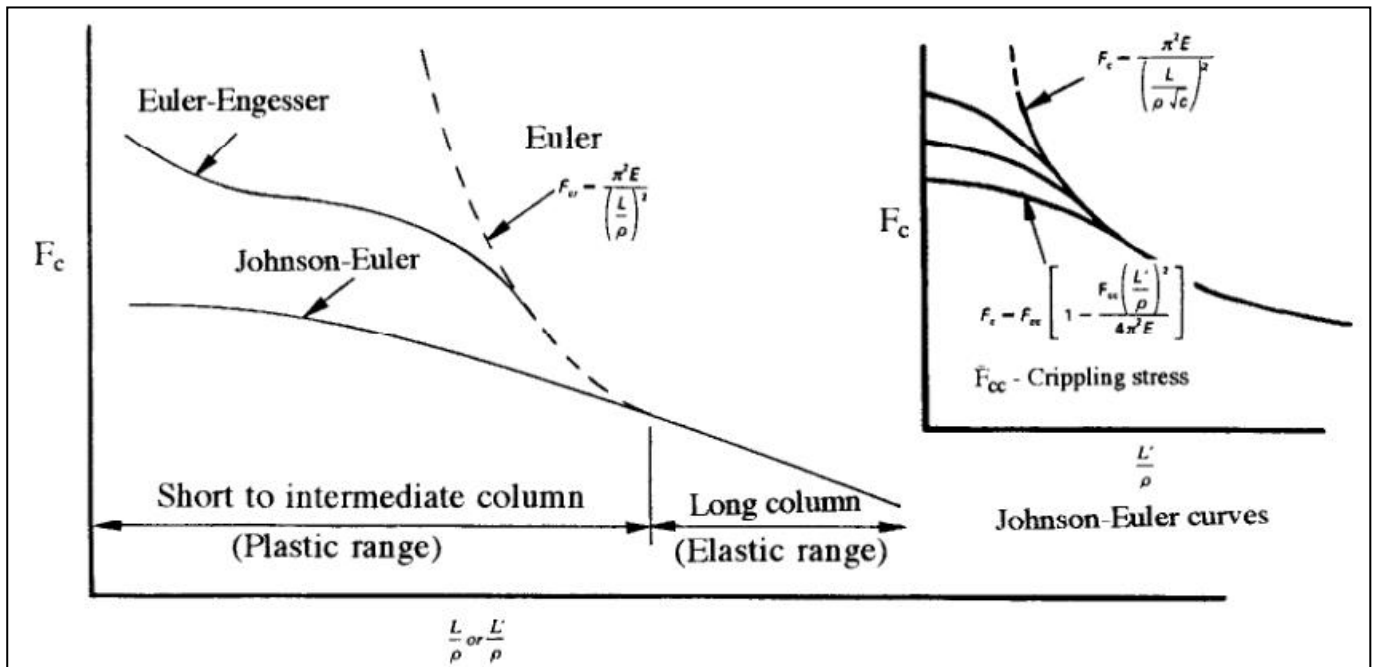


Figure.5.19 –Buckling curves

Loss of stability according to the Euler formula is determined for thin and long rods with  $L'/\rho \geq 80$ .

Loss of stability according to the Euler-Engesser formula is determined for comparisons of the average length and thickness of the rods. For such stubble, the loss of stability is characterized by plastic deformations of the cross section, resulting in destruction at  $P < P_{cr}$  ( $F < F_{cr}$ ). The Euler-Engesser formula is similar to the Euler formula, but it already has a tangent modulus  $E_t$  (tangential).

The third section is characterized mainly by short stubble with a shaped or bent cross section. Such rods are analyzed by the Johnson-Euler formula.

$$F_c = F_{cc} - \frac{F_{cc}^2 \left( \frac{L}{\rho \sqrt{c}} \right)^2}{4\pi^2 E} \quad (5.5)$$

where

$F_c$  is the compression stress;

$F_{cc}$ -stress of crippling;

c-coefficient of braking;

$\rho$ -minimum radius of inertia;

E-compression modulus of elasticity.

In this formula, it appears that the term “kripling stress” is mentioned. This phenomenon – kripling – also applies to cases of loss of adhesion. Kripling is the loss of load-bearing capacity of a structure due to plastic deformations of the cross-section shape. These plastic deformations occur as a result of the local loss of resistance by the individual elements of the cross section, which causes the redistribution of stresses across the cross section. Thus, when the whole structure is still operating under the influence of forces or stresses much smaller than the critical value, in the congested section, the stresses reach a plastic threshold. After that, the material begins to deform plastically, which causes loss of bearing capacity. In particular, sections formed by bending work, which have pronounced angles and free faces of elements, are prone to kripling. The creep stresses for each individual case are mainly determined experimentally, but based on the tests performed for typical sections, typical graphs were constructed. These graphs can be used to determine the critical creep stresses for any section.

Cripling and Jonsin-Euler allowable stress and MS for each upper chord from each cross-sections are shown on figures 5.20 – 5.25.

Chord crippling and Jonson-Euler					$\sqrt{\frac{F_{cy}}{E} \cdot \frac{b}{t}}$					
Element	Edge free	b, in	t, in	b/t		Fcc, psi	b*t, in <sup>2</sup>	Fcc*b*t	Fcc	MS
4	1	0.70	0.10	7	0.58091	68875.4	0.07	4821.28	MS	0.69786
5	0	3.00	0.15	20	1.65973	58582.2	0.45	26362		
6	1	1.00	0.15	6.67	0.55324	71360.8	0.15	10704.1	Fcje	53949
$\Sigma$							0.67	41887.4	MS	0.46513

Figure.5.20 – Cripling and Jonsin-Euler allowable stress and MS from A-A cross-section

Chord crippling and Jonson-Euler					$\sqrt{\frac{F_{cy}}{E} \cdot \frac{b}{t}}$					
Element	Edge free	b, in	t, in	b/t		Fcc, psi	b*t, in^2	Fcc*b*t	Fcc	
4	1	0.70	0.10	7	0.58091	68875.4	0.07	4821.28	MS	59305.6
5	0	2.50	0.12	20.83333333	1.72889	56764.8	0.3	17029.4		0.87468
6	1	1.00	0.12	8.33	0.69156	60075.4	0.12	7209.05	Fcje	48016.7
$\Sigma$							0.49	29059.8	MS	0.51783

Figure.5.21 – Crippling and Jonsin-Euler allowable stress and MS from B-B cross-section

Chord crippling and Jonson-Euler					$\sqrt{\frac{F_{cy}}{E} \cdot \frac{b}{t}}$					
Element	Edge free	b, in	t, in	b/t		Fcc, psi	b*t, in^2	Fcc*b*t	Fcc	
4	1	0.70	0.10	7	0.58091	68875.4	0.07	4821.28	MS	52926.3
5	0	2.50	0.10	25	2.07467	48440.8	0.25	12110.2		0.74321
6	1	1.00	0.10	10.00	0.82987	52975.4	0.1	5297.54	Fcje	52158.5
$\Sigma$							0.42	22229	MS	0.71792

Figure.5.22 – Crippling and Jonsin-Euler allowable stress and MS from C-C cross-section

Chord crippling and Jonson-Euler					$\sqrt{\frac{F_{cy}}{E} \cdot \frac{b}{t}}$					
Element	Edge free	b, in	t, in	b/t		Fcc, psi	b*t, in^2	Fcc*b*t	Fcc	
4	1	0.70	0.10	7	0.58091	68875.4	0.07	4821.28	MS	52926.3
5	0	2.50	0.10	25	2.07467	48440.8	0.25	12110.2		3.44915
6	1	1.00	0.10	10.00	0.82987	52975.4	0.1	5297.54	Fcje	30606
$\Sigma$							0.42	22229	MS	1.57284

Figure.5.23 – Crippling and Jonsin-Euler allowable stress and MS from D-D cross-section

Chord crippling and Jonson-Euler					$\sqrt{\frac{F_{cy}}{E} \cdot \frac{b}{t}}$					
Element	Edge free	b, in	t, in	b/t		Fcc, psi	b*t, in^2	Fcc*b*t	Fcc	
4	1	0.80	0.10	8	0.66389	62215.9	0.08	4977.27	MS	63817
5	0	2.60	0.15	17.33333333	1.43844	65296.7	0.39	25465.7		0.60511
6	1	1.00	0.12	8.33	0.69156	60075.4	0.12	7209.05	Fcje	52211.3
$\Sigma$							0.59	37652	MS	0.31321

Figure.5.24 – Crippling and Jonsin-Euler allowable stress and MS from E-E cross-section

Chord crippling and Jonson-Euler					$\sqrt{\frac{F_{cy}}{E} \cdot \frac{b}{t}}$					
Element	Edge free	b, in	t, in	b/t		Fcc, psi	b*t, in^2	Fcc*b*t	Fcc	
4	1	0.70	0.08	8.75	0.72613	58124.7	0.056	3254.98	MS	44235.2
5	0	2.50	0.08	31.25	2.59333	40588	0.2	8117.6		0.67272
6	1	1.00	0.08	12.50	1.03733	43630.6	0.08	3490.45	Fcje	40489.5
$\Sigma$							0.336	14863	MS	0.53108

Figure.5.25 – Crippling and Jonsin-Euler allowable stress and MS from F-F cross-section

## 5.4 Web buckling.

[1]

Elements 2, 5 and web should be analyzed for different buckling combination.

Should be calculated following buckling cases:

- 1) Compression;
- 2) Bending;
- 3) Shear;
- 4) Compression+ Bending;
- 5) Compression+ Shear.

Buckling stress for a flat plate under in-plane compression load calculated per paragraph 5.1.

Buckling stress for a flat plate under in-plane bending load is:

$$F_{bcr} = K_b \eta_c E (t/b)^2 \quad (5.6)$$

Where  $k_b$  – compressive-buckling coefficients for flat rectangular plates, Fig 5.26,  $E_c$  – Elastic modulus for Compression,  $\nu$  – Poisson ratio,  $t$  – flange thickness,  $b$  – flange width;  $n_c$  – plasticity reduction factor in compression load.

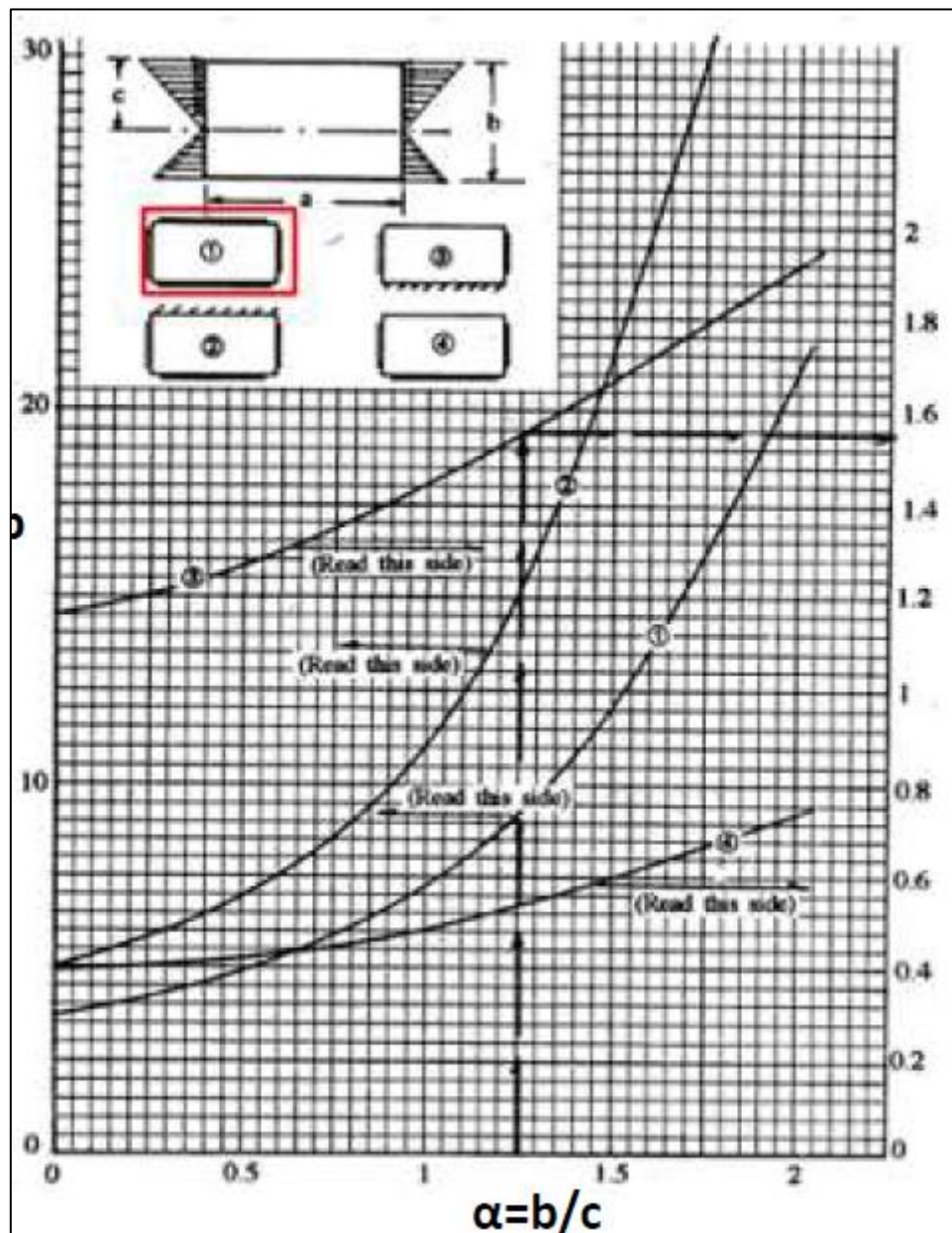


Figure 5.26 - Bending-buckling coefficients for flat rectangular plates. [1]

Buckling stress for a flat plate under in-plane shear load is:

$$F_{bcr} = K_s \eta_s E (t/b)^2 \quad (5.7)$$

Where  $k_s$  – compressive-buckling coefficients for flat rectangular plates, Fig 5.2,  $E_c$  – Elastic modulus for Compression,  $\nu$  – Poisson ratio,  $t$  – flange thickness,  $b$  – flange width;  $n_s$  – plasticity reduction factor in shear load.

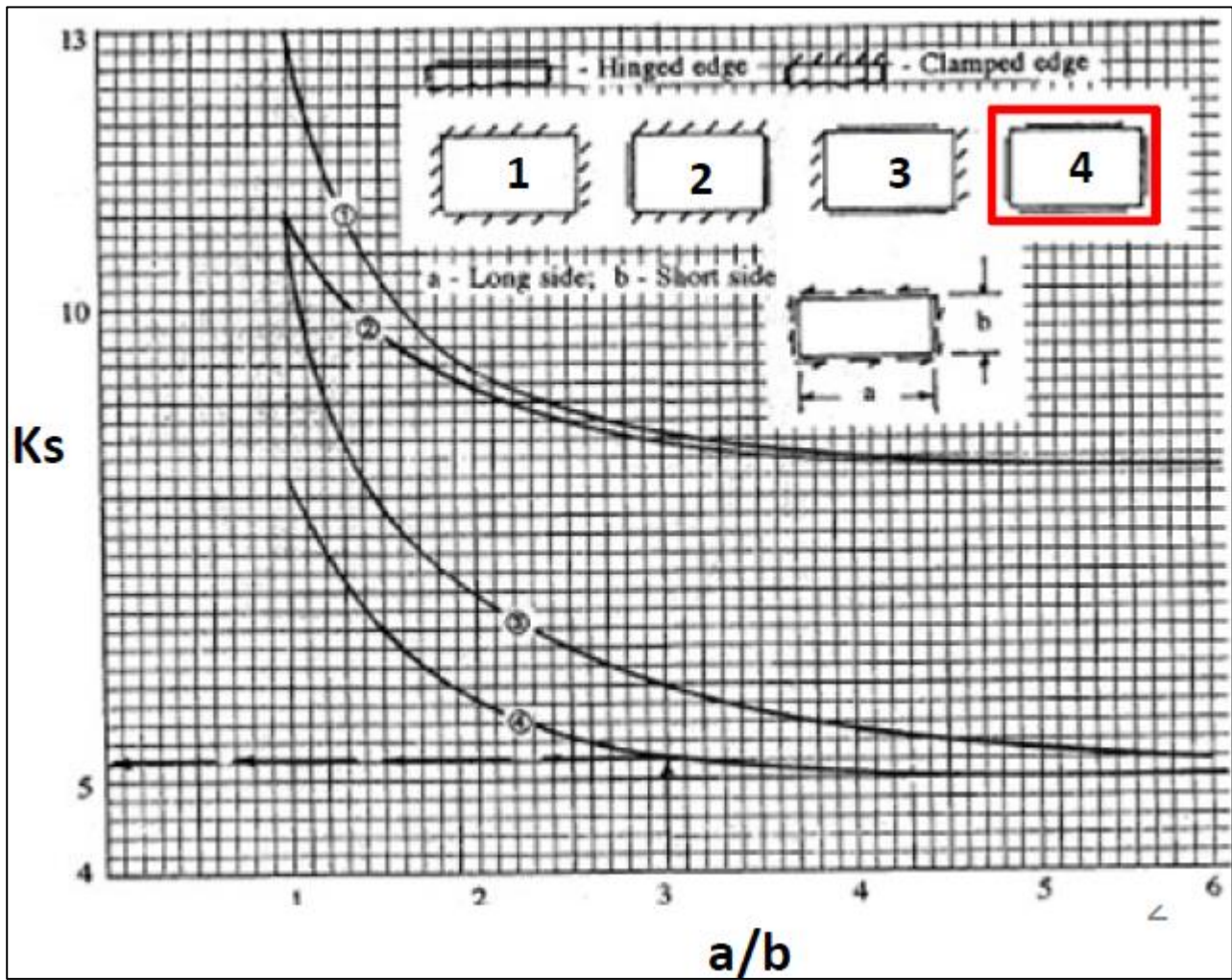


Figure 5.27 - Shear-buckling coefficients for flat rectangular plates. [1]

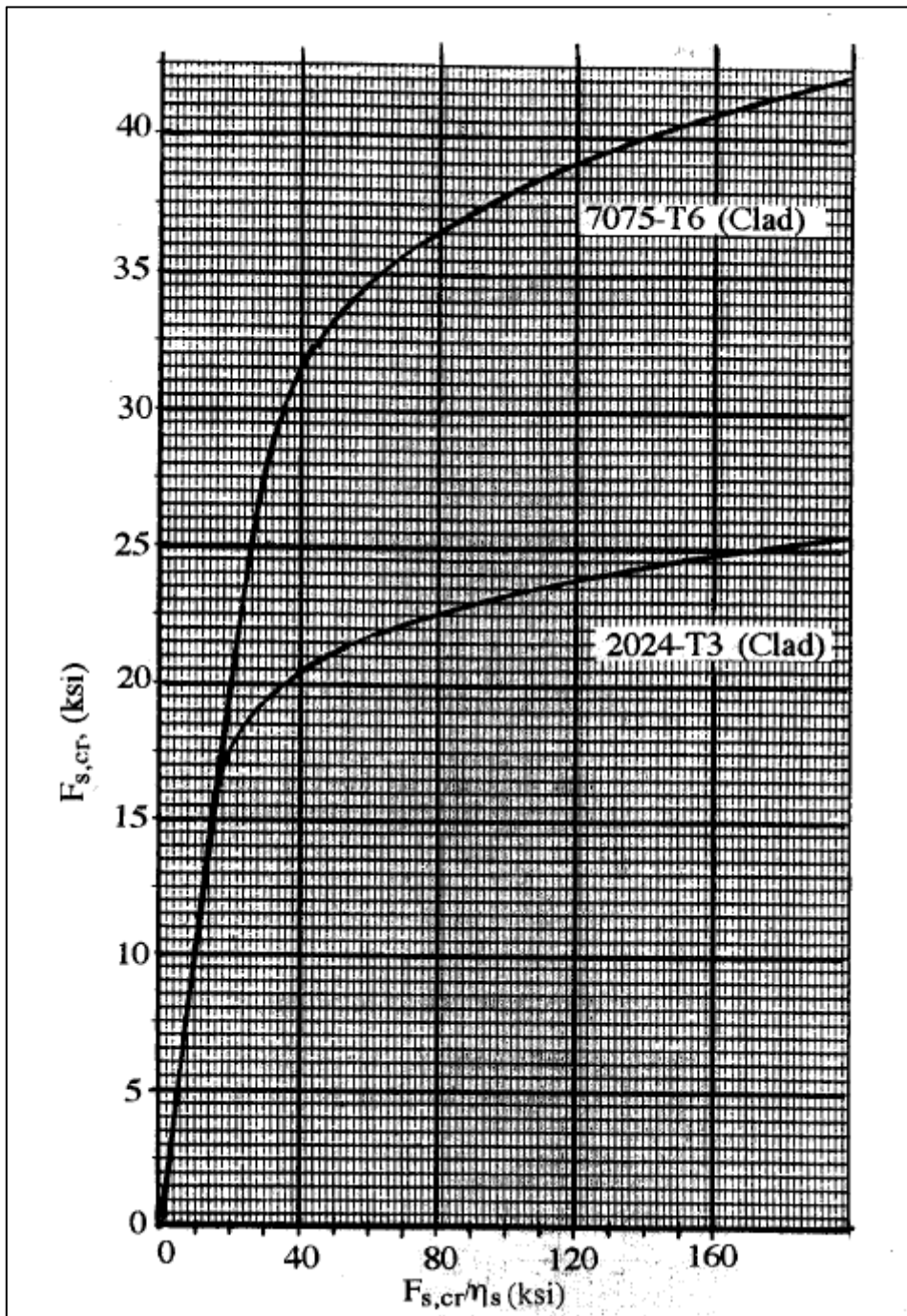


Figure 5.28 - Shear-buckling stress. [1]

Calculate margin of safety for web under combined bending and longitudinal compression.

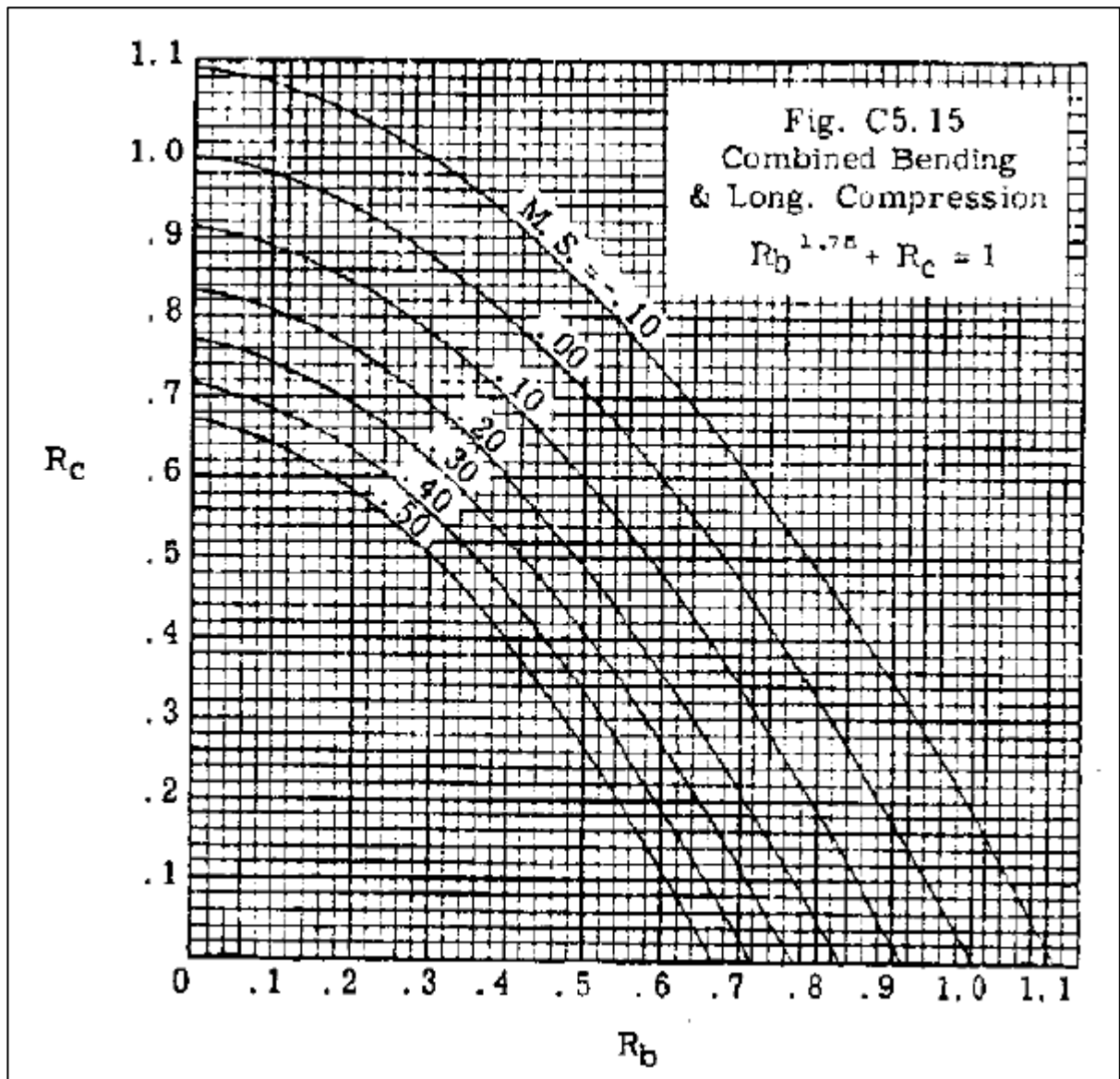


Figure 5.29 – MS for compression + bending. [3]

Calculate margin of safety for web under combined shear and compression.

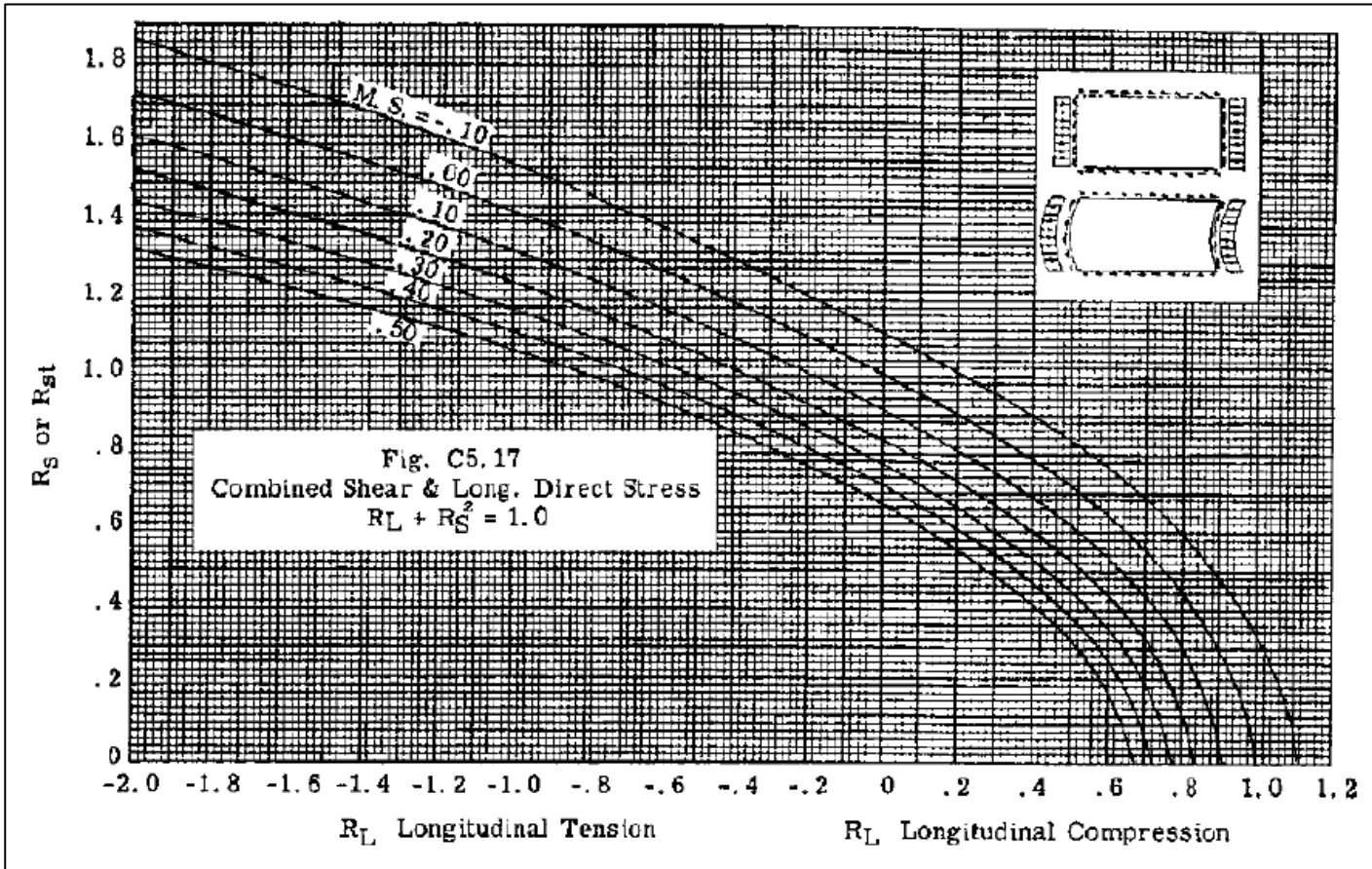


Figure 5.30 – MS for compression + shear. [3]

Result of web buckling analysis for each cross-section are shown on figures 5.31 – 5.36.

Web buckling												
Number of element	b, in	t, in	L, in	(t/b) <sup>2</sup>	L/b	Number of element	MS(b+c)	MS(c+s)				
2	3.00	0.12	22.66	0.001600	7.55333	2	0.25	0.69				
web	4.02	0.10	22.66	0.000619	5.63682	web	0.95	1.07				
5	3.00	0.15	22.66	0.002500	7.55333	5	0.03	0.47				
Number of element	Compression				Bending				Shear			
	Kc	Fc,cr/n	Fc,cr	Rc	Kb	Fb,cr/n	Fb,cr	Rb	Ks	Fs,cr/n	Fs,cr	Rs
2	3.6	61.056	53018.7	0.51669351	7	118.72	62231	0.44021	5	84.8	36600	0.05611
web	3.6	23.6133	23613.3	0.40	17.1	112.163	61596.4	0.15	5	32.7962	28318.5	0.07252
5	3.6	95.4	59675	0.61704245	7	185.5	67236.8	0.55	5	132.5	39500	0.05199

Figure 5.31 – Web buckling analysis for cross-section A-A.

Web buckling													
Number of element	b, in	t, in	L, in	(t/b) <sup>2</sup>	L/b	Number of element	MS(b+c)	MS(c+s)					
									2	2.60	0.10	22.66	0.001479
web	4.98	0.08	22.66	0.000258	4.5502	web	0.01	0.00					
5	2.50	0.12	22.66	0.002304	9.064	5	0.18	0.62					
Number of element	Compression				Bending				Shear				
	Kc	F <sub>c,cr/n</sub>	F <sub>c,cr</sub>	R <sub>c</sub>	Kb	F <sub>b,cr/n</sub>	F <sub>b,cr</sub>	R <sub>b</sub>	Ks	F <sub>s,cr/n</sub>	F <sub>s,cr</sub>	R <sub>s</sub>	
2	3.6	56.4497	51483.235	0.44535633	7	109.763	61364.2	0.37364	5	78.4024	36107.9	0.10366	
web	3.6	9.84758	9847.5831	0.93	17.1	46.776	46184	0.20	5	13.6772	13677.2	0.27366	
5	3.6	87.9206	58653.44	0.53935506	7	170.957	66315.2	0.48	5	122.112	38950.7	0.09609	

Figure 5.32 – Web buckling analysis for cross-section B-B.

Web buckling													
Number of element	b, in	t, in	L, in	(t/b) <sup>2</sup>	L/b	Number of element	MS(b+c)	MS(c+s)					
									2	2.60	0.10	6.56	0.001479
web	5.02	0.08	6.56	0.000254	1.30677	web	0.17	0.06					
5	2.50	0.10	6.56	0.001600	2.624	5	0.13	0.52					
Number of element	Compression				Bending				Shear				
	Kc	F <sub>c,cr/n</sub>	F <sub>c,cr</sub>	R <sub>c</sub>	Kb	F <sub>b,cr/n</sub>	F <sub>b,cr</sub>	R <sub>b</sub>	Ks	F <sub>s,cr/n</sub>	F <sub>s,cr</sub>	R <sub>s</sub>	
2	3.6	56.4497	51483.235	0.41173953	7	109.763	61364.2	0.34544	5	78.4024	36107.9	0.14598	
web	3.6	9.69127	9691.2747	0.78	17.1	46.0336	45689	0.17	5	13.4601	13460.1	0.39161	
5	3.6	61.056	53018.667	0.57265545	7	118.72	62231	0.49	5	84.8	36600	0.14402	

Figure 5.33 – Web buckling analysis for cross-section C-C.

Web buckling													
Number of element	b, in	t, in	L, in	(t/b) <sup>2</sup>	L/b	Number of element	MS(b+c)	MS(c+s)					
									2	2.60	0.10	35.37	0.001479
web	5.00	0.08	35.37	0.000256	7.074	web	5.86	1.06					
5	2.50	0.10	35.37	0.001600	14.148	5	1.77	1.87					
Number of element	Compression				Bending				Shear				
	Kc	F <sub>c,cr/n</sub>	F <sub>c,cr</sub>	R <sub>c</sub>	Kb	F <sub>b,cr/n</sub>	F <sub>b,cr</sub>	R <sub>b</sub>	Ks	F <sub>s,cr/n</sub>	F <sub>s,cr</sub>	R <sub>s</sub>	
2	3.6	56.4497	51483.235	0.11720168	7	109.763	61364.2	0.09833	5	78.4024	36107.9	0.21103	
web	3.6	9.76896	9768.96	0.09	17.1	46.4026	45935	0.02	5	13.568	13568	0.5616	
5	3.6	61.056	53018.667	0.22437043	7	118.72	62231	0.19	5	84.8	36600	0.20819	

Figure 5.34 – Web buckling analysis for cross-section D-D.

Web buckling												
Number of element	b, in	t, in	L, in	(t/b) <sup>2</sup>	L/b	Number of element	MS(b+c)	MS(c+s)				
2	2.50	0.13	22.66	0.002704	9.064	2	0.27	0.63				
web	4.93	0.10	22.66	0.000411	4.59635	web	0.27	0.22				
5	2.60	0.15	22.66	0.003328	8.71538	5	0.02	0.40				
Number of element	Compression				Bending				Shear			
	Kc	F <sub>c,cr/n</sub>	F <sub>c,cr</sub>	R <sub>c</sub>	Kb	F <sub>b,cr/n</sub>	F <sub>b,cr</sub>	R <sub>b</sub>	Ks	F <sub>s,cr/n</sub>	F <sub>s,cr</sub>	R <sub>s</sub>
2	3.6	103.185	60648.08	0.51652072	7	200.637	73000	0.42912	5	143.312	40054.7	0.15943
web	3.6	15.7005	15700.538	0.69	17.1	74.5776	56429.6	0.19	5	21.8063	21505.3	0.29696
5	3.6	127.012	63033.403	0.63075452	7	246.967	73000	0.54	5	176.405	41358.8	0.15441

Figure 5.35 – Web buckling analysis for cross-section E-E.

Web buckling												
Number of element	b, in	t, in	L, in	(t/b) <sup>2</sup>	L/b	Number of element	MS(b+c)	MS(c+s)				
2	2.60	0.08	17.38	0.000947	6.68462	2	0.26	0.56				
web	5.08	0.08	17.38	0.000248	3.42126	web	0.11	0.16				
5	2.50	0.08	17.38	0.001024	6.952	5	0.05	0.37				
Number of element	Compression				Bending				Shear			
	Kc	F <sub>c,cr/n</sub>	F <sub>c,cr</sub>	R <sub>c</sub>	Kb	F <sub>b,cr/n</sub>	F <sub>b,cr</sub>	R <sub>b</sub>	Ks	F <sub>s,cr/n</sub>	F <sub>s,cr</sub>	R <sub>s</sub>
2	3.6	36.1278	36127.811	0.574163	7	70.2485	55562.1	0.37333	5	50.1775	33025.4	2.1E-05
web	3.6	9.4637	9463.6989	0.83	17.1	44.9526	44952.6	0.18	5	13.144	13144	5.4E-05
5	3.6	39.0758	39075.84	0.67676198	7	75.9808	56663.5	0.47	5	54.272	33610.3	2.1E-05

Figure 5.36 – Web buckling analysis for cross-section F-F.

## 6. Floor beam with Frame Joint. Static and fatigue analysis

### 6.1 Static strengths analysis

In this paragraph was analyzed joint floor beam to frame which has 30 fasteners in three rows. This joint loaded shear force, axial force and moment shown on figure 6.1.

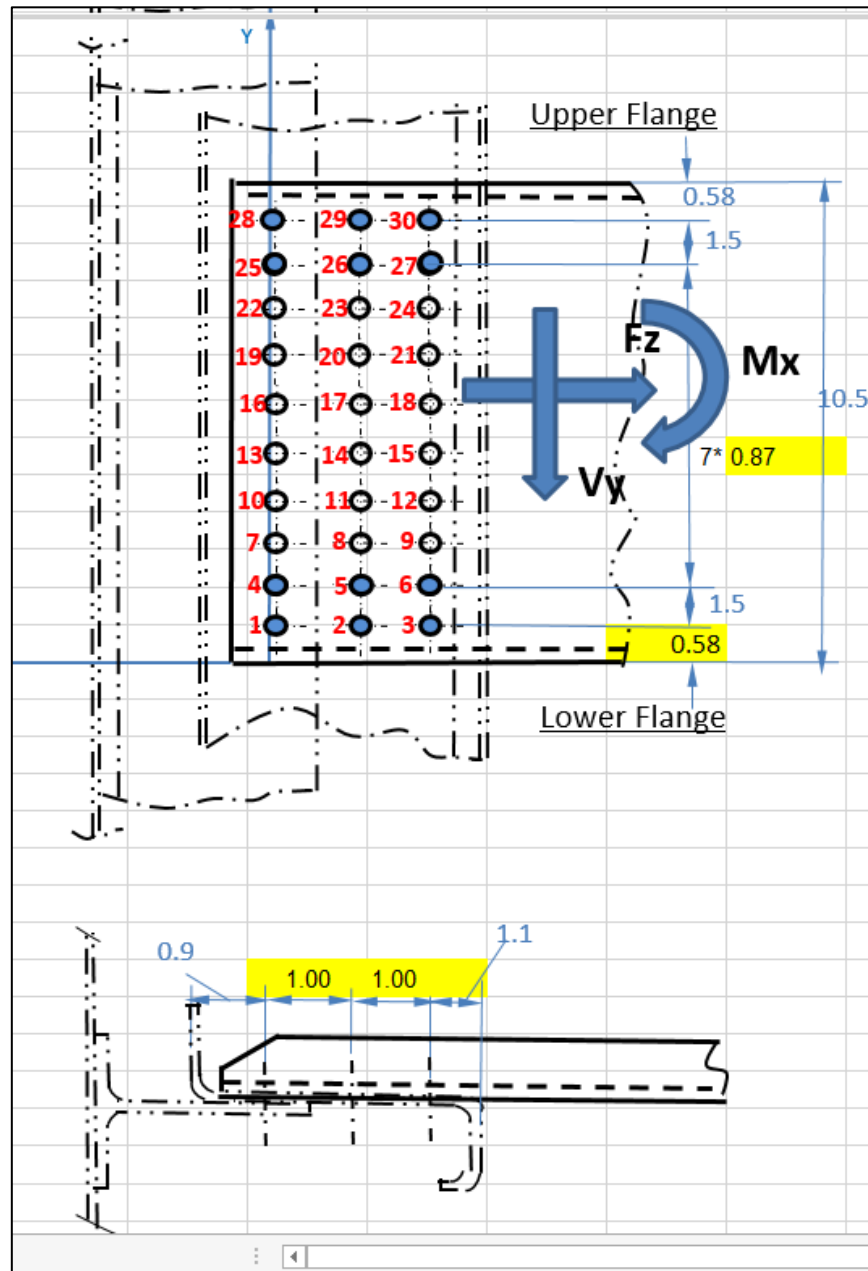


Figure 6.1 - Joint

Due to fasteners different shear and axial forces were redistributed equal to fastener diameter between all 30 fasteners.

Shear force caused by moment was found per formula 6.1

Shear load on given fasteners 1, due to a moment, M:

$$P_{m.1} = M \left( \frac{A_1 \cdot d_1}{\sum A \cdot d^2} \right) \quad (6.1)$$

Where A – Fastener area, d – Distance from centroid of the fastener cluster to given fastener.

Our joint has vertical pitch and horizontal pitch shown on figure 6.1. Were installed rivets with diameter 0.25 in and with diameter 0.156 in. Calculation of centroid is tabulated in Table 7.1.

Material properties for beam:

Ultimate Bearing Stress ( $e/D = 2.0$ ),  $F_{bru(e=2.0)} = 147000$  psi.

Fastener Properties

Fastener Material : 7075-T731 (E)

Ultimate Shear load: For  $d=0.25$  –  $P_{sh}=2230$  (lbs),

for  $d=0.156$  –  $P_{sh}=1230$  (lbs)

Table 6.1 – Calculation of centroid

Fastener ID	Y	Z	D	tweb	A <sub>i</sub>	A <sub>i</sub> *Y <sub>i</sub>	A <sub>i</sub> *Z <sub>i</sub>	A <sub>i</sub> *(Y <sub>i</sub> -Y <sub>cg</sub> ) <sup>2</sup>	A <sub>i</sub> *(Z <sub>i</sub> -Z <sub>cg</sub> ) <sup>2</sup>
	in				in <sup>2</sup>	in <sup>3</sup>	in <sup>3</sup>	in <sup>4</sup>	in <sup>4</sup>
1	0.58	0.00	0.250	0.10	0.049	0.03	0.00	1.07	0.05
2	0.58	-1.000	0.250	0.10	0.049	0.03	-0.05	1.07	0.00
3	0.58	-2.000	0.250	0.10	0.049	0.03	-0.10	1.07	0.05
4	2.08	0.00	0.250	0.10	0.049	0.10	0.00	0.49	0.05
5	2.08	-1.000	0.250	0.10	0.049	0.10	-0.05	0.49	0.00
6	2.08	-2.000	0.250	0.10	0.049	0.10	-0.10	0.49	0.05
7	3.08	0.00	0.156	0.10	0.019	0.06	0.00	0.09	0.02
8	3.08	-1.000	0.156	0.10	0.019	0.06	-0.02	0.09	0.00
9	3.08	-2.000	0.156	0.10	0.019	0.06	-0.04	0.09	0.02
10	3.95	0.00	0.156	0.10	0.019	0.08	0.00	0.03	0.02
11	3.95	-1.000	0.156	0.10	0.019	0.08	-0.02	0.03	0.00
12	3.95	-2.000	0.156	0.10	0.019	0.08	-0.04	0.03	0.02
13	4.82	0.00	0.156	0.10	0.019	0.09	0.00	0.00	0.02
14	4.82	-1.000	0.156	0.10	0.019	0.09	-0.02	0.00	0.00
15	4.82	-2.000	0.156	0.10	0.019	0.09	-0.04	0.00	0.02
16	5.68	0.00	0.156	0.10	0.019	0.11	0.00	0.00	0.02
17	5.68	-1.000	0.156	0.10	0.019	0.11	-0.02	0.00	0.00
18	5.68	-2.000	0.156	0.10	0.019	0.11	-0.04	0.00	0.02
19	6.55	0.00	0.156	0.10	0.019	0.13	0.00	0.03	0.02
20	6.55	-1.000	0.156	0.10	0.019	0.13	-0.02	0.03	0.00
21	6.55	-2.000	0.156	0.10	0.019	0.13	-0.04	0.03	0.02
22	7.42	0.00	0.156	0.10	0.019	0.14	0.00	0.09	0.02
23	7.42	-1.000	0.156	0.10	0.019	0.14	-0.02	0.09	0.00
24	7.42	-2.000	0.156	0.10	0.019	0.14	-0.04	0.09	0.02
25	8.42	0.00	0.250	0.10	0.049	0.41	0.00	0.49	0.05
26	8.42	-1.000	0.250	0.10	0.049	0.41	-0.05	0.49	0.00
27	8.42	-2.000	0.250	0.10	0.049	0.41	-0.10	0.49	0.05
28	9.92	0.00	0.250	0.10	0.049	0.49	0.00	1.07	0.05
29	9.92	-1.000	0.250	0.10	0.049	0.49	-0.05	1.07	0.00
30	9.92	-2.000	0.250	0.10	0.049	0.49	-0.10	1.07	0.05
Σ	-	-	-	-	0.934	4.905	-0.934	10.141	0.623

Center of gravity fastener group coordinates:

$$Y_{c.g.} = \frac{\sum A_i \cdot Y_i}{\sum A_i} = \frac{4.905}{0.934} = 5.25 \text{ in} \quad (6.2)$$

$$Z_{c.g.} = \frac{\sum A_i \cdot Z_i}{\sum A_i} = \frac{-0.934}{0.934} = -1 \text{ in} \quad (6.3)$$

Fastener load components:

$$R_{yv} = -V_y \cdot A_i / \Sigma A_i \quad (6.4)$$

$$R_{zFz} = F_z \cdot A_i / \Sigma A_i \quad (6.5)$$

$$R_{yMx} = -M_x \cdot A_i \cdot (Z_i - Z_{cg}) / [\Sigma A_i \cdot (Y_i - Y_{cg})^2 + \Sigma A_i \cdot (Z_i - Z_{cg})^2] \quad (6.6)$$

$$R_{zMx} = M_x \cdot A_i \cdot (y_i - y_{cg}) / [\Sigma A_i \cdot (Y_i - Y_{cg})^2 + \Sigma A_i \cdot (Z_i - Z_{cg})^2] \quad (6.7)$$

Load Case #8 is most critical for joint.

Table 6.2 – Ultimate joint loads

V <sub>y</sub> (lbs)	Axial (lbs)	M (lbs*in)
-4381	2855	-68197

Table 6.3 – Fastener load components

Fastener ID	R <sub>yv</sub>	R <sub>yMx</sub>	R <sub>zFz</sub>	R <sub>zMx</sub>	R <sub>Σ</sub>	Pshu	Pbru	MS <sub>sh</sub>	MS <sub>br</sub>
	lbs								
1	230	311	150	1452	1691	2230	2940	0.32	0.74
2	230	0	150	1452	1619	2230	2940	0.38	0.82
3	230	-311	150	1452	1604	2230	2940	0.39	0.83
4	230	311	150	986	1258	2230	2940	0.77	1.34
5	230	0	150	986	1159	2230	2940	0.92	1.54
6	230	-311	150	986	1139	2230	2940	0.96	1.58
7	90	121	59	264	385	1230	1838	2.19	3.77
8	90	0	59	264	335	1230	1838	2.68	4.49
9	90	-121	59	264	324	1230	1838	2.80	4.68
10	90	121	59	158	303	1230	1838	3.06	5.07
11	90	0	59	158	235	1230	1838	4.24	6.83
12	90	-121	59	158	219	1230	1838	4.61	7.39
13	90	121	59	53	239	1230	1838	4.15	6.69
14	90	0	59	53	143	1230	1838	7.60	11.84
15	90	-121	59	53	116	1230	1838	9.63	14.88
16	90	121	59	-53	211	1230	1838	4.82	7.69
17	90	0	59	-53	90	1230	1838	12.65	19.39
18	90	-121	59	-53	32	1230	1838	37.31	56.24
19	90	121	59	-158	234	1230	1838	4.26	6.86
20	90	0	59	-158	134	1230	1838	8.17	12.70
21	90	-121	59	-158	104	1230	1838	10.78	16.59
22	90	121	59	-264	294	1230	1838	3.18	5.24
23	90	0	59	-264	224	1230	1838	4.49	7.21
24	90	-121	59	-264	207	1230	1838	4.93	7.86
25	230	311	150	-986	996	2230	2940	1.24	1.95
26	230	0	150	-986	867	2230	2940	1.57	2.39
27	230	-311	150	-986	840	2230	2940	1.66	2.50
28	230	311	150	-1452	1410	2230	2940	0.58	1.08
29	230	0	150	-1452	1323	2230	2940	0.69	1.22
30	230	-311	150	-1452	1305	2230	2940	0.71	1.25

All M.S. are positive, so static strength is enough.

## 6.2 Fatigue joint analysis

In current fatigue analysis are calculated joint with fasteners 28, 29, 30 due to lesser margins of safety.

Firstly below provided bending analysis for operating load:

Table 6.4 – Operation loads

Vy (lbs)	Axial (lbs)	M (lbs*in)
-1366	3048	22074

Fastener dia is 0.25”.

Fastener Material : 7075-T731 (E)

Ultimate Shear load: For  $d=0.25$  –  $P_{sh}=2230$  (lbs)

Sheet thickness is 0.1”.

Assumed effective width is 1.16”.

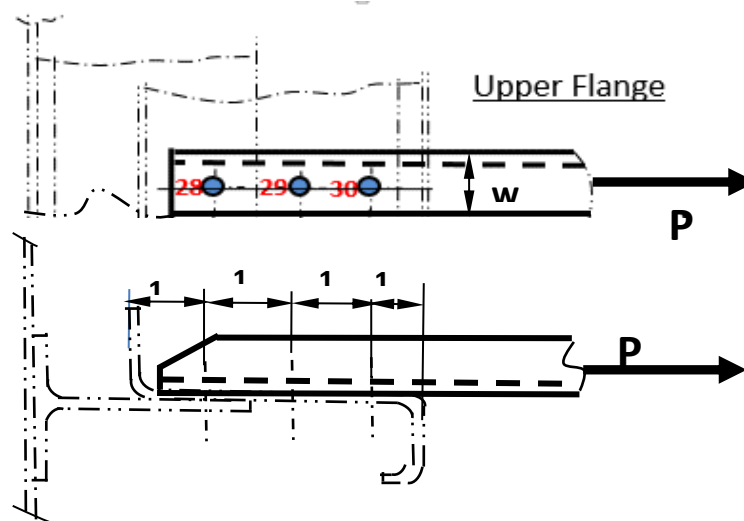


Figure 6.2– Joint

Table 6.5 – Fastener load components

Fastener ID	R <sub>yv</sub>	R <sub>yMx</sub>	R <sub>zFz</sub>	R <sub>zMx</sub>	R <sub>Σ</sub>	Pshu	Pbru	MS <sub>sh</sub>	MS <sub>br</sub>
	lbs								
1	72	-101	160	-470	311	2230	2940	6.16	8.44
2	72	0	160	-470	318	2230	2940	6.01	8.24
3	72	101	160	-470	355	2230	2940	5.29	7.29
4	72	-101	160	-319	162	2230	2940	12.80	17.20
5	72	0	160	-319	174	2230	2940	11.79	15.86
6	72	101	160	-319	235	2230	2940	8.51	11.54
7	28	-39	63	-85	25	1230	1838	47.41	71.33
8	28	0	63	-85	36	1230	1838	33.06	49.88
9	28	39	63	-85	71	1230	1838	16.30	24.84
10	28	-39	63	-51	16	1230	1838	75.80	113.73
11	28	0	63	-51	30	1230	1838	39.65	59.73
12	28	39	63	-51	68	1230	1838	17.00	25.90
13	28	-39	63	-17	47	1230	1838	25.24	38.20
14	28	0	63	-17	53	1230	1838	22.01	33.38
15	28	39	63	-17	81	1230	1838	14.13	21.60
16	28	-39	63	17	80	1230	1838	14.29	21.85
17	28	0	63	17	84	1230	1838	13.57	20.77
18	28	39	63	17	104	1230	1838	10.79	16.62
19	28	-39	63	51	114	1230	1838	9.76	15.07
20	28	0	63	51	117	1230	1838	9.50	14.68
21	28	39	63	51	132	1230	1838	8.30	12.90
22	28	-39	63	85	148	1230	1838	7.29	11.39
23	28	0	63	85	151	1230	1838	7.17	11.21
24	28	39	63	85	163	1230	1838	6.57	10.31
25	72	-101	160	319	480	2230	2940	3.64	5.12
26	72	0	160	319	485	2230	2940	3.60	5.07
27	72	101	160	319	509	2230	2940	3.38	4.77
28	72	-101	160	470	631	2230	2940	2.53	3.66
29	72	0	160	470	634	2230	2940	2.52	3.63
30	72	101	160	470	653	2230	2940	2.41	3.50

Load applied to joint:

$$P_{\text{joint}} = 1891 \text{ lbs} \quad (6.8)$$

For fatigue cycles determination we need calculate safety factor ( concentration factor).

$$K_{tgross} = SF = \left( \frac{\alpha \cdot \beta}{f_g} \right) \left[ \left( \frac{K_{tb} \cdot \Delta P}{D \cdot t} \right) \cdot \theta + \left( \frac{K_{tg} \cdot P}{W \cdot t} \right) \right] \quad (6.9)$$

Gross area stress

$$f_g = \frac{P_{\text{joint}}}{W \cdot t} = \frac{1891}{1.16 \cdot 0.1} = 16300 \text{ psi} \quad (6.10)$$

Explanation of use symbols is shown on figure 6.3.

$\alpha = 0.7$  – for cold worked hole;

$\beta = 0.75$  – for rivets;

Assume that firs fastener take 0.35 from all loads:

$$\Delta P = P_{\text{joint}} \cdot 0.35 = 662 \text{ lbs}$$

For finding  $K_{tb}$  will found  $D/W$  ratio =  $0.25/0.116 = 0.22$

From figure 6.4:

$$K_{tb} = 1.35$$

For finding  $Q$  will found  $t/D$  ratio =  $0.1/0.25 = 0.4$

From figure 6.5:

$$Q = 1.5$$

For finding  $K_{tg}$  will found  $r/c$  ratio =  $0.25/2/1.16/2 = 0.21$

And  $e/c$  ration = 1

From figure 6.6:

$$K_{tg} = 3.7$$

$$SF = \left( \frac{0.7 \cdot 0.75}{16300} \right) \left[ \left( \frac{1.35 \cdot 662}{0.25 \cdot 0.08} \right) \cdot 1.5 + \left( \frac{3.17 \cdot (1891 - 662)}{1.16 \cdot 0.08} \right) \right] = 2.81$$

Net area stress:

$$f_{net} = f_g * \frac{W}{W-D} = 20374 * \frac{1.16}{1.16-0.25} = 20778 \text{ psi} \quad (6.11)$$

Calculate Number of cycles per formula 6.12 from figure :

$$N = 10^{10.2-4.63*\log(f_{net}-5.3)} \quad (6.12)$$

$$N = 49161 \text{ cycles}$$

where:	$\alpha$	– Fastener hole condition factor:
		Standard drilled hole 1.0
		Broached or reamed 0.9
		Cold worked hole 0.7 – 0.8
	$\beta$	– Hole filling factor:
		Open hole 1.0
		Steel lock bolt 0.75
		Rivets 0.75
		Threaded bolts 0.75 – 0.9
		Hi-Lok 0.75
		Taper-Lok 0.5
	$\sigma$	– Reference stress (i.e., $\sigma_{ref}$ ) in the structure
	$\sigma_1$	– Local stress caused by load transfer, $\Delta P$
	$\sigma_2$	– Local stress caused by bypass load, P
	P	– Bypass load
	$\Delta P$	– Load transfer through the fastener
	D	– Fastener diameter
	t	– Splice plate thickness

P	– Bypass load.
W	– Width of the splice plate.
$K_{th}$	– Bearing stress concentration factor, see Fig. 9.12.12
$\theta$	– Bearing distribution factor, see Fig. 9.12.13
$K_{tg}$	– Stress concentration factor, see Fig. 9.12.14

Figure 6.3– Explanation of used symbols [1]

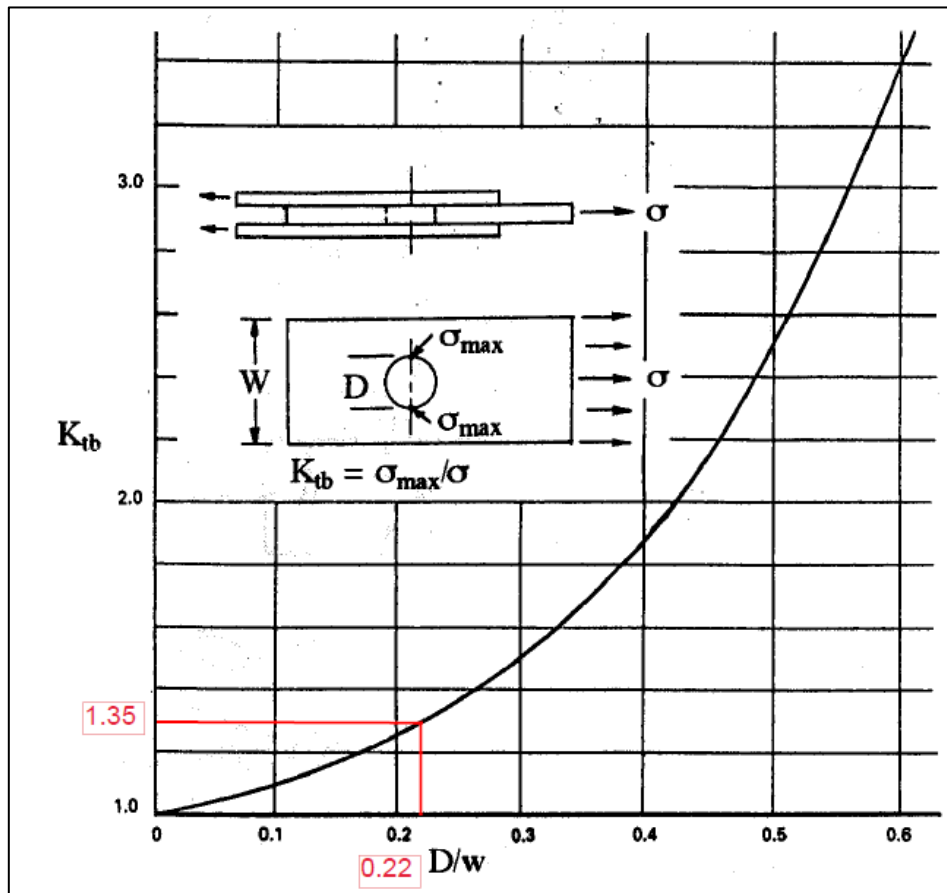


Figure 6.4– Bearing concentration factor [1]

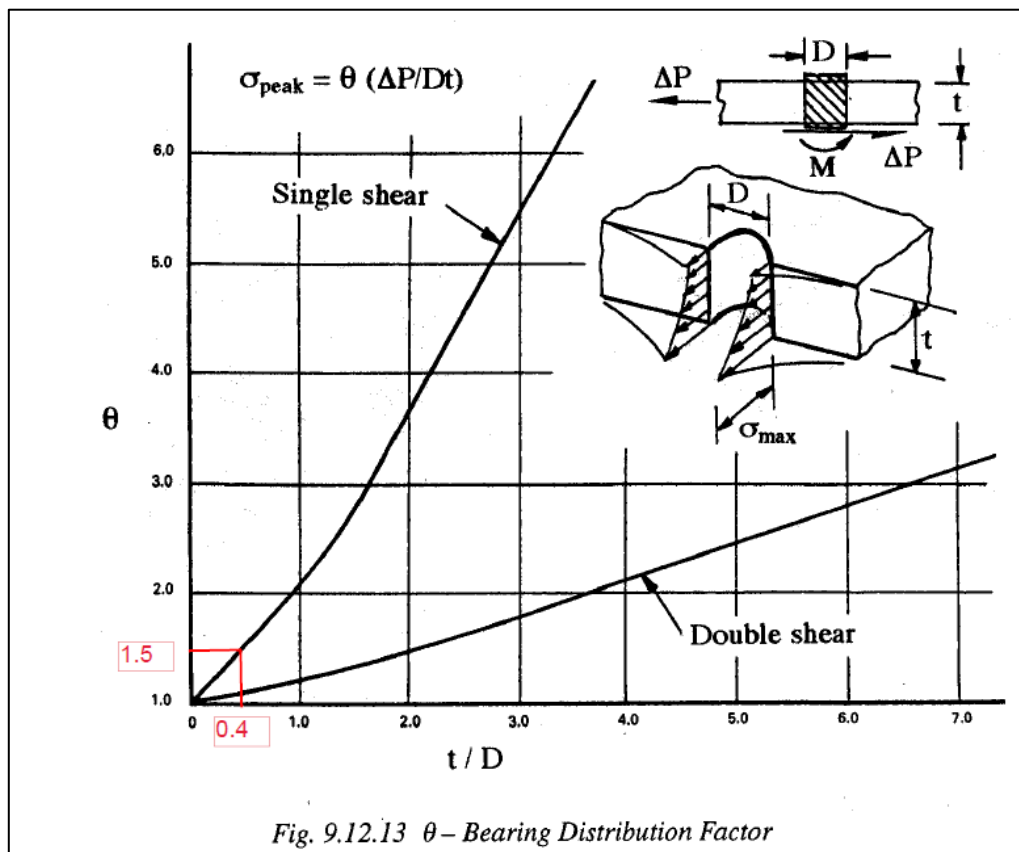


Fig. 9.12.13  $\theta$ – Bearing Distribution Factor

Figure 6.5– Bearing distribution factor [1]

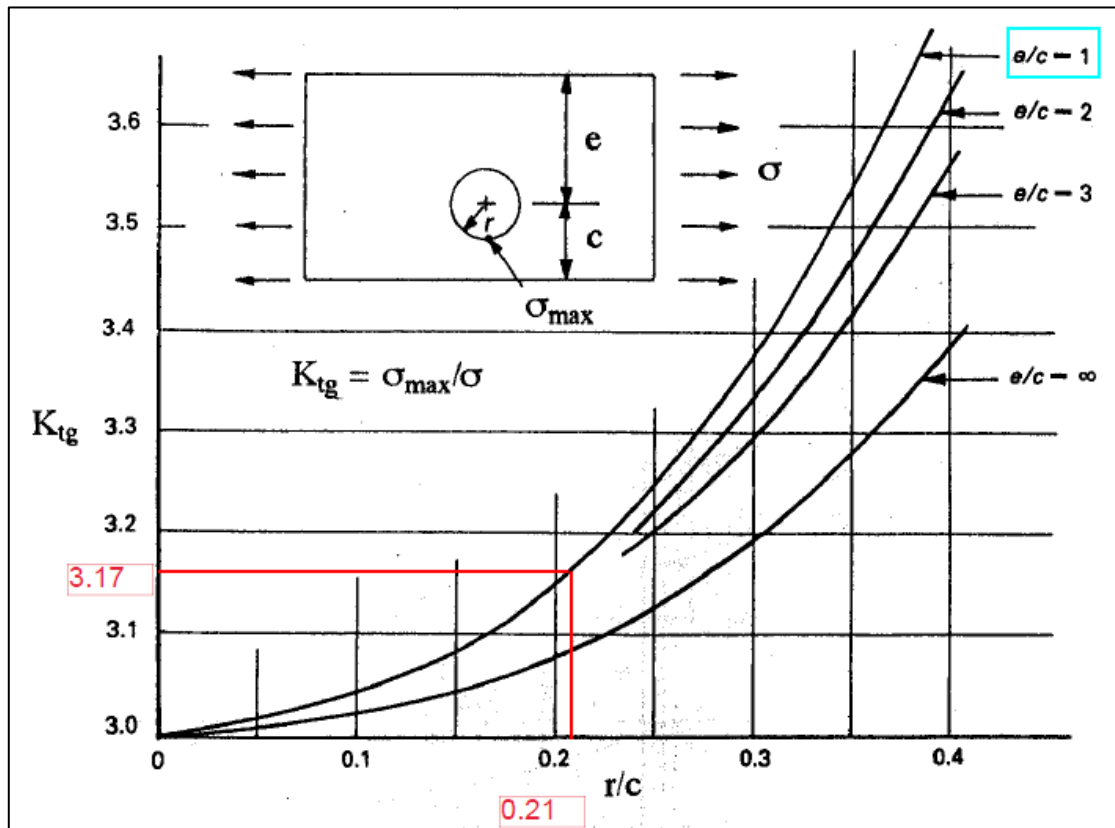


Figure 6.6– Stress concentration factor [1]

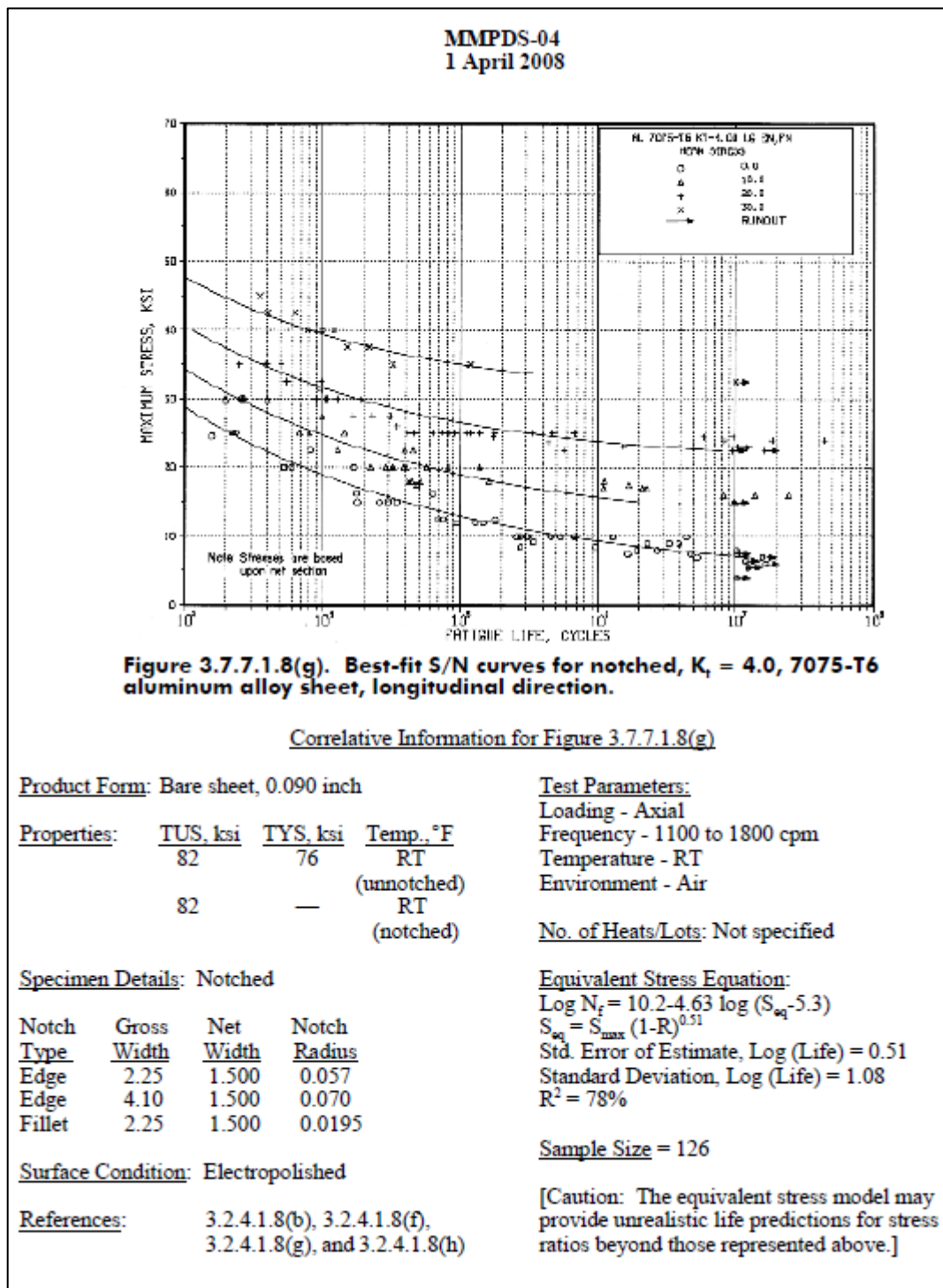


Figure 6.7– Fatigue life cycles [1]

## Startup

The developed beam has one difference in comparison with analogues.

This difference reduced weight of beam which very important for aircraft. Due to airplane has many this beam, weight savings will be significant.

The difference lies in the variable section along the span of the beam. This is very complicated for manufacturing, therefore, more cost. But it should be compensated by increasing payloads weight and reducing fuel consumption.



Figure 7.1– Floor beam with constant geometry

## **Conclusion**

Current floor beam is designed based on typical aircraft methodical and satisfies all requirement FAR25.

All Margins of Safety for cross-section analysis are positives, therefore, static strength is substantiated. Web buckling is the most critical analysis.

All fastened point form joint with frame gave positives Margins of Safety, therefore, static strength is substantiated.

Fatigue calculation for joint with frame gave enough flight cycles for airplane life.

## **Bibliography**

1. Airframe stress analysis and sizing – M.C.Niu (1999)
2. Far-25
3. Analysis and design of flight vehicle structures - Bruhn (1973)
4. Metallic Materials Properties Development and Standardization (MMPDS-11)
5. Commercial Airplane Design Principles.

<https://www.sciencedirect.com/science/article/pii/B9780124199538000127?via%3Dihub>